

---

Doctoral Dissertations

Student Theses and Dissertations

---

Spring 2015

## Characterization of bending fatigue mini-specimens for nuclear materials

Ahmed Suliman R. Haidyrah

Follow this and additional works at: [https://scholarsmine.mst.edu/doctoral\\_dissertations](https://scholarsmine.mst.edu/doctoral_dissertations)



Part of the [Nuclear Engineering Commons](#)

Department: Mining and Nuclear Engineering

---

### Recommended Citation

Haidyrah, Ahmed Suliman R., "Characterization of bending fatigue mini-specimens for nuclear materials" (2015). *Doctoral Dissertations*. 2383.

[https://scholarsmine.mst.edu/doctoral\\_dissertations/2383](https://scholarsmine.mst.edu/doctoral_dissertations/2383)

This thesis is brought to you by Scholars' Mine, a service of the Missouri S&T Library and Learning Resources. This work is protected by U. S. Copyright Law. Unauthorized use including reproduction for redistribution requires the permission of the copyright holder. For more information, please contact [scholarsmine@mst.edu](mailto:scholarsmine@mst.edu).

CHARACTERIZATION OF BENDING FATIGUE MINI-SPECIMENS FOR  
NUCLEAR MATERIALS

by

AHMED SULIMAN R. HAIDYRAH

A DISSERTATION

Presented to the Faculty of the Graduate School of the  
MISSOURI UNIVERSITY OF SCIENCE AND TECHNOLOGY

In Partial Fulfillment of the Requirements for the Degree

DOCTOR OF PHILOSOPHY

In

NUCLEAR ENGINEERING

2015

Approved by

Carlos H. Castaño, Advisor  
Joseph W. Newkirk, Co-advisor  
Muthanna H. Al Dahhan  
Hyoung K. Lee  
Xin Liu

© 2015

Ahmed Suliman R. Haidyrah

All Rights Reserved

## **PUBLICATION DISSERTATION OPTION**

This dissertation consists of the following five papers that have been submitted for publication as follows:

Pages 18 -26 have been published to the TRANSACTIONS OF AMERICAN NUCLEAR SOCIETY 2014, volume 111, No.1, on page 620-623.

Pages 27 -41 have been published in TMS SUPPLEMENTAL PROCEEDINGS. Materials and fuels for the current and advanced nuclear reactors IV, 2015, on page 1225-1232.

Pages 42-63 has been submitted for publication in JOURNAL OF NUCLEAR MATERIALS.

Pages 64-93 has been submitted for publication in JOURNAL OF NUCLEAR MATERIALS.

Pages 94-111 are intended for submission in JOURNAL OF TESTING AND EVALUATION.

## ABSTRACT

The bending fatigue of mini-specimen was used to study fatigue properties of nuclear materials and compare the obtained results with that of reference data of full size specimen. This Krouse-type was made of austenitic (SS304 & SS316), HT9 ferritic martensitic steel and Incoloy alloy MA956 oxide dispersion strengthens (ODS) and machined with waterjet. A comparison between the mini-specimens and the standard specimen ASTM B593 had similar design but a smaller size. The stress range values for the Krouse-type design were found to be lower than that of the standard one. The bending fatigue machine VSS-40H was designed and LEF-150 was modified with a specially designed adapter to test the fatigue of the mini-specimen. The mini-specimen bending fatigue (Krouse-type) of HT9 was tested as-received and Incoloy alloy MA956 was tested as-received and thermal aging conditions. Consequently, the S-N curve for both HT9 and Incoloy alloy MA956 were defined. The fatigue endurance limits were measured to be 94 MPa for HT9 and 132 MPa for Incoloy alloy MA956. The finite element model code ABAQUS was used to estimate the level of stress in the bent mini specimen. The plots indicated that the 3-parameter Weibull distribution fits the data well. The correlation coefficient value for 3-parameter Weibull was increased by 33.66 % for the HT9, 30.88% for the as-received and 26.51% for the thermal aging for Incoloy alloy MA956. The thermal aging treatment on the mini specimens was not much impact on the fatigue life. The analysis of error propagation of specimen's stress has been observed that the most of the error is due to length and deflection measurements. Thus this Krouse-type was seen as the solution to studying fatigue of irradiated specimen as it solved the challenge of limitation of space in research reactors.

## ACKNOWLEDGMENTS

I would like to thank to my advisor, Dr.Carlos H. Castaño, for supporting, encouragement, guiding and patience during my study, without his help, this work would not have been possible. Castaño is someone you will never forget once you meet him. I will forever be thankful to my co-advisor , Dr. Joseph W. Newkirk , has been helpful in providing advice and suggestions to improve my work and for assisting me in several aspects. I also have to extend thanks to the members of my advisory committee, Professors Muthanna H. Al Dahhan,Hyoung K. Lee, Xin Liu for their helpful and suggestions in general.

The love and encouragement from my wife, Nouf K. Balobaid, for her unlimited love, patient and made my living more enjoyable. Big hugs to my daughters Madhawi, Yara and Arwa for bringing a great joy to my live. Thank you for my father in law Khamis A. Balobaid, this man is always asking about my study progress. I really appreciated to my mother, brothers and sisters for support and advise me all time.

Thanks a lot to my friend Saad Mohammed Alqahtani and special thanks are extended to those who accompanied me during my study in Rolla: Mohammed Yousaf, Amer Al-Shareef and Naser Zouli.

Utmost appreciation to my sponsor work King Abdul-Aziz City of Science & Technology (KACST) for support and funding my studying. Without their support none of this would have been possible.

Finally, I would love to dedicate this research to the soul of my father Suliman R.Haidyrah who encouraged me to be the best.

## TABLE OF CONTENTS

	Page
PUBLICATION DISSERTATION OPTION .....	iii
ABSTRACT.....	iv
ACKNOWLEDGMENTS .....	v
LIST OF ILLUSTRATIONS.....	x
LIST OF TABLES.....	xiii
<b>SECTION</b>	
1. PURPOSE OF THIS RESEARCH.....	1
2. INTRODUCTION.....	2
2.1. SCOPE OF THE WORK.....	2
2.2. OVERVIEW OF ADVANCED TESTING REACTOR (ATR).....	3
2.3. SETUP THE MINI-SPECIMEN (KROUSE-TYPE) AT ATR.....	5
3. LITERATURE REVIEW.....	8
3.1. DEVELOPMENT OF MINI SPECIMEN BENDING FATIGUE SPECIMENS.....	8
3.2. DESIGN OF BENDING FATIGUE MACHINE.....	9
3.3. FATIGUE RESPONSE FOR IRRADIATED REACTOR MATERIALS.....	9
3.4. INFLUENCE OF THERMAL AGING ON FATIGUE LIFE.....	11
4. EXPERIMENTAL SETUP AND MEASUREMENT TECHNIQUES.....	12
4.1. FATIGUE MACHINE.....	12
4.1.1. LFE-150 Testing Machine.....	12
4.1.2. VSS-40M Variable Speed Miniature Sheet Specimen Fatigue Testing Machine.....	15
4.2. MINI SPECIMEN (KROUSE-TYPE) DESIGN.....	16
4.3. MEASUREMENT TECHNIQUES.....	17
<b>PAPER</b>	
I. AN EXPERIMENTAL STUDY ON BENDING FATIGUE TEST WITH A KROUSE - TYPE FATIGUE SPECIMEN.....	18
INTRODUCTION.....	18
SPECIMENS.....	18

FATIGUE TEST MACHINE.....	21
ABAQUS MODEL .....	22
RESULTS AND DISCUSSIONS .....	23
CONCLUION .....	24
ACKNOWLEDGMENTS.....	25
REFERENCES .....	25
II. Characterization a Bending Fatigue Mini-Specimen Technique (Krouse-type) of Nuclear Materials.....	27
Abstract .....	27
Introduction .....	27
Specimens.....	28
Experimental procedure .....	30
Material and Specimen Preparation .....	30
Micro hardness test.....	32
Tensile Test .....	33
Bending fatigue Test .....	34
FEA model .....	35
Results and Discussion.....	36
Conclusion.....	39
References .....	40
III. Weibull statistical analysis of Krouse -type bending fatigue in nuclear materials of HT9 .....	42
ABSTRACT .....	42
1. Introduction .....	43
2. Experimental procedure .....	43
2.1. Specimens .....	43
2.2. Material and specimen preparation .....	45
2.3. Metallographic examination.....	46
2.4. Bending fatigue test.....	47
2.5. Stress calculation method.....	49
2.6. Finite element modeling.....	50
3. Analysis of error propagation.....	51
4. Statistics analysis of fatigue data.....	51



5. Results and discussion.....	53
6. Conclusion and future work .....	61
Acknowledgments .....	62
References .....	62
IV. Influence of thermal aging on the mini specimen (Krouse - type) bending fatigue of nuclear materials .....	64
ABSTRACT .....	64
1. Introduction .....	65
2. Experimental procedure .....	65
2.1. Specimens .....	65
2.2. Material and experiment.....	67
2.3. Finite element modeling.....	72
2.4. Statistics analysis of fatigue data.....	74
3. Results and discussion.....	76
3.1. S-N curve.....	76
3.2. Microstructural characterization.....	78
3.3. Irradiation damage of incoloy alloy MA956.....	83
3.4. Hardness .....	84
3.5. Analysis of error propagation.....	84
3.6. Statistics analysis of fatigue data.....	85
4. Conclusion and future work .....	91
References .....	92
V. A Comparison of Bending Fatigue Specimens (Krouse - Type) for Nuclear Materials .....	94
ABSTRACT .....	94
Introduction .....	95
Experimental Procedure .....	96
Specimens.....	96
Material and Specimen Preparation .....	99
Thermal Aging Treatment.....	101
Bending Fatigue Test.....	101
Finite Element Modeling.....	103
Results and Discussion.....	104

Conclusion.....	110
References .....	110
SECTION	
5. CONCLUSION & FUTURE WORK .....	112
APPENDIX.....	115
REFERENCE.....	118
VITA .....	119

## LIST OF ILLUSTRATIONS

SECTION	Page
Figure 2.1. ATR core .....	4
Figure 2.2. Capsule loaded in basket .....	7
Figure 3.1. Comparison of the fatigue lives for ferritic/martensitic steels (MANET and HT9) in the unirradiated and irradiated conditions as a function of temperature .....	10
Figure 3.2. High Cycle fatigue strength of Incoloy alloy MA956.....	11
Figure 4.1. LEF-150.....	13
Figure 4.2. Schematic diagram of mini specimen adapters .....	14
Figure 4.3. Schematic design of the mini specimen adapters .....	15
Figure 4.4. Diagram of the VSS-40H mini specimen Krouse bending fatigue equipment.....	16
<b>PAPER I</b>	
Figure 1. Sketch of the Krouse-type fatigue test specimen .....	19
Figure 2. Schematic view of the wedge-shaped beam's length .....	20
Figure 3. The failure crack at the specimen's lower cross section area.....	21
Figure 4. Measured deflection .....	22
Figure 5. Stress distribution on the Krouse-type specimen model .....	23
Figure 6. Results for the mini specimen compared with full size specimen results obtained for 304 stainless steel.....	24
<b>PAPER II</b>	
Figure 1. Sketch of the mini fatigue test specimen .....	29
Figure 2. Steps prepared HT9 specimen .....	31
Figure 3. (a) As-Received mini specimen, (b) polished mini specimen.....	32
Figure 4. Testing set-up for tensile test for mini specimens .....	33
Figure 5. Testing set-up for bending fatigue for mini specimen size .....	35
Figure 6. Stress results for the Krouse-type specimen model.....	36
Figure 7. Measured Vicker hardness of polished HT9 .....	37

Figure 8. Optical micrographs of polished surface finish and ground surface finish for mini-specimen .....	38
--	----

Figure 9. Results for as-received and polished surface finish Mini-specimen for HT9 compared with stainless steel 304. ....	39
---	----

### PAPER III

Fig. 1. Sketch of the mini fatigue test specimen .....	44
--	----

Fig. 2. Bending fatigue equipment.....	48
--	----

Fig. 3. Schematic design of the fatigue test system. ....	48
---	----

Fig. 4. Stress distribution on the Krouse -type specimen model at 15 N.....	50
---	----

Fig. 5. Experimental results for the mini specimen compared with FEA (ABAQUS) results obtained for HT9 .....	54
--	----

Fig. 6. S-N curves for HT9. ....	55
----------------------------------	----

Fig. 7. S-N Curve for mean fatigue life .....	56
---	----

Fig. 8. Sample of SEM .....	57
-----------------------------	----

Fig. 9. SEM images of mini specimen.....	58
--	----

Fig. 10. Plot of 2-parameter Weibull distribution.....	60
--	----

Fig. 11. Plot of 3-parameter Weibull distribution.....	61
--	----

### PAPER IV

Fig. 1. Diagram for the mini fatigue test specimen.....	66
---	----

Fig. 2. LEF-150 bending fatigue machine .....	70
---	----

Fig. 3. VSS-40H bending fatigue machine .....	71
---	----

Fig. 4. Stress distribution of the model .....	73
--	----

Fig. 5. Comparison of the fatigue lives for INCOLOY ALLOY MA956 in the as-received and thermal aging conditions at different stress levels .....	76
--	----

Fig. 6. S–N curves for INCOLOY ALLOY MA956 each marker corresponds to a tested specimen .....	77
---	----

Fig. 7. SEM of as-received specimen .....	78
---	----

Fig. 8. SEM of Thermal aging .....	79
------------------------------------	----

Fig. 9. SEM obtained by etch test for, (a) as-received.....	80
---	----

Fig. 10. Optical Microscopy obtained by etch test .....	81
---	----

Fig. 11. XRD patterns of (a) as-received before fatigue test .....	82
Fig. 12. Damage profile of Incoloy alloy MA956 steel.....	83
Fig. 13. Microhardness profiles on specimen .....	84
Fig. 14. Lognormal distribution fit under stress level at 563 MPa, 408 MPa, and 275 MPa and 132 MPa stress levels .....	87
Fig 15. Probability Plot of 563 MPa, 408 MPa, 275 MPa and 132 MPa stress level.....	89
Fig. 16. Probability Plot of 563 MPa, 408 MPa, 275 MPa and 132 MPa stress level.....	90
 PAPER V	
FIG.1. Sketch of specimen type-1.....	96
FIG.2. Sketch of specimen type-2.....	97
FIG.3. Sketch of specimen type-3.....	97
FIG.4. Sketch of specimen type-4.....	98
FIG.5. Physical geometry of specimen types.....	101
FIG.6 .Experiment device of bending fatigue.....	102
FIG.7. Stress analysis for the specimen types.....	103
FIG.8. Results for specimen type-1 for 304 stainless steel compared with typical stainless steel 304L .....	105
FIG.9.Results for specimen type-2 for 304 stainless steel compared with typical 304 stainless steel .....	106
FIG.10. Results for specimen type-3 for 304 stainless steel compared with typical stainless steel 304L.....	107
FIG.11.Results for specimen type-1 for 304 stainless steel compared with typical stainless steel 304L. ....	108

## LIST OF TABLES

SECTION	Page
Table 1.1. Approximate number of specimen fit into ATR capsule positions .....	6
<b>PAPER II</b>	
Table 1. Mini Fatigue Test Specimen dimensions comparing with ASTM B593 Standard .....	29
Table 2. Hardness test (HRB) result for HT9 .....	32
<b>PAPER III</b>	
Table 1. Mini Fatigue Test Specimen dimensions comparing with ASTM B593 Standard. ....	45
Table 2. Chemical composition .....	46
Table 3 . Mechanical properties of HT9 .....	46
Table 4. Error Analysis Calculation.....	58
<b>PAPER IV</b>	
Table 1. Mini Fatigue Test Specimen dimensions comparing with ASTM B593 Standard. ....	67
Table 2. Chemical composition (in wt %) .....	68
Table 3 . Mechanical properties of alloy .....	68
Table 4. Error Analysis Calculation.....	85
Table 5. Weibull parameters summary .....	88
<b>PAPER V</b>	
Table 1. Chemical composition (in wt %) of 304 stainless steel .....	99
Table 2 . Mechanical properties of 304 stainless steel.....	100
Table 3. Simulated and experimental comprising results .....	109
Table 4. Error Analysis Calculation [8].....	109

## **SECTION**

### **1. PURPOSE OF THIS RESEARCH**

Specific objective of this research are to (1) validate the use of bending fatigue specimens (Krouse-type) to create the S-N curve with known fatigue curves (i.e. SS 304), (2) study and create the S-N curve for fatigue behavior for some materials such as HT9, Incoloy alloy MA956, (3) study thermal aging and the effect the thermal on fatigue behavior, (4) setup the mini-specimen (Krouse-type) at ATR.

## 2. INTRODUCTION

### 2.1. SCOPE OF THE WORK

To achieve required goals of new reactor design, new materials that have high radiation swelling resistance and stability that can withstand high temperatures is recommended. Only materials that meet these high standards were recommended to be used. It was suggested using Ferritic/Martensitic steel. Although it experiences reduction of mechanical properties above 600 C °, it has a good resistance when it comes to neutron irradiation induced charges of up to 150 dpa. A good example is HT9 and MA 956. They react in a cyclic load if used in a nuclear reactor. This is mainly because of the automatic frequency control mode of operation it also experience changing pressure and load. It is advised to know the fatigue properties of a material before subjecting them to nuclear reactor.

To determine a material fatigue property, a cycle to failure S-N curve is typically used. For this research we will study the bending fatigue. Here a material is slightly bend until it breaks. The results are recorded using an x and y axis. The x axis is used to record the number of time the materials is bend while the y axis records the bending stress of the specimen. In theory it will look like a concave up curve that reaches a lower horizontal asymptote called the endurance limit. This is where the amount of cycles the sample can undergo without failing. Accurate S-N curve is a variable tool that determines which material will fatigue will induce fatigue.

The primary research main objective was creating an S-N curve for stainless steel 304 using the HT9 and MA956 was necessitated by its uniqueness and that it also meets the established materials for this kind of research. It began by testing the stainless steel 304 sample for this research.

This research utilized the mini specimens to create an S-N curve for nuclear materials. The base design is a modified Krouse type specimen. The specimen was placed in a controlled displacement bending fatigue machine. The specimen had already been investigated by the materials science and Engineering department of Missouri SST to study it for bending fatigue of AA705-T6 an aluminum alloy [3]. The result from these research will go a long way in researching other materials once an the results are



established. This will lead to testing every material under different conditions such as thermal aging condition, after irradiations, or even welding. More investigations will be discussed later in this research.

New research had to be incited that had superior radiation and corrosion resistance that could improve the economy, performance of the current nuclear materials with the possibility of creating new ones for future reactors and structural materials of fusion reactors. These materials had to provide sufficient reliability and also well stable mechanical properties under a wide range of temperature and a high neutron dose. Nuclear reactors operate under load conditions that cause cyclic loads that need internal and structure components that cause fatigue to achieve this we measure mechanical properties of the material to estimate its safe operating life. This has been hampered by lack of space in nuclear test reactors that could irradiate a full size fatigue specimen in sufficient quantities. Studying is a challenge due to space limitation in reactors (e. ATR). We proposed the use of Krouse-type material such as stainless steel 304L, 316L, HT9 and MA 956 oxide dispersion strength (ODS) on a majority of experiments that produce address irradiation issues in nuclear materials putting in mind the suitability of a mini-specimen (Krouse-type) bending fatigue under cycle fatigue conditions.

The bending fatigue mini specimen technique is ultimately crosscutting since fatigue is an important basic characteristic of nuclear materials that needs to be studied. It is suitable for advanced reactor materials, and will help characterize materials in a variety of conditions (as-received, polished, and irradiated). The small size of the machine will allow it to be introduced in a hot cell. The smaller sample will allow for more efficient use of existing irradiated materials and enable fabrication of smaller fatigue specimens from previously examined nuclear materials.

## **2.2. OVERVIEW OF ADVANCED TESTING REACTOR (ATR)**

The key objective for this research is irradiating the mini specimen bending fatigue at advanced testing reactor (ATR). The ATR is a high flux test reactor cooled with water, and whose serpentine design allows large power variations among its flux traps. ATR's curved fuel arrangement makes it possible for fuel to remain close on all

sides of the flux positions, something that would otherwise be more difficult in a rectangular grid. This reactor comes with nine neutron flux traps and 68 irradiation positions in the reactor's main reflector tank as shown in Figure 2.1. Each of these tanks may contain a number of experiments. The size of experiment positions varies from 0.5 to 5 inches in diameter and is 48 inches long. The peak thermal flux is  $1 \times 10^{15}$  n/cm<sup>2</sup>-sec while its fast flux is  $5 \times 10^{14}$  n/cm<sup>2</sup> at its 250 MW full power. It has a hydraulic shuttle irradiation that allows the insertion and removal of experiments during the reactor operation. Pressurized water reactor loops make it possible for loops to be performed at potential PWR operating conditions [2].

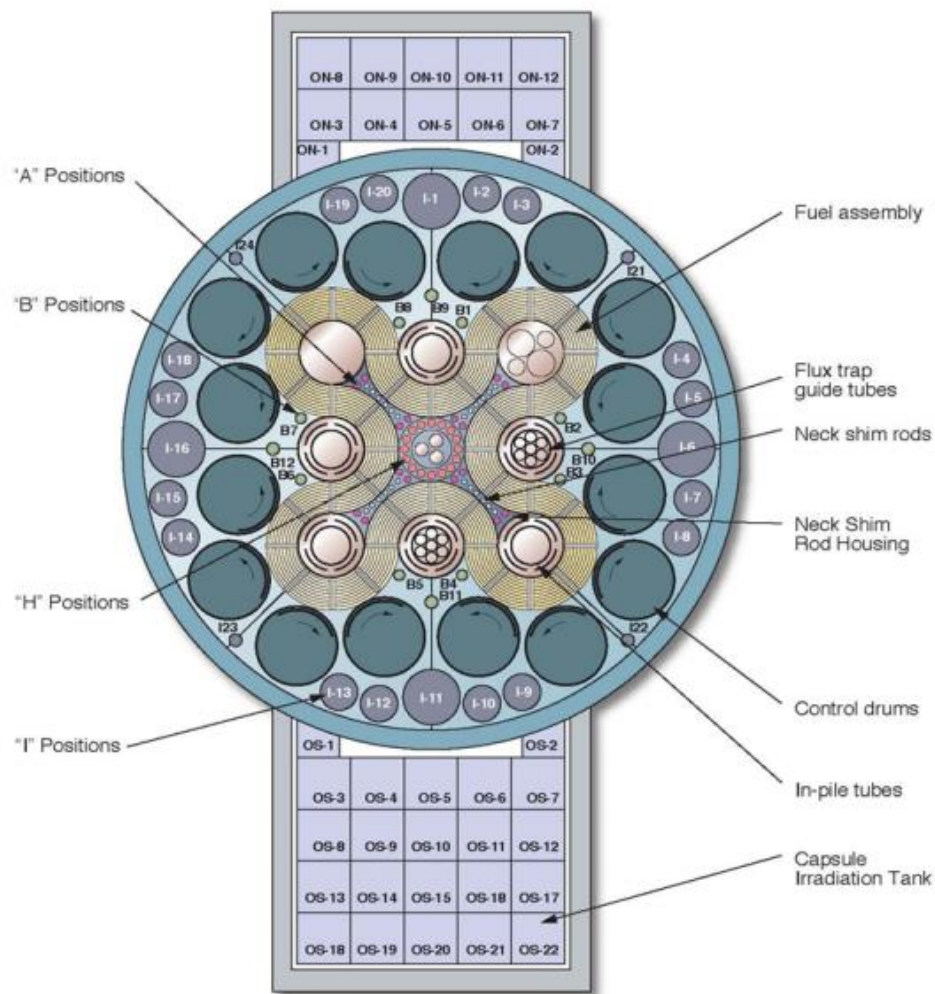







Figure 2.1. ATR core.

### **2.3. SETUP THE MINI-SPECIMEN (KROUSE-TYPE) AT ATR**

The position A and B are candidate irradiation positions to irradiate the mini specimen (Krouse-type) size. The different size and potential number of the specimen fit into ATR at irradiation positions are shown in Table 2.1. When the positions A and B are appointed for irradiation of a particular experiment, an irradiation capsule are going to be designed. The irradiation capsule isn't sealed however permit the experiment specimens to be up-to-date with the reactor primary agent to forestall excessive temperature. The mini specimen (Krouse-type) size can rely upon the capsule size and also the want for temperature insulation. Once the target specimen's size has been determined, target fabrication should slot in to those dimensions.

The length of the capsules are different from several centimeters to full core height of 1.2 meters. They also different in diameter from 12 mm or less for the small irradiation positions to more than 120 mm for the larger irradiation positions. Then, the capsule will fit inside a basket as shown in Figure 2.2. The capsules area unit typically contained in an irradiation basket that radially locates the capsules within the irradiation position and vertically positions them among the ATR core [3]. The target specimens are inserted into the ATR inside "experiment assemblies." The components of these assemblies are the targets, the capsule, and the basket. The capsule serves to provide a boundary to contain the target material and isolate it from the reactor primary coolant. The capsule is designed with an internal annulus generally filled with an inert gas such as helium or argon. The basket serves as the housing of the capsule and is designed to mate with the irradiation position in the reactor.

Table 2.1. Approximate number of specimen fit into ATR capsule positions

No.	Description							Specimen Size
	Position	Diameter of Position (mm)	Height Of Position (mm)	Max specimen width (mm)	Specimen length (mm)	Number of specimen fit the diameter of position	Total Specimens	
1	A	15.9	1219.2	6.77	13	≈ 3	≈ 276	
	B	22.2	1219.2	6.77	13	≈ 5	≈ 460	
2	A	15.9	1219.2	17.53	29.34	≈ 0.90	≈ 41	
	B	22.2	1219.2	17.53	29.34	≈ 1.27	≈ 88	
3	A	15.9	1219.2	19.93	50.72	≈ 0.80	≈ 19	
	B	22.2	1219.2	19.93	50.72	≈ 1	≈ 24	
4	A	15.9	1219.2	25.34	57.15	≈ 0.63	≈ 13	
	B	22.2	1219.2	25.34	57.15	≈ 0.87	≈ 18	
5	A	15.9	1219.2	33.61	63.14	= No fit	= No fit	
	B	22.2	1219.2	33.61	63.14	= No fit	= No fit	

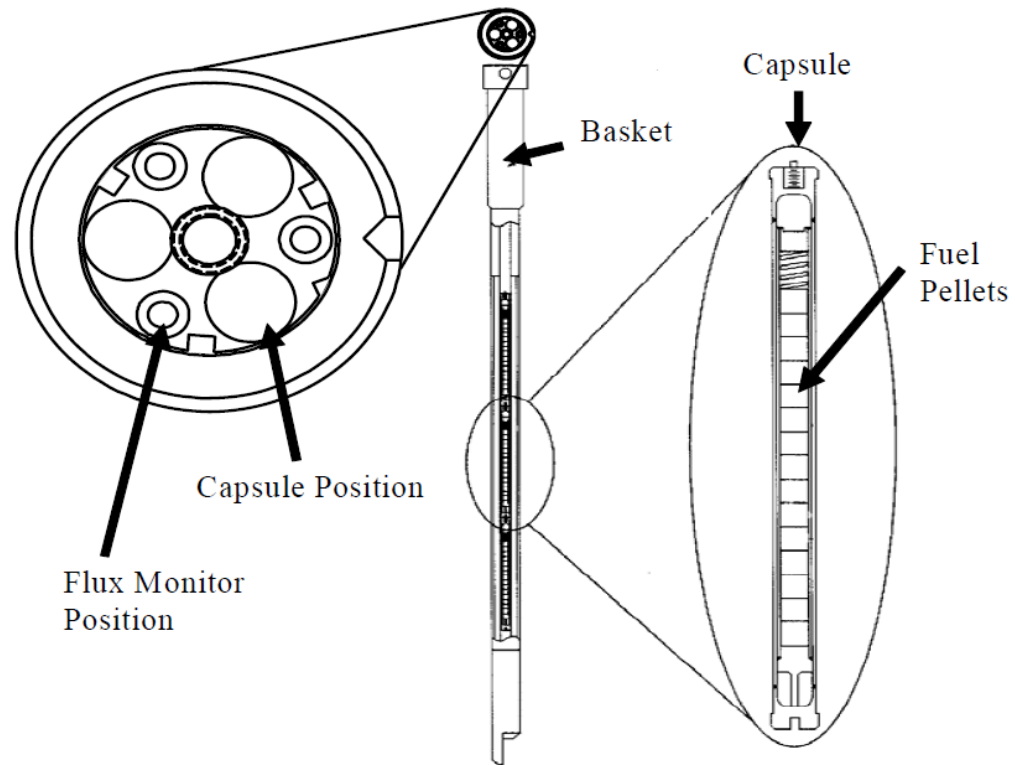


Figure 2.2. Capsule loaded in basket.

After experiment assemblies (target specimen, capsule and basket) have cooled and safe to handling and transport, the capsule is removed from the basket and placed inside Nuclear Regulatory Commission (NRC) container by ATR Canal Operations. The loading and transport to Post Irradiation Examination (PIE) facilities are conducted by INL and will be shipped to hot fuel examination facility (HFEEF). Because the specimens will be highly radioactive, all the work will be done in HFEEF facilities. Mechanical manipulators take the place of human hands, so it must be very careful about cutting open the capsule and removing the specimen without damaging the specimen.

### **3. LITERATURE REVIEW**

Relevant literature was found and surveyed in order to gain ideas of how to create method performing bending fatigue experiments and executing S-N curves for nuclear materials. The results are shown below followed by a brief summary of what was performed and how it can relate to our project.

#### **3.1. DEVELOPMENT OF MINI SPECIMEN BENDING FATIGUE SPECIMENS**

ASTM B593 standard used helps determine the capability of the material to resist cracks and other mechanical failures due to repeated use and strains. The results of the test are used to determine the effects on materials and give data on selecting proper copper alloy materials. The bending fatigue machine is a constant deflection, fixed cantilever machine. The specimens will be clamped at one end and will be deflected with a concentrated load. The test specimens are mounted to the machine and flex until failure, and the data is then recorded. It is important that each specimen is properly cut to ensure good test results. Improper or bad workmanship on the test specimens will result in unsatisfactory results. We must ensure that our testing method is similar to that of this paper so that we can receive valuable data. This is an official testing method so we must know what guidelines apply to our testing and follow them [4].

C. M. Obermark and R. S. Mishra were used miniature size specimens for fatigue test of a 7075-T6 copper-alloy. The small size of the specimens is commonly used in nuclear industry for evaluating material properties. The specimens were hybrids of the Krouse-type bending specimens. With the small size, axial loads are the only measurements taken. Each specimen was cut down to 1 mm thickness and left with the milled edges for the experiment. Using a crank driven DC motor, each of the specimens was linearly bent until failure. Specimen failure was sensed by snap-action switch upon breakage. Four stresses were taken at levels of 190, 220, 240, and 300 MPa using high cycle fatigue testing to develop S-N curves. The results from this experiment will help us

by being an example of how to analyze our data. The overall process of this experiment is very good and can serve as an example for our work[5].

### **3.2. DESIGN OF BENDING FATIGUE MACHINE**

Cao, H., Yang, P., & Bao, B [4,6] were created a machine to study the bending fatigue of flexible electronics. A stepper motor was used to apply the load to the sample. To ensure that the load can be varied, a screw nut body was used. It is a similar mechanism to that of our machine. One feature of the machine is that it can count cycles and shut off when a sample has failed. Unfortunately, the failure criterion for an electronic sample is different than that of a metal sample. The actual functioning capability of the electronic sample is taken into consideration for its failure. This means that I cannot apply its method for stopping the motor to my machine. However, this design does use an infrared counter to determine the number of cycles. Ultimately, this paper detailed how they created a bending fatigue machine that could be operated unattended. Although its method for stopping the testing is not applicable to our technique, we can keep it mind that this design favors an infrared sensor in order to measure cycles. In addition, if we experience difficulty with our mechanism for varying our load, we can consider the mechanism used by this design, which the authors say has “smooth motion, high precision, and a large reduction ratio.” In addition, this paper supports a brushless stepper motor because it controls speed well and has good position accuracy. We can use this paper for ideas of refining or improving the loading mechanism.

### **3.3. FATIGUE RESPONSE FOR IRRADIATED REACTOR MATERIALS**

G. R. R. and B. A. Chin [1] were irradiated and tested miniature specimens of stainless steel 316. A miniature rectangular specimen is used with “dimensions of 30.1625x4.7625x.762 mm with a gauge length of 6.35 mm.” Another specimen used for bending fatigue is a miniature disk with a diameter of 3 mm. The gauge is 1.5 mm formed by two radii and has a thickness of 0.254 mm. The first specimen was made by milling while the other by electrical discharge machining prior to electropolishing. The materials were tested using a cantilever flexural fatigue machine. The rectangular and disk specimens were tested at various temperatures. The rectangular followed a trend

while the disk seemed to have a worse fatigue life at higher temperatures. The method for testing using a bending fatigue machine was very successful giving great results for each specimen. Differing results depends on the geometry and size of the specimen. This paper reinforces the fact that we must keep a consistent shape to my specimen. Obviously it will not drastically change, but the process of making the specimen must be consistent so that our dimensions do not change. Additionally, this paper shows that miniature fatigue specimens give good fatigue data.

M. Li and J. Stubbins [7] were studied the fatigue lives for AISI 316 stainless steel and HT9 in the unirradiated and irradiated conditions at various temperatures. There is very little influence of irradiation on the fatigue life at low temperature. At a very high temperature, the fatigue life decreases following irradiation. Only limited data are available for the fatigue response of this class of materials following irradiation. There is very little influence of irradiation on the fatigue life at low temperature for HT9. At a very high temperature, the fatigue life decreases following irradiation. Figure 3.1 shows the fatigue responses of MANET with HT9 before and after irradiation.

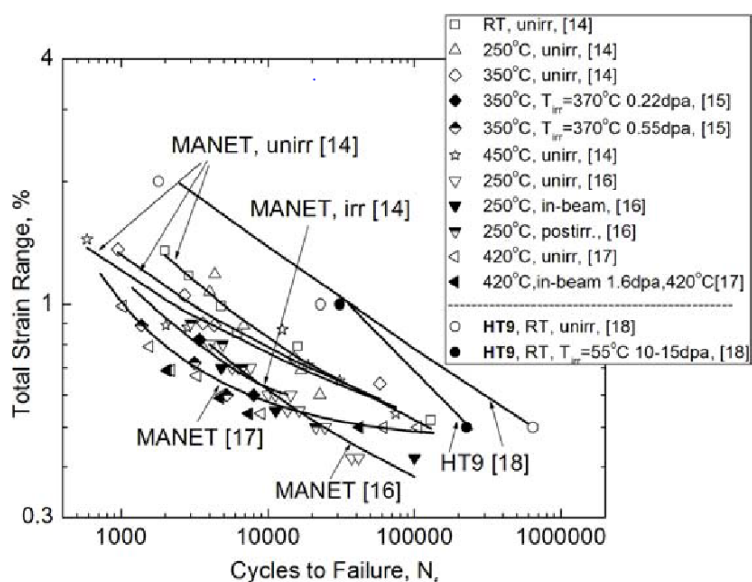


Figure 3.1. Comparison of the fatigue lives for ferritic/martensitic steels (MANET and HT9) in the unirradiated and irradiated conditions as a function of temperature.



### 3.4. INFLUENCE OF THERMAL AGING ON FATIGUE LIFE

Raymond et al [8] was performed thermal aging experiment at 600 C° and 700 C° and created the S-N curve with stress ratio (R= -1) at frequency 90 Hz for Incoloy alloy MA956. It can be seen that from Figure 3.2, the stress of specimens aged with 600 C° is slightly higher than specimens aged with 700 C°.

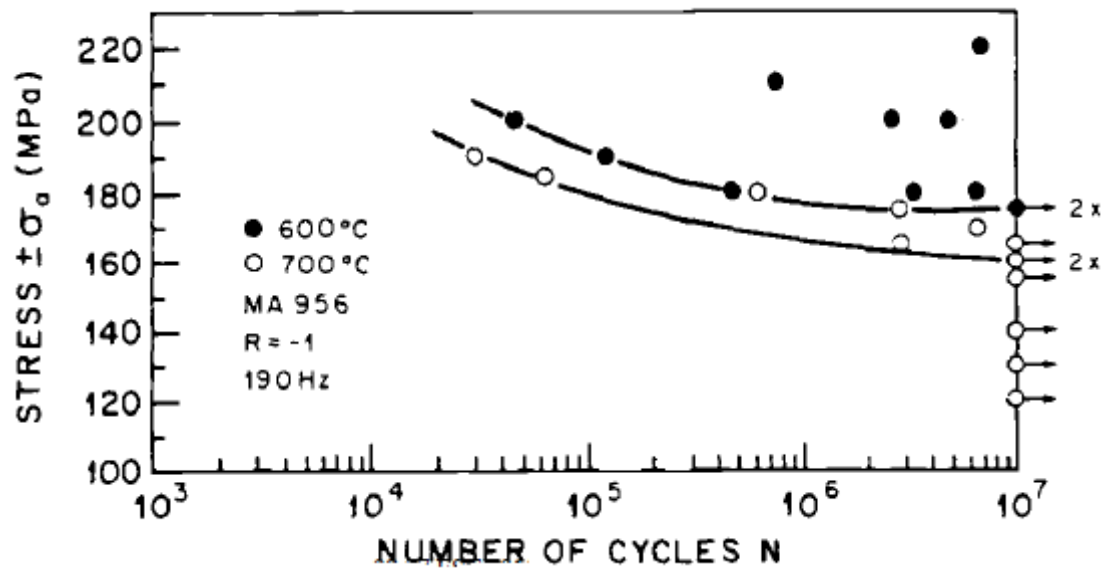


Figure 3.2. High Cycle fatigue strength of Incoloy alloy MA956.

This paper demonstrates the profile of S-N curve and the influence of the thermal aging on the fatigue life for Incoloy alloy MA956.

## **4. EXPERIMENTAL SETUP AND MEASUREMENT TECHNIQUES**

### **4.1.FATIGUE MACHINE**

**4.1.1. LFE-150 Testing Machine.** The LFE-150 testing machine is a universal unit designed for testing a component, device or specimen requiring oscillatory or reciprocating actuation as shown in Figure 4.1. The machine provides constant amplitude cyclic motion at a preset stroke, adjustable from zero to two inches. It is compact, bench mounted and consists of a rigid welded frame, variable speed motor and control, variable throw crank connected to a reciprocating platen, a failure cutoff circuit and a predetermining cycle counter. The basic load capacity of the machine is 150 pounds at the reciprocating platen. The reciprocating platen stroke is infinitely adjustable from 0 to 2 inches. The stroke is changed by adjusting the crank eccentricity through the access opening in the end plate of the machine. Four clamp screws are loosened and the crank adjustable pinion gear rotated to obtain the desired total stroke as initiated on the etched graduation on the crank face [7].

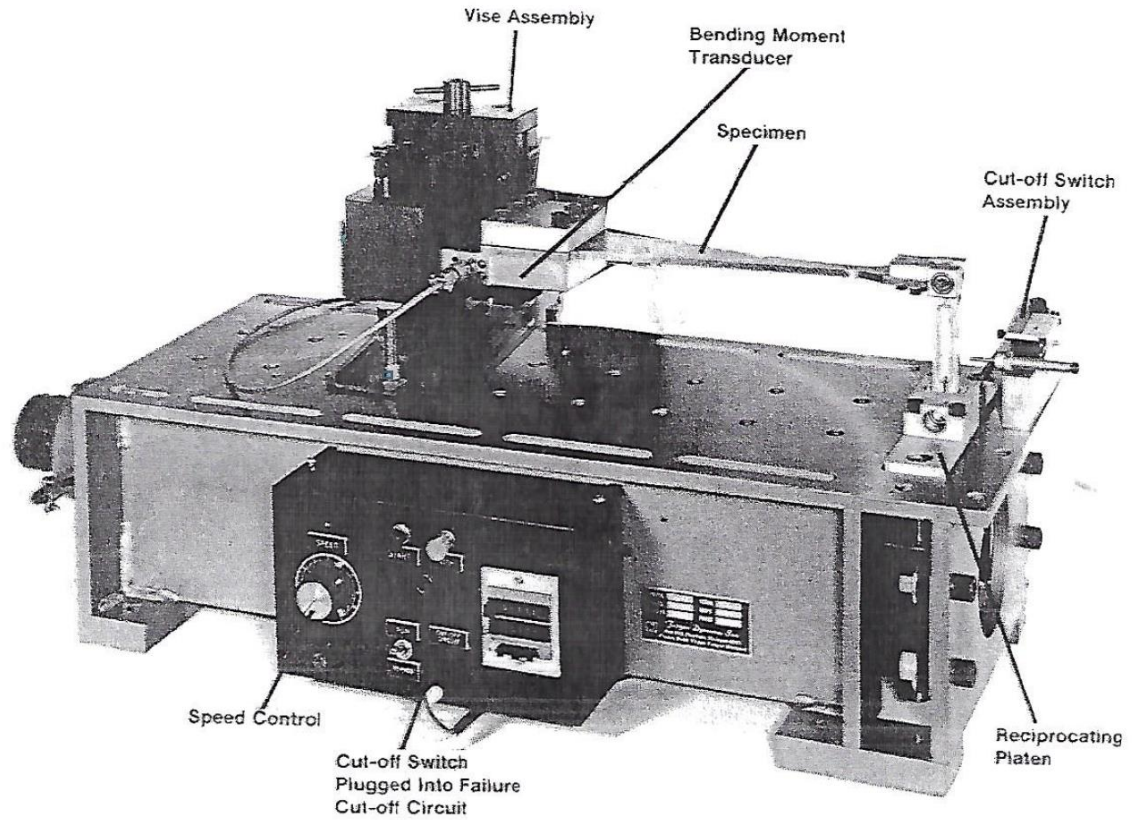


Figure 4.1. LFE-150.

In order to test mini specimen, the LFE-150 was modified to fit small specimen. The adapters were designed as shown in Figure 4.2 & 4.3.

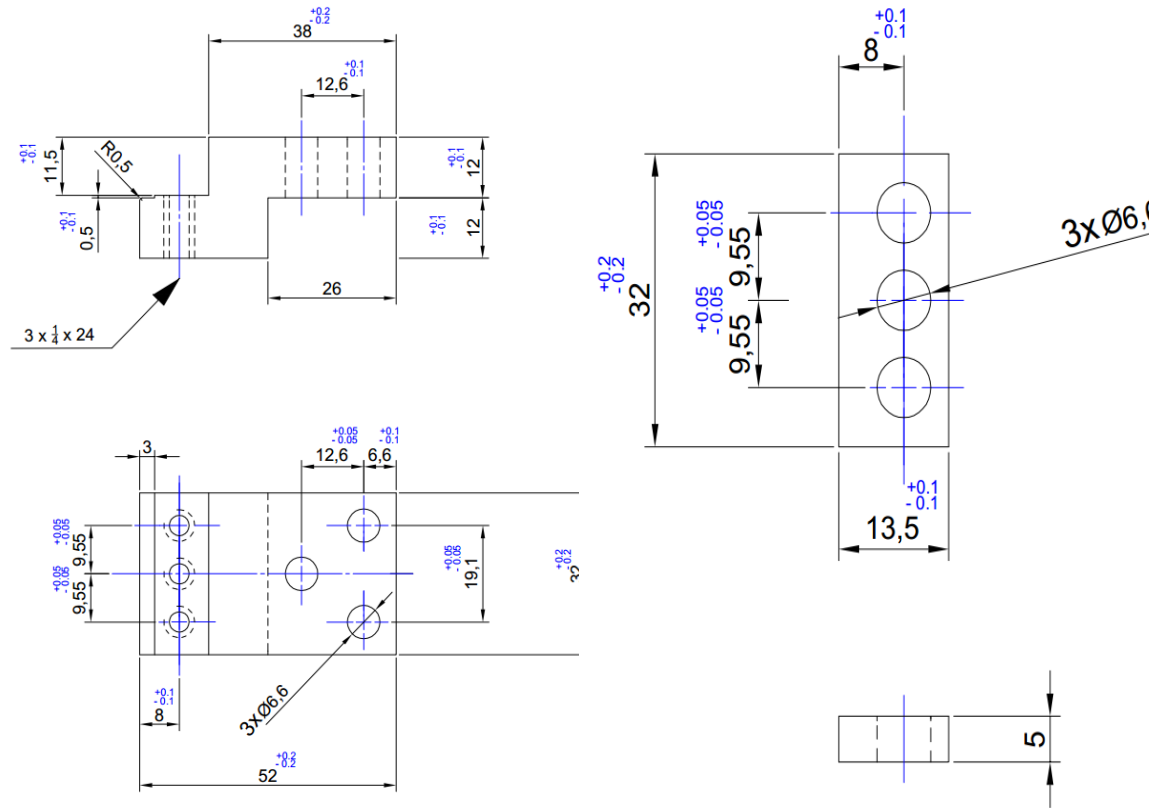


Figure 4.2. Schematic diagram of mini specimen adapters.

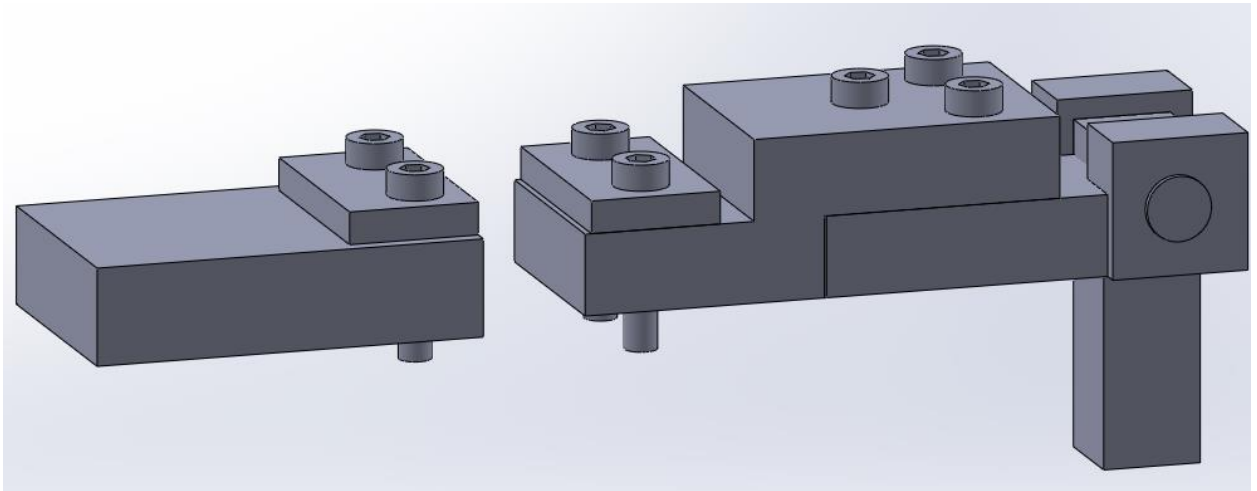


Figure 4.3. Schematic design of the mini specimen adapter.

**4.1.2. VSS-40M Variable Speed Miniature Sheet Specimen Fatigue Testing Machine.** The VSS-40H is designed for the flexural testing of sheet material under all ranges of stress. The machine subjects the specimen to a constant deflection amplitude cyclic deformation. Means are provided to use the test specimen as its own dynamometer. This feature permits setting the initial mean stress and stress range with the specimen in its actual test position. The machine is a compact, bench mounted unit consisting of a rigid welded frame, viable speed motor and control, adjustable bending deflection indicator and weight pan are included with machine shipped with no load cell. The connecting rod has a force capacity of 40 pounds and a maximum stroke of 2 inches. The unit measures 17"X15.3"X9.5" as shown in Figure 3.4.

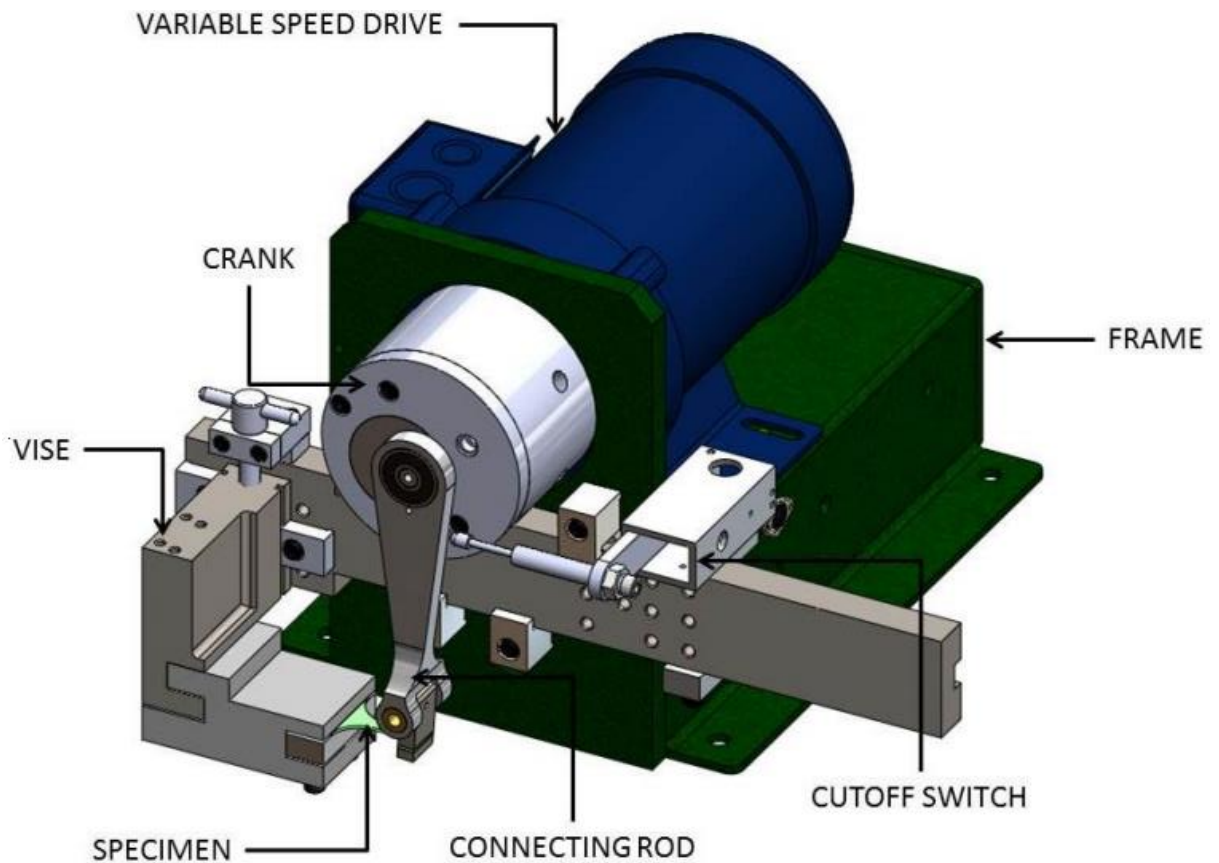


Figure 4.4. Diagram of the VSS-40H mini specimen Krouse bending fatigue equipment.

#### 4.2. MINI SPECIMEN (KROUSE-TYPE) DESIGN

The Krouse -type mini-specimen design is useful because the stress is uniform all the whole area of specimen. The specimen design was very precise and created by using a CNC machine, water jet and EDM because a defined and accurate shape would be much easier analyzed. The specimen preparation for fatigue analysis was carried out according the dimensions recommended by the ASTM standard B593 [9] and machined with the EDM. The EDM machining does not introduce any stresses into the material and no side pressures are created.

### 4.3. MEASUREMENT TECHNIQUES

In order to measure the stress for each specimen, we need to calculate the deflection and the specimens' dimensions. The designs of LFE-150 and VSS-40H fatigue machine have no way of mounting a load cell to the unit to apply the force. The LFE-150 unit has a bending moment load cell and would measure the force on the samples in lbs of bending moment. The issue with testing mini-specimen is that this moment is extremely low, causing the manufacturing of this load cell to be extremely difficult. We have had a much easier time dialing in deflection and our results have been extremely consistent. A digital gauge (with a precision of  $\pm 3.048 \mu\text{m}$ ) was used to measure deflection simultaneously for the specimen and the reciprocating arm. The contact point tip of the digital gauge was placed on the top of the specimen to measure the deflection in mm. The specimens' dimensions were measured using a digital caliper (with a precision of  $\pm 25.4 \mu\text{m}$ ).

## PAPER

### I. AN EXPERIMENTAL STUDY ON BENDING FATIGUE TEST WITH A KROUSE - TYPE FATIGUE SPECIMEN

Ahmed S. Haidyrah<sup>1</sup>, Carlos H. Castaño<sup>1</sup> and Joseph W. Newkirk<sup>2</sup>

<sup>1</sup>Nuclear Engineering, Missouri University of Science & Technology, 224 Fulton Hall, Rolla, MO, USA 65401

<sup>2</sup>Materials Science & Engineering, Missouri University of Science & Technology, 282 McNutt Hall, Rolla, MO, USA 65401

#### INTRODUCTION

Comprehension of fatigue property of various materials is of significant importance to success of both existing and future nuclear systems. This knowledge can be used to predict behavior of a reactor under oscillating load conditions. An S-N curve was used to determine fatigue properties of a material. The material under examination is repeatedly bent until it fails to take the stress. The number of cycles before the material broke is recorded and plotted against the bending stress. The Krouse-type design utilized in this study is similar to a standard specimen with respect to geometry though it is smaller in size [1]. The ASTM B593 standard is used to test the mini-specimens fatigue properties [2]. A LEF-150 bending fatigue machine was modified to generate the S-N curve of the stainless steel 304 material, which is typically used in the primary piping of light water nuclear reactors [3]. This machine provides a constant amplitude cyclic motion at a pre-set stroke adjustable from zero to two inches. The pre-set stroke produced a specimen deflection for calculating the stress.

#### SPECIMENS

The specimen shape and dimensions used in this study is shown in Figure 1. The specimen were modified from the dimensions recommended by the ASTM standard B593 [9]. The Krouse-type specimen was used and made of stainless steel 304, and machined with a using Computer Numerical Control (CNC). Straight line of the specimen as shown in Figure 2 makes an angle of 10° with the horizontal axis with the specimen clipped at the widest end of specimen. The bending is simulating by drawing two straight lines from a



point A where it is a point of application of force on the specimen along the edges intersect [5].

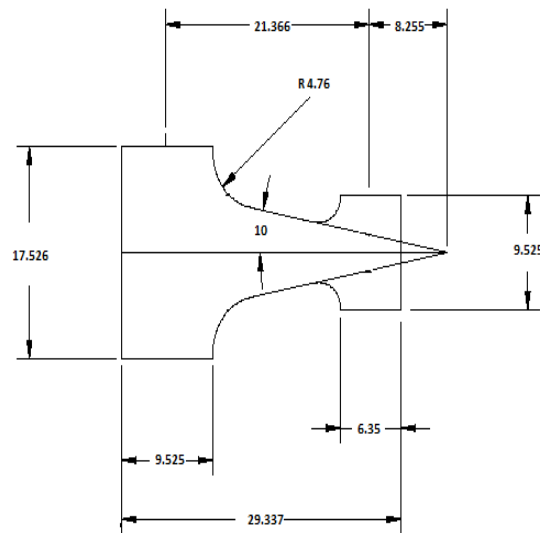


Figure 1. Sketch of the Krouse-type fatigue test specimen.

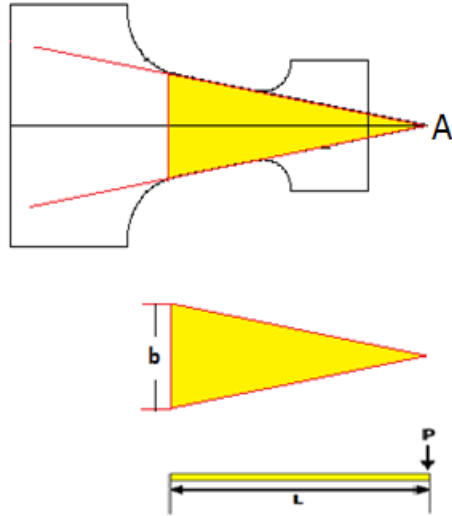


Figure 2. Schematic view of the wedge-shaped beam's length.

The maximum bending stress can be calculated with the following [5].

$$S = \frac{6PL}{bt^2} \quad (1)$$

where  $S$  is the desired bending stress in MPa ,  $L$  is the distance between the connecting pin (apex of triangle) and the point of stress (or the length of the wedge shaped beam in mm ), as depicted in Figure 2 [10].  $t$  is the specimen thickness in mm ,  $b$  is the width of the specimen at a distance  $L$  from the point of load application in mm and  $P$  is the force in Newton.  $P$  can be calculated as

$$P = \frac{St^2b}{6L} \quad (2)$$

The formula for the deflection of a triangular shape is [11].

$$D = \frac{SL^2}{Et} \quad (3)$$

where  $D$  is the deflection in mm, and  $E$  is the modulus of elasticity. This triangular shape is advantageous because the stress is constant along the length of the test section.

### **FATIGUE TEST MACHINE**

The LFE-150 testing machine was used to test the fabricated mini-specimen. In order to test mini specimen, the LFE-150 was modified to fit small specimen.

The LEF150 actuates the specimen by means of an eccentric cam. This cam allows the deflection to be changed and, thus, change the load on the specimen [11].

The test mini specimens were in as-milled condition and were in the same condition as-received. Each test specimen was supported by a cantilevered beam and was subjected to an alternating force at one end. The wide end was attached to a bed plate while the thin end was cyclically deflected. This end was tested for a high cycle fatigue life at various stresses until the fatigue crack had propagated through the specimen as shown in Figure 3.



Figure 3. The failure crack at the specimen's lower cross section area.

A digital gauge with a precise of  $\pm 3.048 \mu\text{m}$  was used to measure deflection, the contact point tip of the digital gauge was placed on the specimen, toward the small end as depicted in Figure 4.

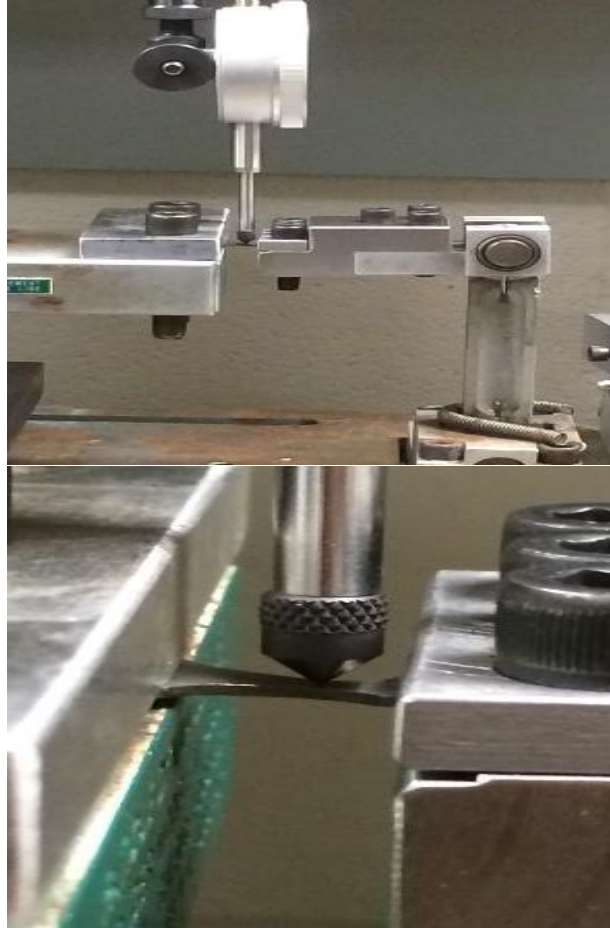


Figure 4. Measured deflection

The calculated stresses and number of cycles to failure shown in Figure 6.

### **ABAQUS MODEL**

The Krouse-type specimen for stainless steel 304 is simulated by using FEA code ABAQUS with the purpose of studying the maximum stress distribution and deflection. The maximum stress is shown in Figure 5. It can be seen clearly from Figure 6 that the simulated by ABAQUS is in accordance with the corresponding experimental specimen.

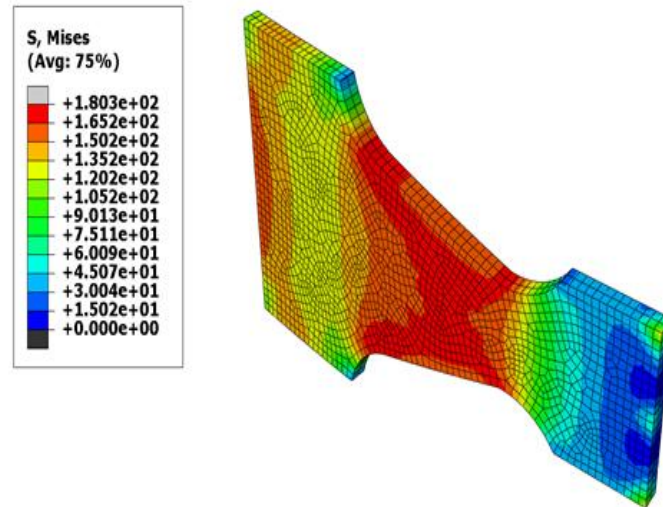


Figure 5. Stress distribution on the Krouse-type specimen model.

## RESULTS AND DISCUSSIONS

Typical S-N curve used for stainless steel 304 was used to compare the bending fatigue test results with the fatigue life test results. Because the machine did not have a force transducer, the length of the crank stroke was adjusted until the desired loads were obtained. A digital gauge (with a precision of  $\pm 25 \mu\text{m}$ ) was used to measure deflection simultaneously for the specimen and the reciprocating platen. The relationship between the specimen's deflection and the stroke range is linear. Thus as the stroke range increased, the deflection increased.

Each specimen was tested to failure. The data was recorded and plotted in terms of bending stress as a function of failure cycles. The specimen's geometry and material properties were used to calculate the stress [9]. Equation 2 was used to calculate the bending stress. Figure 6 illustrates the relationship between stress and the number of cycles

for stainless steel 304. These results were compared to reference data for full size specimens obtained from NAS [12]. This comparison revealed that the stress range values for the Krouse-type specimens were lower than the accepted values. Therefore, the differing results were influenced by both the geometry and size of specimen [13].

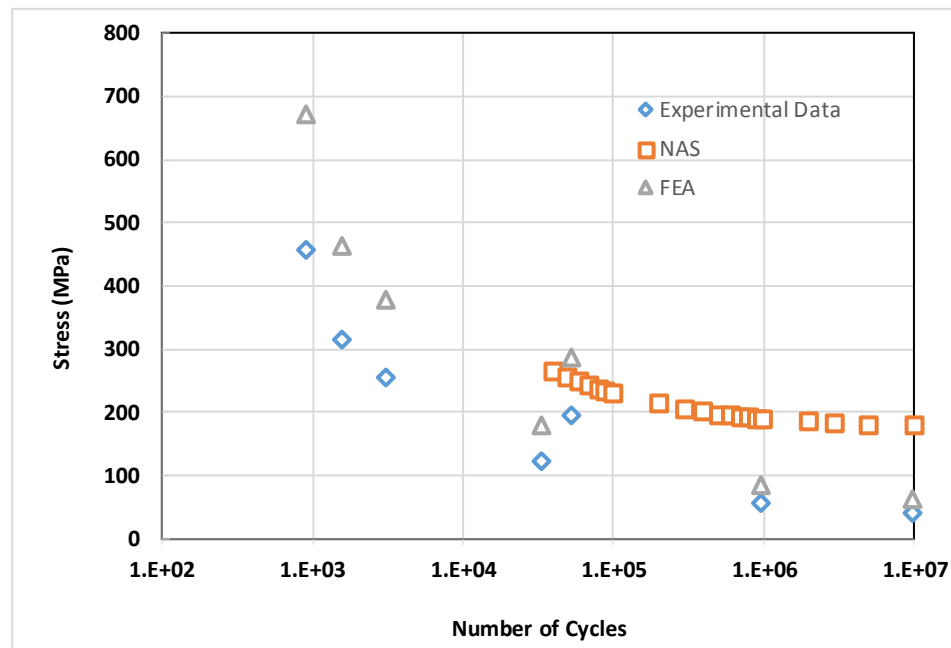


Figure 6. Results for the mini specimen compared with full size specimen results obtained for 304 stainless steel.

## CONCLUION

This experiment was carried out to verify the Krouse - type fatigue specimen for material under constant deflection. The fatigue test was modified using a bending fatigue machine as a method for testing. The results suggest a lower stress than that listed in accepted data. These results support the need for additional nuclear material testing and research.

Once we fix our testing technique post irradiation fatigue tests can be conducted very soon.

## ACKNOWLEDGMENTS

The first author's graduate program is funded by the King Abdul-Aziz City for Science & Technology, Saudi Arabia.

## REFERENCES

- [1] T. S. M. Corporation, "INCOLOY alloy INCOLOY ALLOY MA956."
- [2] J. R. Kennedy, S. Robertson, R. Soelberg, and C. Knight, "ATR NSUF," 2013.
- [3] R. V Furstenuau and S. B. Grover, "The Advanced Test Reactor Irradiation Facilities and Capabilities," in *PHYTRAI: First International Conference on Physics and Technology of Reactors and Applications*, 2007, p. 8.
- [4] G. R. R. and B. A. Chin, "Development of miniature bending fatigue specimens," *J. Nucl. Mater.*, vol. 181, pp. 2–4, 1991.
- [5] C. M. Obermark and R. S. Mishra, "Development of a Reversible Bending Fatigue Test Bed to Evaluate Bulk Properties Using Sub-Size Specimens."
- [6] H. W. Cao, P. Yang, and B. Z. Bao, "Design of Bending Fatigue Machine for Flexible Electronics," *Adv. Mater. Res.*, vol. 383–390, pp. 483–489, 2011.
- [7] M. Li and J. Stubbins, "Fatigue Response and Life Prediction of Selected Reactor Materials," *J. ASTM Int.*, vol. 1, no. 5, p. 11334, 2004.
- [8] R. C. Benn, R. Benn, and P. Relationships, "Microstructure and Property Relationships in Oxide Dispersion Strengthened Alloys," pp. 238–268, 2015.
- [9] ASTM, "Standard Test Method for Bending Fatigue Testing for Copper-Alloy Spring Materials," *Annu. B. ASTM Stand.*, vol. 96, pp. 3–7, 2009.
- [10] P. Gohil, H. N. Panchal, S. M. Sohail, and D. V Mahant, "Experimental and FEA Prediction of Fatigue Life in Sheet Metal ( IS 2062 ) Authors International Journal of Applied Research & Studies," *Int. J. Appl. Res. Stud.*, vol. II, no. I, pp. 1–8, 2013.

- [11] Fatigue Dynamics Inc., “Instruction Manual Model LFE-150 Variable Speed Life,Fatigue analysis.pdf.” Walled Lake ,MI 48390, p. 47.
- [12] North American Stainless, “Flat Products Stainless Steel Grade Sheet,” Ghent, KY 41045-9615.
- [13] G. R. R. and B. A. Chin, “Development of a Miniature-Disk Bending Fatigue Specimen,” *Am. Soc. Test. Mater.*, pp. 267–274, 1993.



## II. Characterization a Bending Fatigue Mini-Specimen Technique (Krouse-type) of Nuclear Materials

Ahmed S. Haidyrah<sup>1</sup>, Joseph W. Newkirk<sup>2</sup>, Carlos H. Castaño<sup>1</sup>

<sup>1</sup>Nuclear Engineering, Missouri University of Science & Technology, 224 Fulton Hall, Rolla, MO, USA 65401

<sup>2</sup>Materials Science & Engineering, Missouri University of Science & Technology, 282 McNutt Hall, Rolla, MO, USA 6540

**Keywords.** bending fatigue test, bending fatigue mini specimen, S-N curve, Krouse Specimen.

### Abstract

A bending fatigue mini-specimen (Krouse-type) was used to study the fatigue properties of nuclear materials for (SS304, HT9). The objective of this paper is to provide fatigue data for HT9 ferritic-martensitic steel and SS304 using a mini-specimen (Krouse-type) suitable for reactor irradiation studies. These mini-specimens are similar in design to that described in the ASTM B593 standard. A bending fatigue machine was modified to test the mini-specimen's dimensions. This study was conducted to evaluate the high cycle bending fatigue behavior of HT9 and SS304 and compare its bending properties with simulations conducted with the Abaqus FEA code. Other properties tensile strength and hardness tests were also conducted. The S-N fatigue results were affected by polishing of surface and bending fatigue reported values for HT9 were lower than typical S-N curve for SS304.

### Introduction

Fatigue is a material degradation developed under cyclic stress. Understanding the fatigue property of various materials is important to the success of both current and future nuclear systems. This understanding can be used to predict the behavior and lifetime of reactor components under oscillating load conditions. In a bending fatigue experiment the material under examination is repeatedly bent until failure occurs. The number of cycles before the material breaks is recorded and plotted against the bending stress. The Krouse-type design or cantilever flat sheet utilized in this study is similar in geometry to a

ASTM standard specimen though it is smaller in size [5]. The ASTM B593 [9] standard is used to test the mini-specimens fatigue properties. HT9 is one of the candidate materials for advanced nuclear reactors [14]. HT9 has an excellent thermal conductivity and irradiation resistance and has been considered for in-core applications of advanced nuclear reactors [3]. A specially modified LEF-150 bending fatigue machine was used to generate the S-N curve of the HT9. This machine provided a constant amplitude cyclic motion at an adjustable pre-set stroke adjustable from zero to two inches. The pre-set stroke produced a reliable specimen deflection for calculating the stress [11].

### **Specimens**

The specimen developed is a mini-specimen (Krouse-type) and is shown in Figure 1. The specimen was modified from the dimensions recommended by the ASTM standard B593 [2]. The Krouse-type specimen was used and machined with a using a water jet. The straight lines of the specimen as shown in Figure 2 makes an angle of  $26^\circ$  with the horizontal axis. The bending is also simulated by drawing two straight lines from a point of load where it is a point of application of force on the specimen along the edges intersect [15]. All specimens' dimensions were measured using a digital caliper (with a precision of  $\pm 25.4 \mu m$ ) and optical microscopy including an accuracy measurements as shown in Table 1.

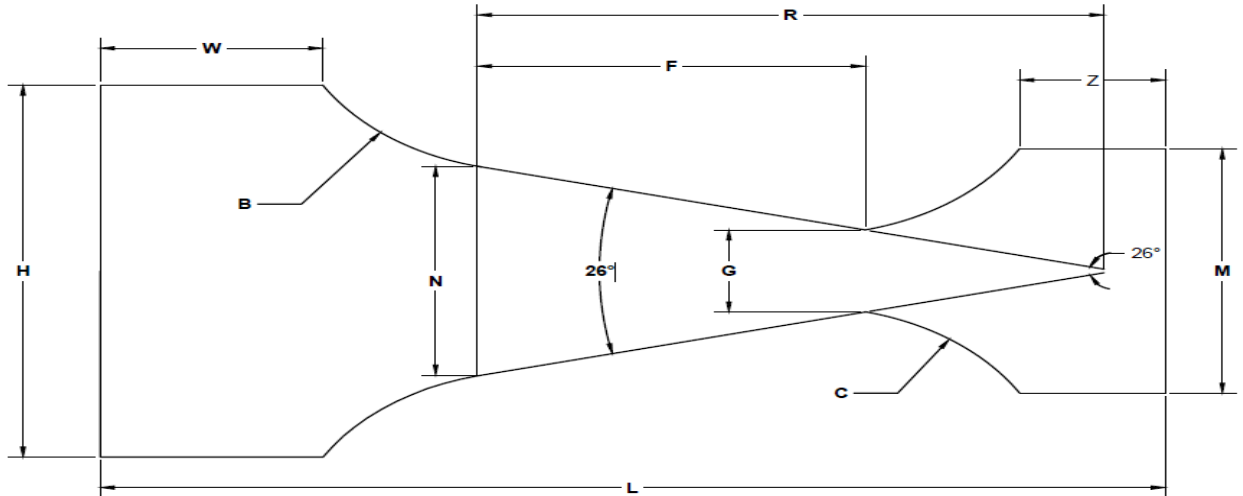


Figure 1. Sketch of the mini fatigue test specimen (all dimensions are in millimetres) [3].

Table 1. Mini Fatigue Test Specimen dimensions comparing with ASTM B593 Standard

Letter #	Description	ASTM B593 Standard specimen dimension, in [mm]	Mini fatigue test specimen (Krouse- type) dimension, mm
<b>F</b>	Gage length	-	<b>4.97 ±0. 1</b>
<b>H</b>	Width of grip section	1.38 in	<b>6.59 ±0. 3</b>
<b>M</b>	Width of grip section	0.75 in	<b>4.33 ±0. 1</b>
	Thickness	0.008 to 0.031 in (0.203 to 0.787 mm)	<b>1.09 ±0. 1</b>
<b>L</b>	Overall length	2.31 in	<b>13.67 ±0.1</b>
<b>G</b>	width of reduced section		<b>1.45 ±0. 1</b>
<b>W</b>	Length of grip section	0.75 in	<b>2.86±0. 1</b>
<b>Z</b>	Length of grip section	0.5 in	<b>1.87±0.1</b>
<b>C</b>	Radius of fillet, min	3/8 in	<b>3.18±0. 1</b>
<b>B</b>	Radius of fillet, min	3/8 in	<b>3.18±0. 1</b>
<b>R</b>	Distance between the connecting pin (apex of triangle) and the point of load	-	<b>8.04±0.1</b>
<b>N</b>	Width of the specimen at a distance R from the point of load application	-	<b>3.70±0.1</b>

The maximum bending stress can be calculated with the following equation.

$$S = \frac{DEt}{L^2} \quad (1)$$

where S is the desired bending stress in MPa, L is the distance between the connecting pin (apex of triangle) and the point of load in mm. The specimen thickness in mm is represented by t and D is the deflection in mm, and E is the modulus of elasticity. This value (P) can be calculated as

$$P = \frac{St^2b}{6L} \quad (2)$$

Where P is the force in Newton and the width of the specimen at a distance L from the point of load application in mm is represented by b.

The formula for the deflection of a triangular shape is [11].

$$D = \frac{SL^2}{Et} \quad (3)$$

where D is the deflection in mm, and E is the modulus of elasticity. This triangular shape is advantageous because the stress is constant along the length of the test section.

## **Experimental procedure**

### **Material and Specimen Preparation**

The samples were cut from HT9 rod. A diameter of the rod was 1.5 in. A thin cylinder of around 2 mm thickness was first cut from the rod via a band saw. This cylinder is milled by using a milling machine ensures flatness of the surface [16]. The HT9 plate was machined with a using water jet machine to generate mini specimens (Krouse-type) as shown in Figure 2.

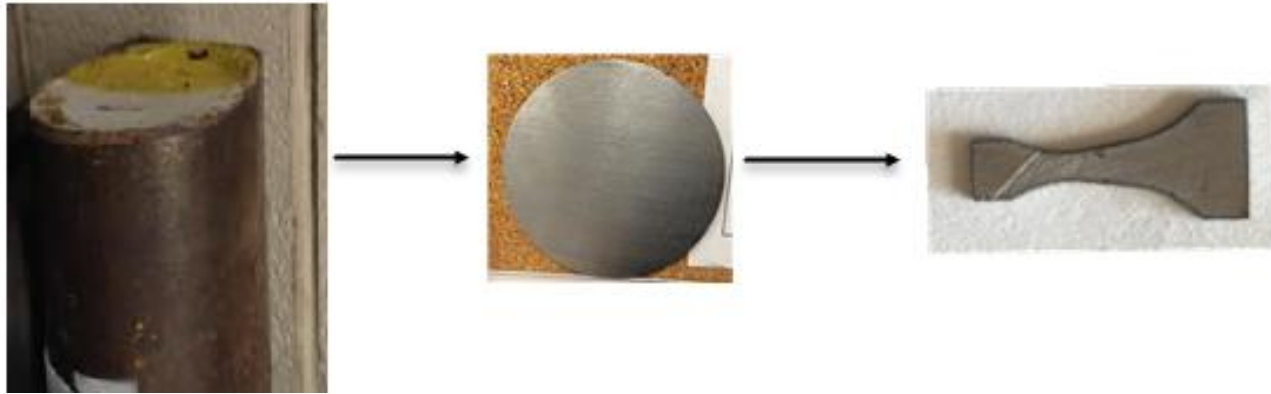


Figure 2. Steps prepared HT9 specimen.

Some specimens were kept in as-received condition, while the edges were kept in as milled condition as shown in Figure 3 and some specimens were polished with 320 SiC (Silicon Carbide) foil to remove 100  $\mu\text{m}$  from the surface, followed by using an MD largo disk to remove another 100  $\mu\text{m}$  thickness from the surface and using MD-chem disk for polishing with used Diapro 3  $\mu\text{m}$  and after that polished with MD-CHEM pad for 2 minutes and 30 second with OPS 0.4  $\mu\text{m}$  polishing, and thorough these steps rinsing water between each steps to eliminate particles from the last step that could cause new scratches.

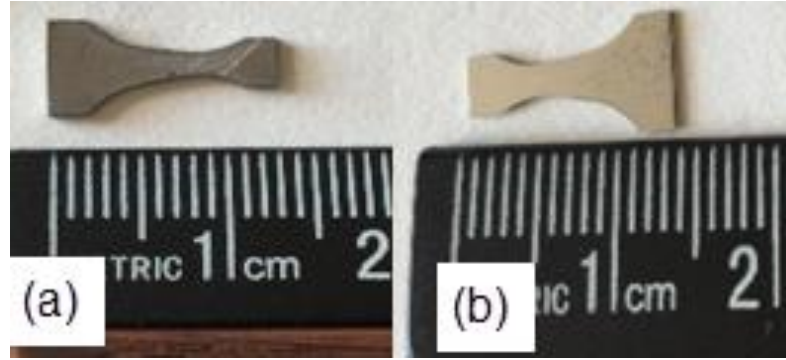


Figure 3. (a) As-Received mini specimen, (b) polished mini specimen.

### Micro hardness test

Two methods of measuring hardness were used in this study, hardness testing (Rockwell hardness test, HRB) and micro hardness testing (Vickers, HV). The hardness was measured at different locations as shown in Table 2.

Table 2. Hardness test (HRB) result for HT9

No.	Hardness (HRB)
1	99
2	100
3	96
4	96
5	98

The micro hardness was measured at different distances and with a 9.81 N indentation load. The mini specimen (Krouse-type) was cut, mounted, and polished. The hardness was then measured across the thickness of the sample.

## Tensile Test

Because fatigue always occurs under tensile loading and the fatigue increases as the tensile strength increases. The material with the residual tensile stresses will be the most susceptible to fatigue cracking. Fatigue is usually has a direct relationship with tensile, as tensile strength increases, the endurance limit increases[17]. It is important to know tensile, yield stress and ultimate tensile stress (UTS) for HT9 and compare with reference data. Tensile testing was conducted on mini-specimen .Grips for the mini specimens (Krouse-type) were designed and manufactured as shown in Figure 4. The grips were machined out of stainless steel alloy and threaded for easy attachment in the universal tester [16].

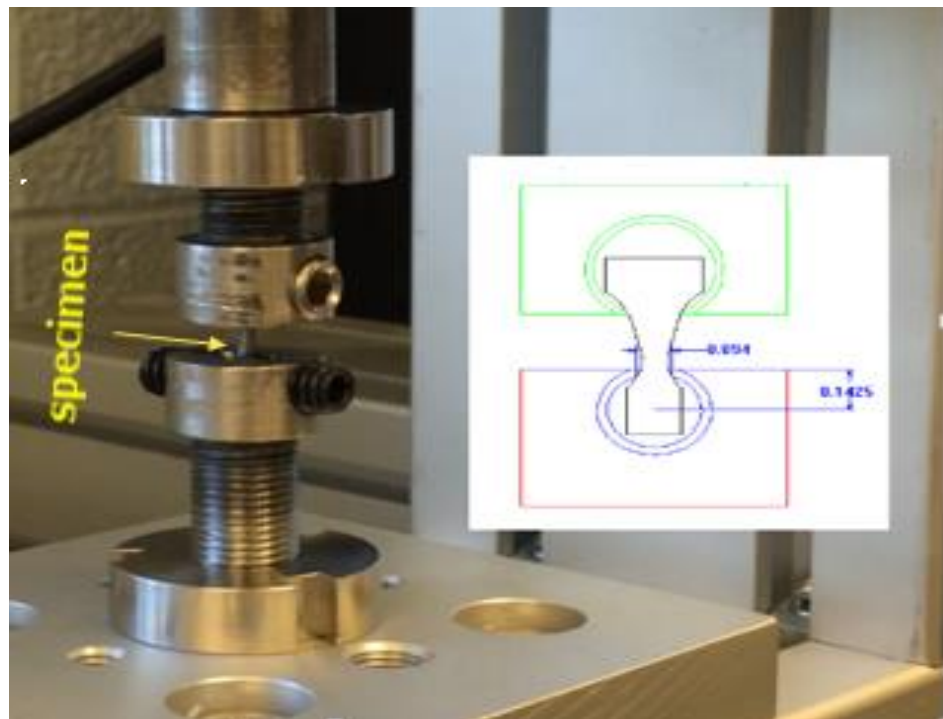


Figure 4. Testing set-up for tensile test for mini specimens.

### **Bending fatigue Test**

Each test specimen was loaded in the unit and set a deflection and run at a low speed to simulate the bending fatigue and subjected to an alternating deflection at one end. The wide end was attached to a bed plate while the thin end was cyclically deflected. This end was tested for a high cycle fatigue life at various stresses until the fatigue crack had propagated through the specimen pictured in Figure 8. The length of the crank stroke was adjusted until the desired loads were obtained. A digital gauge (with a precision of  $\pm 25 \mu\text{m}$ ) was used to measure deflection simultaneously for the specimen and the reciprocating arm. The relationship between the specimen's deflection and the stroke range is linear. Thus as the stroke range increases, the deflection increases. The digital indicator is denoted by the yellow arrow was used to measure the deflection and the contact point tip of the indicator was placed on the top of the specimen denoted by yellow arrow toward the small end depicted in Figure 5 [3]. Each specimens was tested to failure as shown in Figure 9.



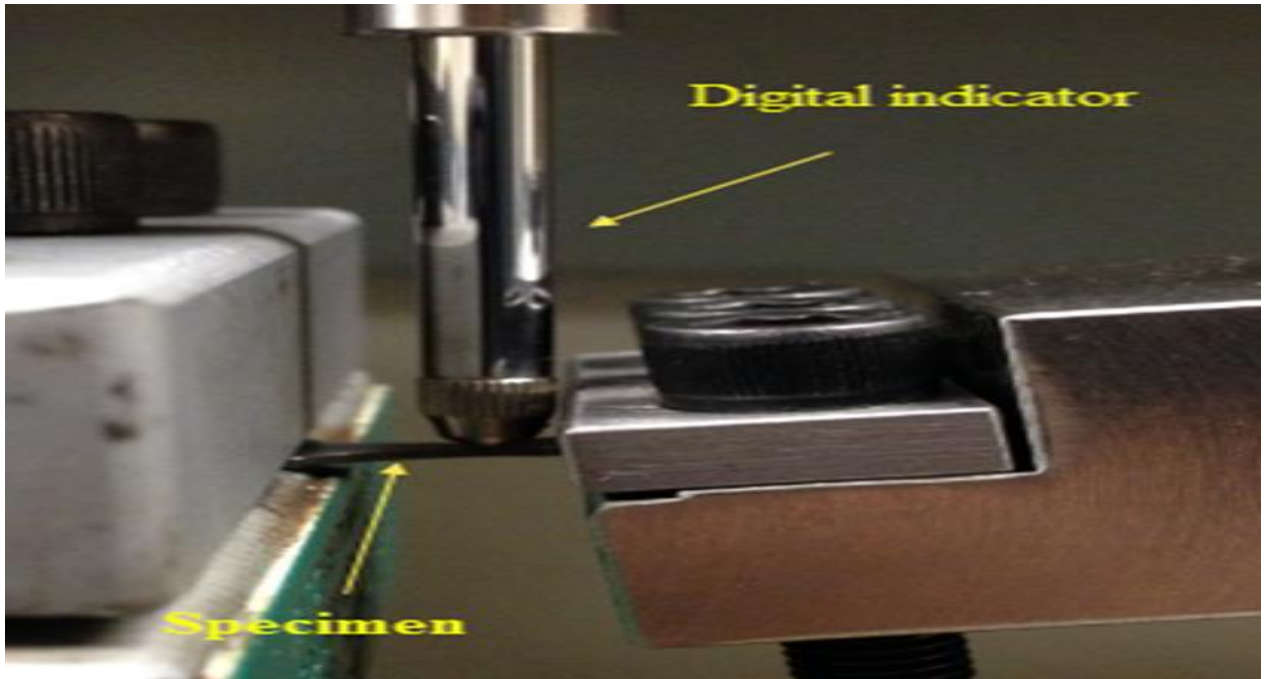


Figure 5. Testing set-up for bending fatigue for mini specimen.

### **FEA model**

A FEA code ABAQUS of this test was carried out with the Krouse -type specimen for HT9 using various load (from 1 N to 22 N). Figure 6 shows the stress distribution and the maximum stress for mini specimen with 1.29 mm thickness.

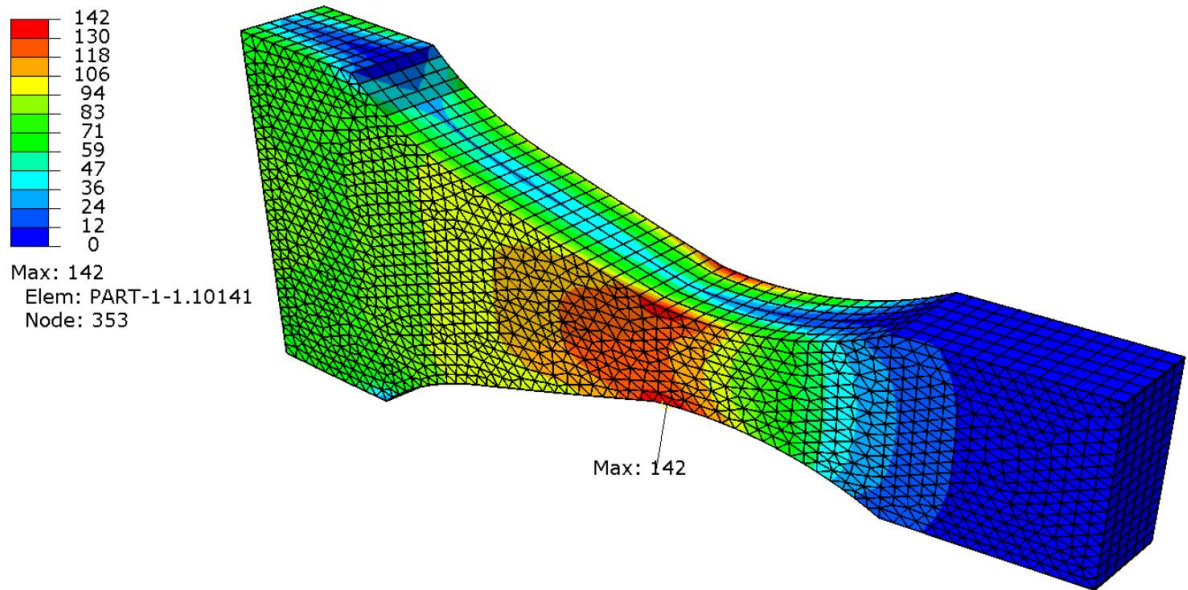


Figure 6. Stress results for the Krouse-type specimen model.

## Results and Discussion

Micro-hardness was measured in the polished surface of the specimen. The average hardness of the HT9 increased by approximately 1 HRB. The Vickers hardness measurements were made and the results were in Rockwell B scale. Figure 7 provides the measured hardness as a function of distance from the surface.

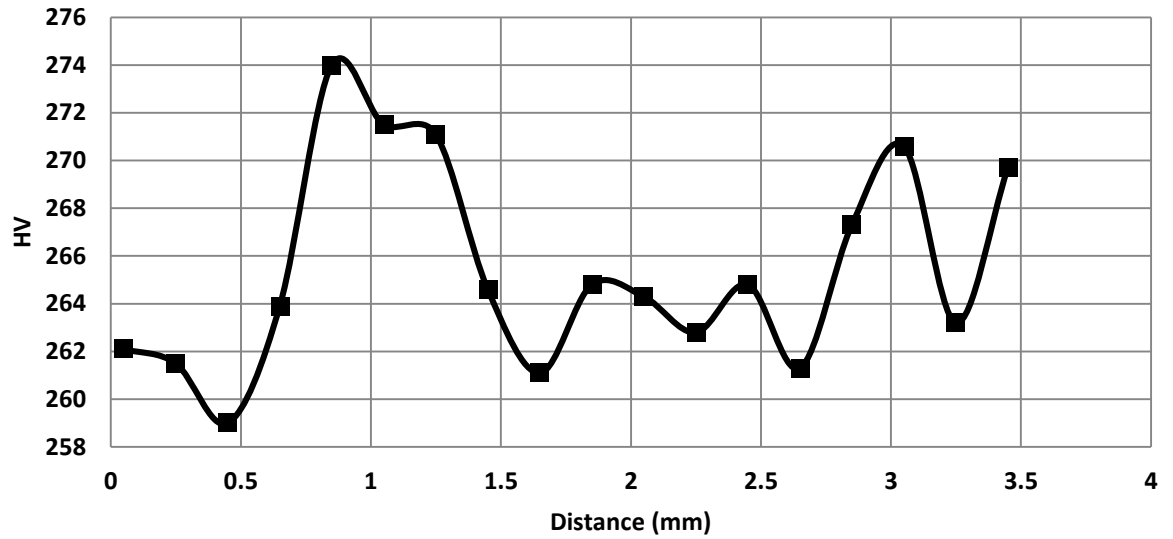


Figure 7. Measured Vicker hardness of polished HT9.

The tensile test with mini specimen was done with ultimate tensile stress, UTS (723.1 MPa) and reference data yield stress (768.076 MPa) and UTS (954.924 MPa). Scratches and cracks initiation that cause decreases in fatigue life and these scratches were removed by mechanical polishing as shown in Figure 8.

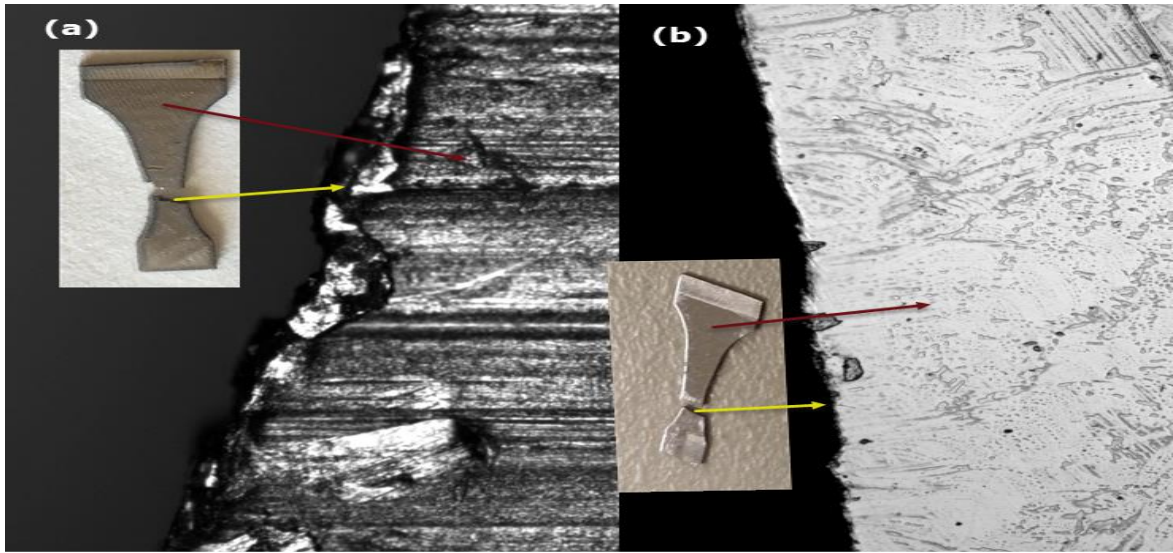


Figure 8. Optical micrographs of polished surface finish and ground surface finish for mini-specimen, (a) shows surface and expected post failure in the gage section condition of as received mini specimen, (b) shows polished surface finish and failure in the gage section.

The data was recorded and plotted in terms of bending stress as a function of failure cycles. The specimen's geometry and material properties were used to calculate the stress [2]. Equation 1 was used to calculate the bending stress. Figure 9 illustrates the relationship between stress and the number of cycles for HT9. The bending fatigue behavior of HT9 was determined on polished and as-received finishes as presented in Figure 9.

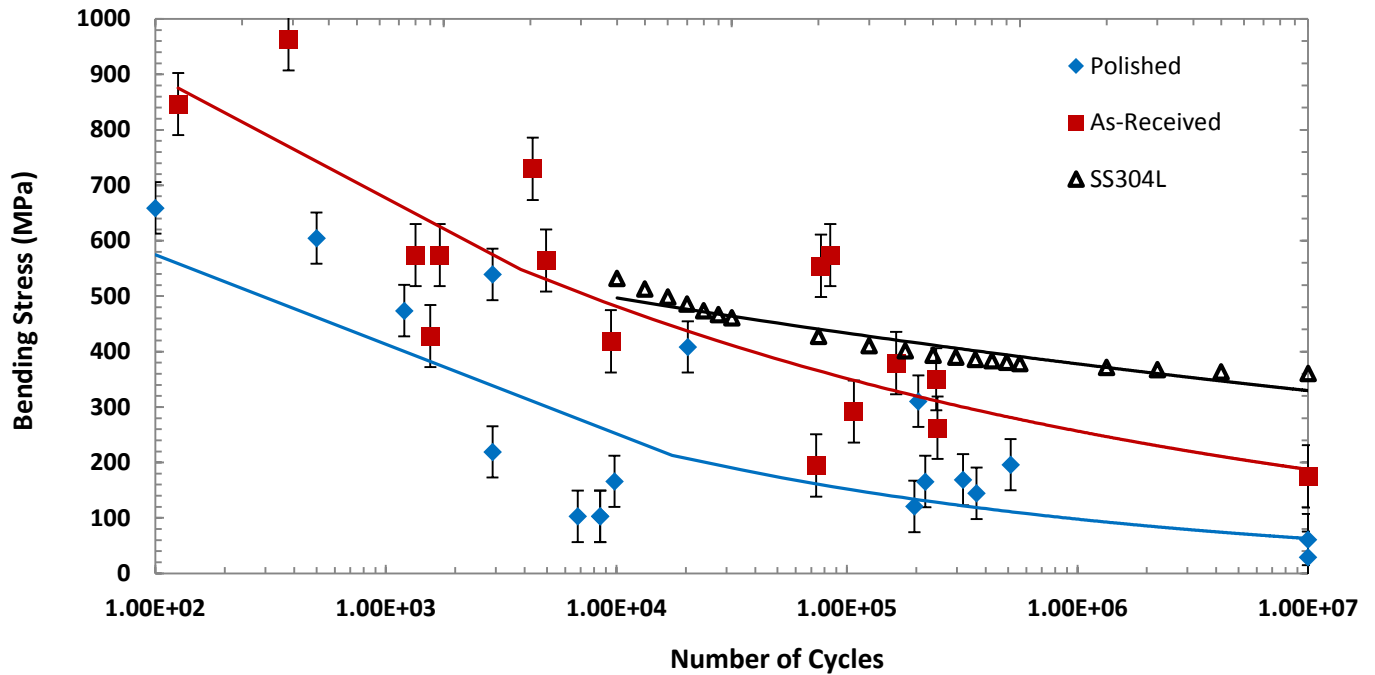


Figure 9. Results for as-received and polished surface finish mini specimen for HT9 compared with stainless steel 304.

The S-N curve used for stainless steel 304 [8] was used to compare the bending fatigue test results with fatigue life for HT9. The results is comparison exposed that the stress range values for the polished (Krouse-type) specimens were lower than as-received specimen and typical stainless steel 304 [12]. Therefore, the fatigue life was affected by the polish surface finish. This comparison revealed that the stress range values for the Krouse-type specimens were lower than the stainless steel 304. Therefore, the differing results were influenced by the geometry, surface finish and size of specimen.

## Conclusion

This work was done to verify a bending fatigue mini-specimen technique (Krouse-type) and create the S-N curve for HT9 under constant deflection. The measured fatigue life was lower than that listed in accepted data for 304 stainless steel for polished mini specimens. While the fatigue results were affected by the polishing of the surface finish,

the fatigue results were too spread to obtain good S-N curves. We are planning to prepare new specimens with higher volumes to try to reduce surface effects and obtain a more reliable fatigue measurements suitable for mini-specimens. The primary fracture surface of the mini specimens will be analyzed by scanning electron microscopy (SEM) to determine the level and morphology of failure for further work. These results indicate the need for additional material testing and substantial further research is required.

## References

- [1] T. S. M. Corporation, "INCOLOY alloy INCOLOY ALLOY MA956."
- [2] J. R. Kennedy, S. Robertson, R. Soelberg, and C. Knight, "ATR NSUF," 2013.
- [3] R. V Furstenuau and S. B. Grover, "The Advanced Test Reactor Irradiation Facilities and Capabilities," in *PHYTRAI: First International Conference on Physics and Technology of Reactors and Applications*, 2007, p. 8.
- [4] G. R. R. and B. A. Chin, "Development of miniature bending fatigue specimens," *J. Nucl. Mater.*, vol. 181, pp. 2–4, 1991.
- [5] C. M. Obermark and R. S. Mishra, "Development of a Reversible Bending Fatigue Test Bed to Evaluate Bulk Properties Using Sub-Size Specimens."
- [6] H. W. Cao, P. Yang, and B. Z. Bao, "Design of Bending Fatigue Machine for Flexible Electronics," *Adv. Mater. Res.*, vol. 383–390, pp. 483–489, 2011.
- [7] M. Li and J. Stubbins, "Fatigue Response and Life Prediction of Selected Reactor Materials," *J. ASTM Int.*, vol. 1, no. 5, p. 11334, 2004.
- [8] R. C. Benn, R. Benn, and P. Relationships, "Microstructure and Property Relationships in Oxide Dispersion Strengthened Alloys," pp. 238–268, 2015.
- [9] ASTM, "Standard Test Method for Bending Fatigue Testing for Copper-Alloy Spring Materials," *Annu. B. ASTM Stand.*, vol. 96, pp. 3–7, 2009.
- [10] P. Gohil, H. N. Panchal, S. M. Sohail, and D. V Mahant, "Experimental and FEA Prediction of Fatigue Life in Sheet Metal ( IS 2062 ) Authors International Journal of Applied Research & Studies," *Int. J. Appl. Res. Stud.*, vol. II, no. I, pp. 1–8, 2013.

- [11] Fatigue Dynamics Inc., “Instruction Manual Model LFE-150 Variable Speed Life,Fatigue analysis.pdf.” Walled Lake ,MI 48390, p. 47.
- [12] North American Stainless, “Flat Products Stainless Steel Grade Sheet,” Ghent, KY 41045-9615.

### III. Weibull Statistical analysis of Krouse -type bending fatigue in nuclear materials of HT9

Ahmed S. Haidyrah<sup>1</sup>, Joseph W. Newkirk<sup>2</sup>, Carlos H. Castaño<sup>1\*</sup>

<sup>1</sup>Nuclear Engineering, Missouri University of Science & Technology, 224 Fulton Hall, Rolla, MO, USA 65401

<sup>2</sup>Materials Science & Engineering, Missouri University of Science & Technology, 282 McNutt Hall, Rolla, MO, USA 6540

**Keywords.** Bending fatigue test, bending fatigue mini specimen, S-N curve, Krouse, Weibull distribution, mean life, Minitab 17.

#### ABSTRACT

A bending fatigue mini-specimen (Krouse-type) was used to study the fatigue properties of nuclear materials. The objective of this paper is to study fatigue for HT9 ferritic-martensitic steel using a mini-specimen (Krouse-type) suitable for reactor irradiation studies. These mini-specimens are similar in design (but smaller) to those described in the ASTM B593 standard. The mini specimen was machined by waterjet and tested as-received. The bending fatigue machine was modified to test the mini-specimen with a specially designed adapter. The cycle bending fatigue behavior of HT9 was studied under constant deflection. The finite element model code ABAQUS was used to estimate the stress in the bent mini specimen. The S-N curve was created and mean fatigue life was analyzed using mean fatigue life. In this study, the Weibull function was predicted probably for high stress to low stress at 563, 310 and 265 MPa. The commercial software Minitab 17 was used to calculate the distribution of fatigue life under different stress levels. The simulation results are compared with experimental data for HT9. The stress obtained experimentally was slightly higher than the calculated by simulations. We have used 2 and 3- parameters Weibull analysis to introduce the probability of failure. The plots indicated that the 3- parameter Weibull distribution fits the data well.

---

\* Corresponding author. Tel:+1 (573) 341-676

E-mail address: Email: [castanoc@mst.edu](mailto:castanoc@mst.edu) (Carlos H. Castaño)



## 1. Introduction

Understanding fatigue of materials is important to both current and future nuclear systems. This understanding can be used to predict the behavior and lifetime of reactor components under oscillating load conditions. Fatigue is becoming more important as nuclear systems age [1]. In a bending fatigue experiment the material under examination is repeatedly bent until failure occurs. Fatigue life before the material breaks is recorded and plotted against bending stress. The Krouse-type design or cantilever flat sheet utilized in this study is similar in geometry to an ASTM standard specimen though it is smaller in size [2]. The ASTM B593 [3] standard is used to test the mini-specimens fatigue properties. HT9 is one of the candidate materials for advanced nuclear reactors [4]. HT9 has an excellent thermal conductivity and irradiation resistance and has been considered for in-core applications of advanced nuclear reactors [3]. In this study, the FEA code ABAQUS was used to verify the area of maximum stress on the specimen. The Weibull distribution function has been used for the analysis of fatigue scattering problems because of its excellent applicability and accuracy, although, it needs a lot of experimental data. The Weibull distribution is examined to determine how well or bad the data fit a straight line. In some cases the bad fit may relate to the quality of the data or behavior of the failure [5].

## 2. Experimental procedure

### 2.1. Specimens

The specimen used is a mini-specimen (Krouse-type) as shown in Fig. 1. The specimen was modified from the dimensions recommended by the ASTM standard B593 [2]. The Krouse-type specimen was machined with waterjet. The straight lines of the specimen as shown in Fig.1 make an angle of  $26^\circ$  with the horizontal axis. The bending is done by applying force at the point where two straight lines along the specimen straight edges intersect (apex of triangle in Fig. 1) [6]. All specimens' dimensions were measured using a digital caliper and/or optical microscopy. Measurements of the specimen including tolerances are shown in Table 1.

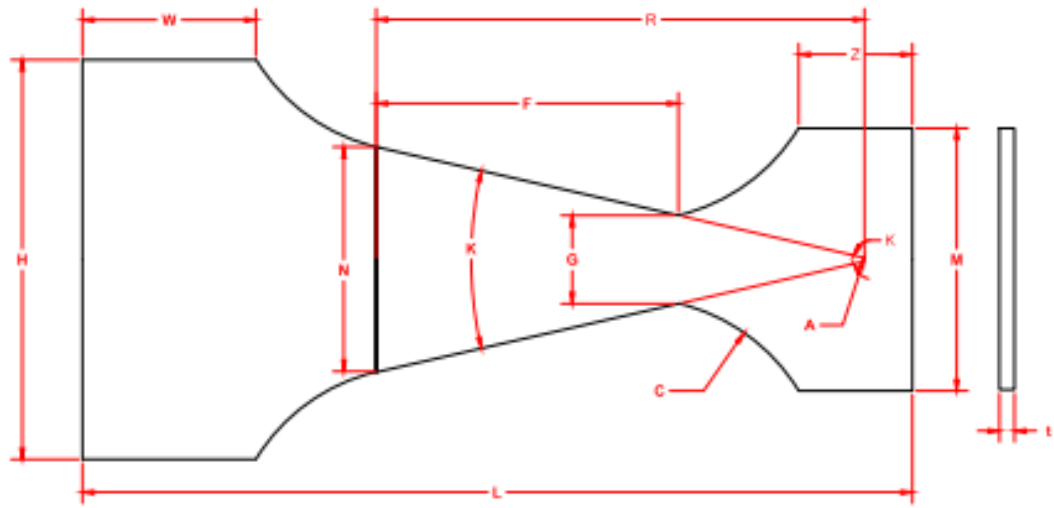


**Fig. 1.** Sketch of the mini fatigue test specimen (all dimensions are in millimeters) [3].

**Table 1**  
Mini Fatigue Test Specimen dimensions comparing with ASTM B593 Standard.

	Description	ASTM B593 Standard specimen dimension, in [mm]	Mini fatigue test specimen (Krouse-type) dimension, mm
<b>F</b>	Length of test region	-	<b>4.97 ±0. 1</b>
<b>H</b>	Width of grip section 1	1.38 in(35.052mm)	<b>6.59 ±0. 2</b>
<b>M</b>	Width of grip section 2	0.75 in(19.05 mm)	<b>4.33 ±0. 1</b>
<b>t</b>	Thickness	0.008 to 0.031 in (0.203 to 0.787 mm)	<b>1.09 ±0. 01</b>
<b>L</b>	Overall length	2.31 in(58.674 mm)	<b>13.67 ±0.01</b>
<b>G</b>	width of narrowest section	-	<b>1.45 ±0. 2</b>
<b>W</b>	Length of grip section 1	0.75 in(19.05 mm)	<b>2.86±0. 1</b>
<b>Z</b>	Length of grip section 2	0.5 in(12.7 mm)	<b>1.87±0.1</b>
<b>C</b>	Radius of fillet 2	3/8 in(9.525 mm)	<b>3.18±0. 1</b>
<b>B</b>	Radius of fillet 1	3/8 in(9.525 mm)	<b>3.18±0. 1</b>
<b>R</b>	Distance between the connecting pin (apex of triangle) and the width N of the specimen	-	<b>8.04±0.29</b>
<b>N</b>	Width of the specimen at a distance R from the point of load application	-	<b>3.70±0.29</b>
<b>K</b>	Angle make from two straight lines of the specimen with horizontal axis	-	<b>26°</b>

## 2.2. Material and specimen preparation.

The chemical composition and mechanical properties of HT9 are listed in Tables 2 and 3. The samples were cut from an HT9 rod with a diameter of 3.25 in. A thin section of around 0.0787 in (2 mm) thickness was first cut from the rod using a band saw. This cylinder is milled using a polishing machine ensuring flatness of the surface [7]. The HT9 plate was then machined with a using a water jet to generate the Krouse-type mini specimens.

**Table 2**  
Chemical composition (in wt %) of HT9 [8]

Composition	304 Stainless steel
Cr	11.94
Ni	0.62
Al	0.01
C	0.21
Cu	0.02
Mn	0.69
Co	0.03
Mo	1.03
Si	0.30
P	0.013
W	0.48
Ti	<0.01
V	0.30
Fe	84.36

**Table 3**  
Mechanical properties of HT9

Properties	
Modulus of Elasticity, MPa	$1.72 \times 10^5$
Ultimate Tensile Strength, MPa	955
Yield Strength, MPa	768
Hardness, HRB	99

### 2.3. Metallographic examination

The microstructure of the specimen was characterized by scan electron microscopy (SEM) to study surface morphology and points of failure. Failed specimens were also characterized by optical microscopy.

#### 2.4. *Bending fatigue test*

A LEF-150 bending fatigue machine as shown in Fig. 2 was used to generate the S-N curve of the HT9 at room temperature at a frequency 60 Hz with a stress ratio  $R$  of -1. After testing, the fractured specimens were examined using optical microscopy [9]. The mini specimens were tested in a specially modified adapters as shown in Fig. 2. This machine provided a constant amplitude cyclic motion with an adjustable pre-set stroke adjustable from zero to two inches [10]. The pre-set stroke produced a reliable specimen deflection for calculating stress. Each test specimen was loaded in the unit with a fix deflection, and are initially run at a low speed. The wide end was attached to a bed plate while the thin end is cyclically deflected. The length of the crank stroke was adjusted until the desired loads were obtained. A digital gauge (with a precision of  $\pm 25 \mu\text{m}$ ) was used to measure deflection simultaneously for the specimen and the reciprocating arm. The relationship between the specimen's deflection and the machine stroke range was verified as linear. The digital indicator was used to measure the deflection and the contact point tip of the indicator was placed on the top of the specimen [11]. The number of cycles are recorded and stress level is calculated from the beam equation (7).

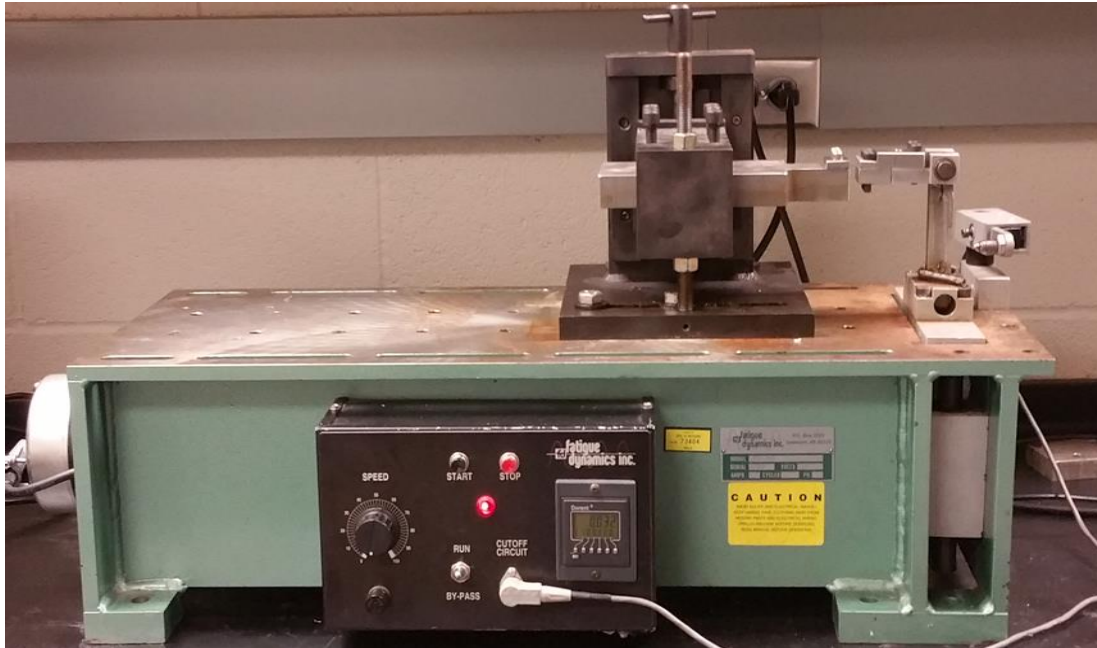


**Fig. 2.** Bending fatigue equipment.

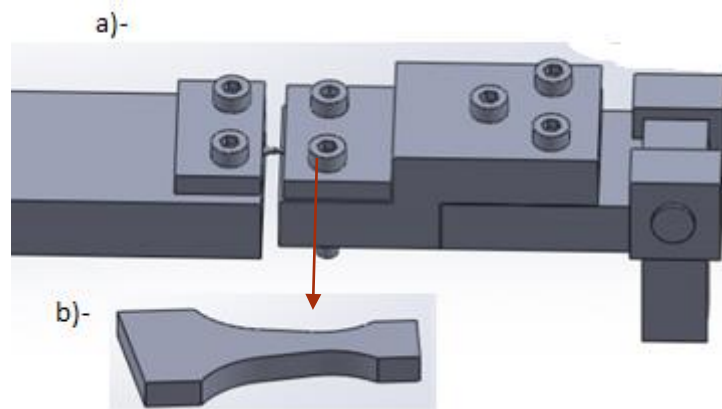


**Fig. 3.** Schematic design of the fatigue test system. a) Adapters, b) Mini-specimen.

### 2.5. Stress calculation method

The maximum bending stress can be derived for a rectangular beam from the flexure formula [12].

$$\sigma = \frac{MC}{I} \quad (1)$$

where  $\sigma$  is the desired bending stress in MPa, M is bending moment where P is force in Newton and L is length in mm, C is distance from neutral axis =  $\left(\frac{t}{2}\right)$ , where t is thickness in mm and I is moment of inertia =  $\left(\frac{bt^3}{12}\right)$ .

From equation (1),

$$\sigma = \frac{6PL}{bt^2} \quad (2)$$

L is the distance between the connecting pin (apex of triangle) and the point of load in mm (in Figure1) and P is the force in Newton. The specimen thickness in mm is represented by t and the width of the specimen at a distance L from the point of load application in mm is represented by b.

$$\Delta = \frac{\sigma L^2}{Et} \quad (3)$$

where  $\Delta$  is the deflection in mm, and E is the modulus of elasticity in MPa. Therefore, the bending stress in the linear (triangular) region of our sample can be calculated with the following equation.

$$\sigma = \frac{\Delta Et}{L^2} \quad (4)$$

The force can be calculated from equation 2,

$$P = \frac{\sigma t^2 b}{6L} \quad (5)$$

The relation between deflection and force

$$P = \frac{\Delta Et^3 b}{6L^3} \quad (6)$$

The formula for the deflection of a triangular shape is [13].

$$\Delta = \frac{SL^2}{Et} \quad (7)$$

### 2.6. Finite element modeling

The finite element code ABAQUS was used to determine the area of maximum stress and uniformity of the stress applied as shown in Fig. 4. This technique applies the load at the end of small grip section (free end) of the specimen and evaluate the bending stress. The Krouse-type specimen for HT9 is simulated by using FEA code ABAQUS with the purpose of studying the maximum stress distribution and deflection. The maximum stress is shown in Fig.4.

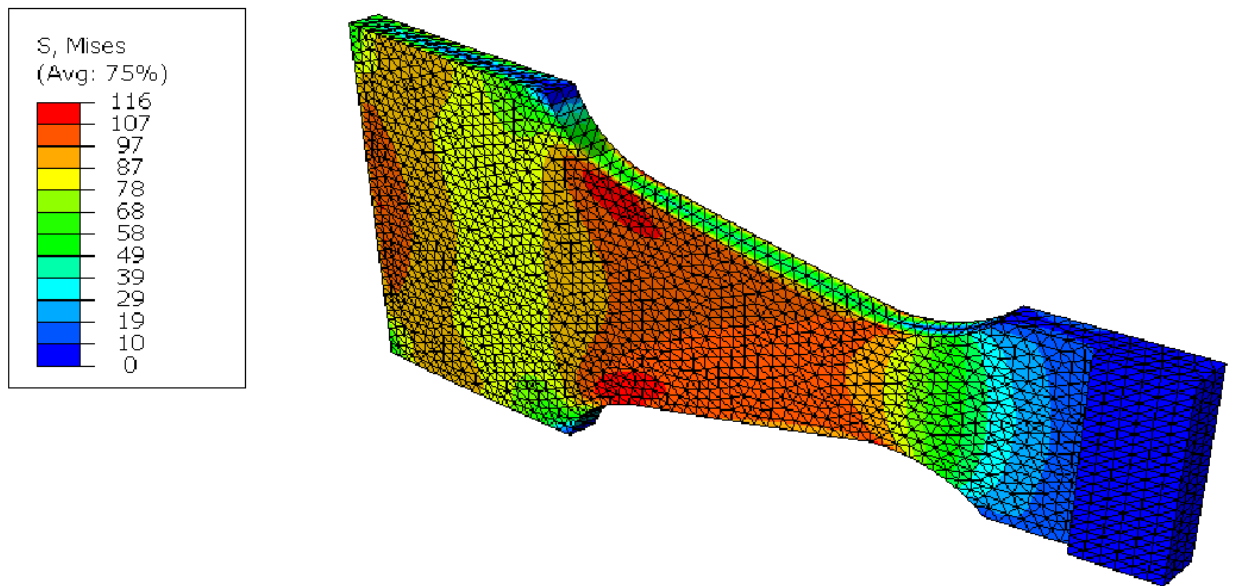


**Fig. 4.** Stress distribution on the Krouse -type specimen model at 15 N



### 3. Analysis of error propagation

Because the variation in the measurements and difficulty to measure the deflection and length of specimen due to the limited of the specimen size, the error analysis calculation is needed. We perform an error propagation analysis of equation 3 as follows [14].

$$\sigma_u^2 = \left( \frac{\partial}{\partial \Delta} \left( \frac{\Delta t E}{L^2} \right) \right)^2 \cdot \sigma_D^2 + \left( \frac{\partial}{\partial t} \left( \frac{\Delta t E}{L^2} \right) \right)^2 \cdot \sigma_t^2 + \left( \frac{\partial}{\partial E} \left( \frac{\Delta t E}{L^2} \right) \right)^2 \cdot \sigma_E^2 + \left( \frac{\partial}{\partial L} \left( \frac{\Delta t E}{L^2} \right) \right)^2 \cdot \sigma_L^2 \quad (8)$$

$$\sigma_u = \pm \sqrt{\left( \frac{Et}{L^2} \cdot \sigma_\Delta \right)^2 + \left( \frac{E\Delta}{L^2} \cdot \sigma_t \right)^2 + \left( \frac{t\Delta}{L^2} \cdot \sigma_E \right)^2 + \left( -\frac{2E\Delta t}{L^3} \cdot \sigma_L \right)^2} \quad (9)$$

### 4. Statistics analysis of fatigue data

Because of the variation in dimensions, hardness and surface finish, etc., the fatigue life data will fluctuate from one specimen to another [15]. The Weibull distribution analysis is a life distribution model with 2-parameter and 3-parameter are used to model extreme values such as failure times and fracture strength. The probability density function (PDF) of 2- parameter distribution can be expressed as [16];

$$f(t) = \frac{\beta}{\eta} \left( \frac{t}{\eta} \right)^{\beta-1} e^{-\left( \frac{t}{\eta} \right)^\beta} \quad \eta \geq 0, \beta \geq 0 \quad (10)$$

where  $\beta$  and  $\eta$  are the shape and scale parameters respectively. The shape parameter  $\beta$ , represents at which 63.2% of the specimen should have failed. A higher scale parameter indicate that the overall durability of the product is better.  $t$  is the failure cycles in this study. By integrated equation 10, the cumulative density function (CDF) is obtained in equation 11 [16].

$$F_f(t) = 1 - e^{-\left(\frac{t}{\eta}\right)^\beta} \quad (11)$$

$$F_s(t) = 1 - F_f(t) \quad (12)$$

Where  $F_f(x)$  is probability of failure and  $F_s(x)$  is the probability of survival. If the natural logarithm of both sides of the equation (9) are taken, the following equation (10) can be written.

$$\ln\left(\ln\left(\frac{1}{1 - F_f(t)}\right)\right) = \beta \ln(t) - \beta \ln(\eta) \quad (13)$$

Comparing this equation with the liner form  $y = mx + b$ , leads into

$$y = \ln\left(\ln\left(\frac{1}{1 - F_f(t)}\right)\right), \quad m = \beta, \quad \text{and } b = -\beta \ln(\eta)$$

Each value for failure probability was used a Bernard's median rank formula [17]

$$MR = \frac{i - 0.3}{n + 0.4} \quad (14)$$

Where (  $i$  ) is the number of the data point in ascending order and (  $n$  ) is the total number of data points in the specimen. The equation was used for calculate for each stress value.

$$y = \ln\left(\ln\left(\frac{1}{1 - MR}\right)\right), \quad \text{and } X = \ln(N) \quad (15)$$

The Weibull analysis for estimation of the 3- parameter.

$$F(t) = 1 - e^{-\left[\left(\frac{t-\gamma}{\eta}\right)^\beta\right]} \quad (16)$$

where,  $\gamma$  is minimum life or threshold parameter . If the logarithm of both sides of the equation (16) are taken, the following equation (17) can be written.

$$\ln\left(\ln\left(\frac{1}{1 - F(t)}\right)\right) = \beta \ln(t - \gamma) - \beta \ln(\eta) \quad (17)$$

$$y = \ln \left( \ln \left( \frac{1}{1-F_f(t)} \right) \right), m = \beta, \text{ and } b = -\beta \ln(\eta) \quad (18)$$

$$y = \ln \left( \ln \left( \frac{1}{1-MR} \right) \right), \text{ and } x = \ln(t - \gamma) \quad (19)$$

It is an important to calculate mean time to failure  $\mu$  [16]

$$\mu = \eta \cdot \Gamma \cdot \left( 1 + \frac{1}{\beta} \right) \quad (20)$$

where  $\Gamma$  is gamma function

## 5. Results and discussion

### Finite element modeling

The stress differences between the experimental and simulated results present in Figure 5. The force obtained from equation (6) was used to simulate the experiment by ABAQUS. It can be seen clearly from Figure6, the stress is lower than the experimental one.

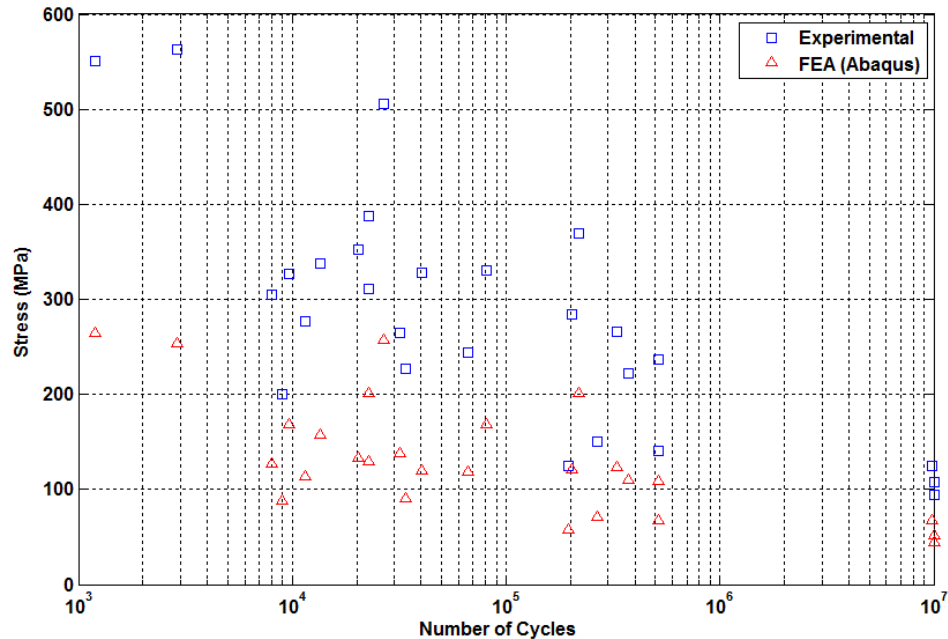


**Fig. 5.** Experimental results for the mini specimen compared with FEA (ABAQUS) results obtained for HT9.

The main reason the differences between the experimental and simulated in stress because of the dimensional inaccuracies on the deflection and length due to limited size of each specimen. The value of stress is related to the deflection and length of each specimen. Moreover, the FEA code ABAQUS simulations is used determine the maximum stress in each specimen for its deflection.

### Generation of S-N curve

The results of the total 130 specimens fatigue as-received testing are summarized in Fig.6 in the form of a Wöhler-diagram that describe the fatigue life that specimens survive at a constant stress amplitude. These specimens were tested with different stress. The stress amplitudes were chosen so as to obtain failure in the range of 563 to 108 MPa of load stress.

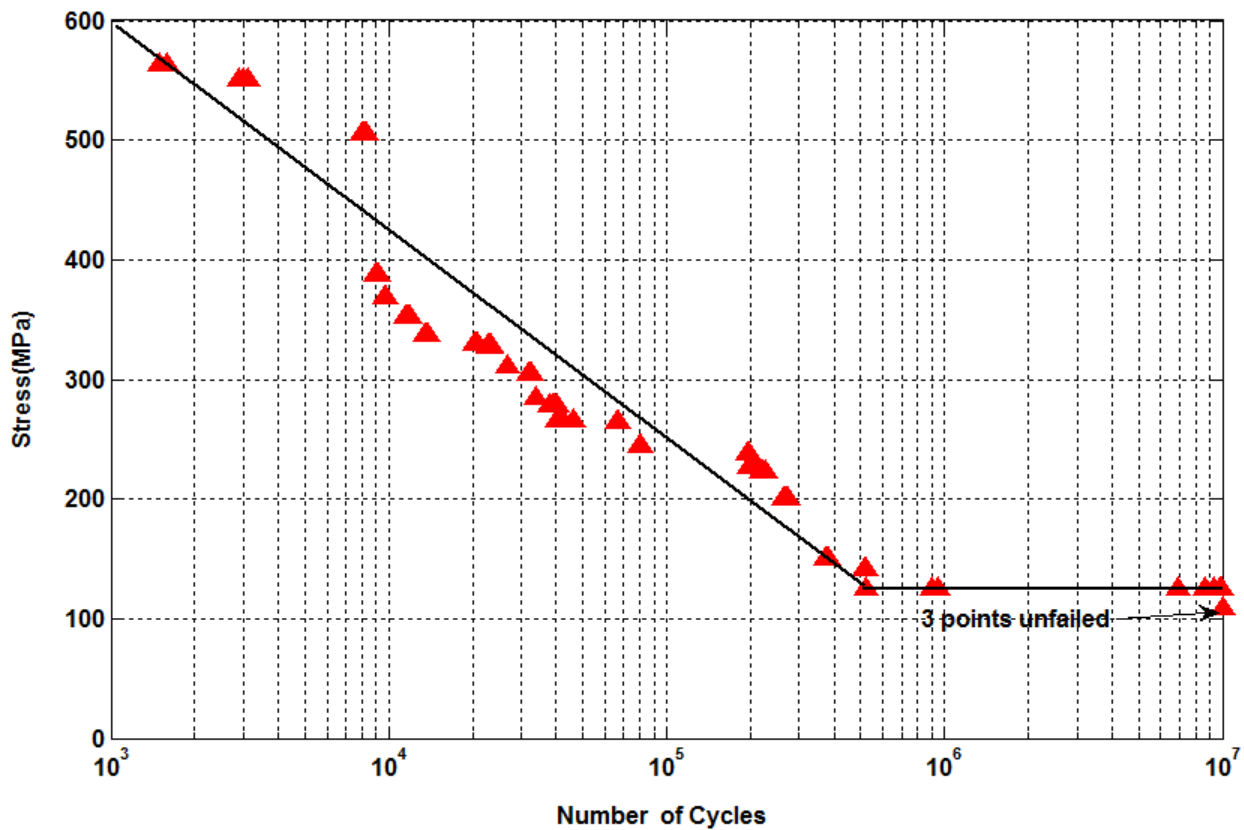


**Fig. 6.** S–N curves for HT9.

The mean fatigue life corresponding to each stress was calculated from equation (20).

The S–N curve is plotted for mean fatigue life as shown in Figure 7.

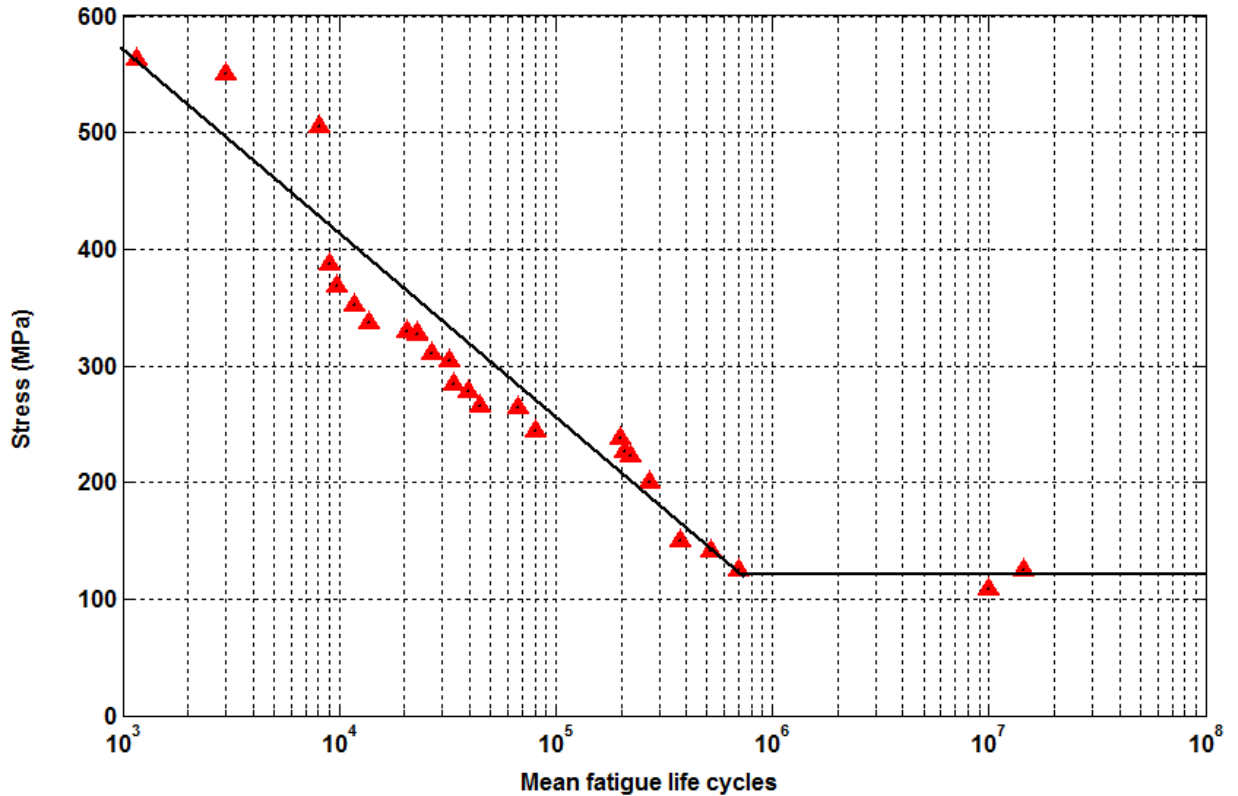


**Fig. 7.** S-N Curve for mean fatigue life.

### **Metallographic examination**

The initial microstructure of as-received for mini-specimen was characterized by SEM. Figure 8 shows the microstructures of edges of the mini specimen. The microstructure displays evidence of point of failure. Figure 8 (b) shows that the edges are sharp and need additional polishing.

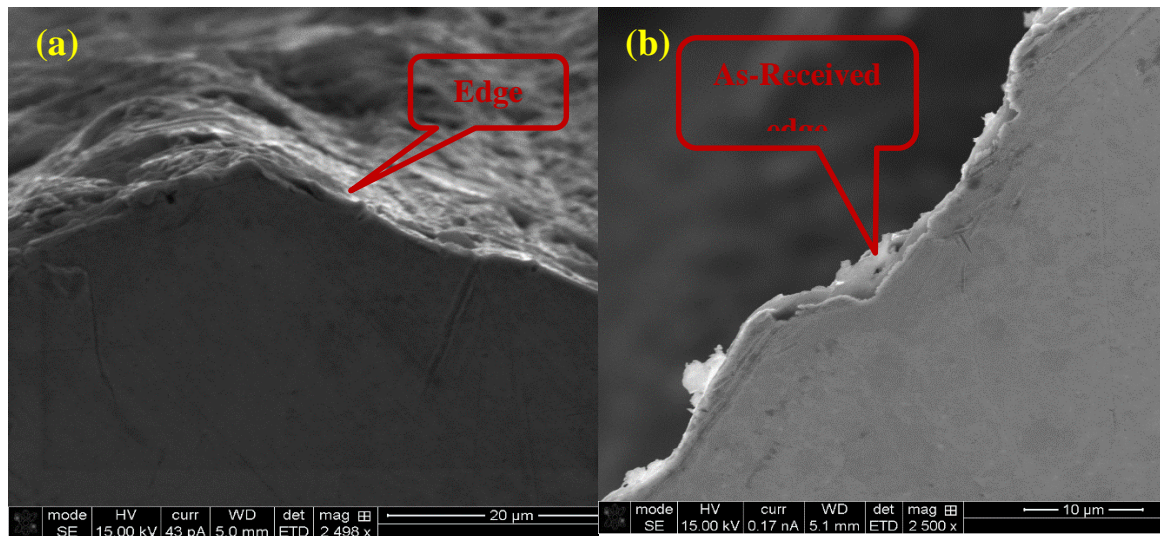


**Fig. 8.** Sample of SEM showing (a) edge of mini specimen (b) surface of specimen.

The fatigue failure occurs in three stages, initiation, crack growth (propagation) and final fracture. The SEM images illustrate fatigue fractures at the surface of the broken area of specimen. The fatigue fractures called striations, the striation is actually a crack that result from stress load as shown in Fig. 9.

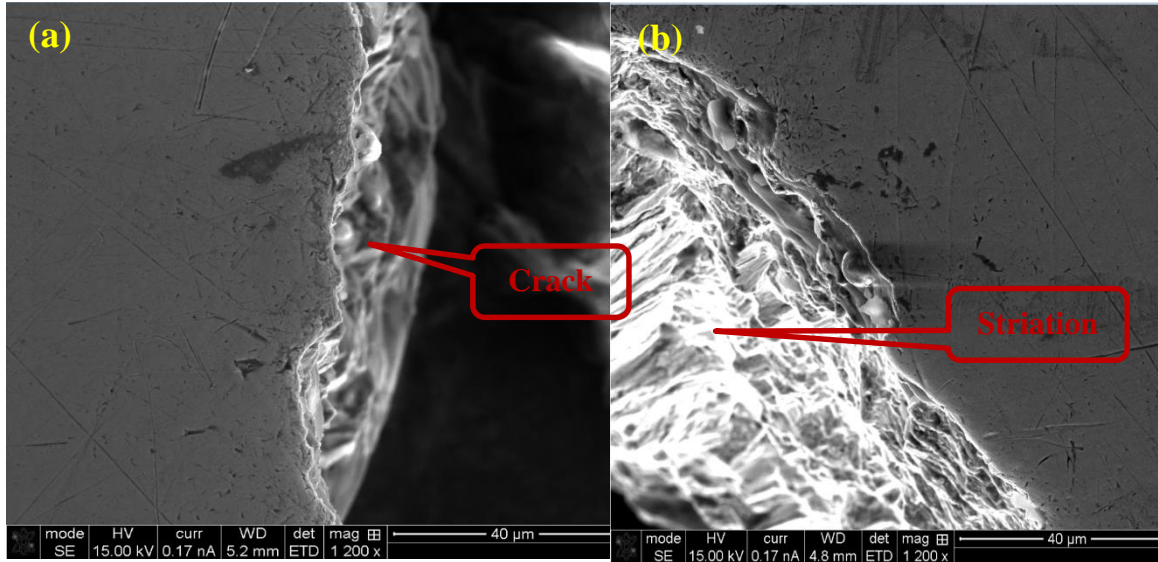


**Fig. 9.** SEM images of mini specimen showing, (a) the failure crack at the neck of the specimen after fatigue test, (b) fatigue striations at the fracture site.

### Analysis of Error Propagation

Table 4 shows an example of one specimen that are measured and repeated five times. The effect of specimen's dimensions on analysis error is listed in Table 4. It has been observed that most of the error is due to length (L) and deflection ( $\Delta$ ) measurements.

**Table 4**

Error Analysis Calculation

Specimen	L	b	t	$\Delta$	$\left(\frac{Et}{L^2} \cdot \sigma_{\Delta}\right)^2$	$\left(\frac{E\Delta}{L^2} \cdot \sigma_L\right)^2$	$\left(-\frac{2E\Delta t}{L^3} \cdot \sigma_L\right)^2$	$\sigma_u$	$\sigma$	$\sigma \pm \sigma_u$
Measured1	5.43	3.1	1.1	0.075	1683	42	2778	67	482	482±67
Measured2	5.07	2.98	1.1	0.076	2214	57	4305	81	561	561±81
Measured3	4.85	3.22	1.08	0.088	2549	91	7261	100	696	696±100
Measured4	5.44	3.14	1.09	0.071	1640	38	2418	64	451	451±64
Measured5	4.84	2.71	1.12	0.076	2764	69	5897	93	626	626±93
Average	5.12	3.03	1.01	0.077	2170	59	4532	81	563	563±81
St. Dev	$\sigma_L$	$\sigma_b$	$\sigma_t$	$\sigma_{\Delta}$	E					
	0.296	0.2	0.0148	0.004	1.72E+05					



It can be shown from the Table 4 that five measurements were taken for one specimen in order to reach a good estimate of the true stress value, the true stress value remains fundamentally unknowable. The errors are depend on the measurement accuracy of deflection and length of specimen.

### **Statistics analysis of fatigue data**

For the statistical analysis, we have chosen the cycle life data under stress level at 563, 310 and 265 MPa. The 2 and 3-parameter Weibull distribution of these test are calculated by commercial software Minitab 17. Figures 10 and 11 show the distribution fit plots of the test data with 95 % confidence level. The centreline is the trend line and the outer lines are the 95% confidence level. This distribution helps us to evaluator the distribution fit by viewing how the data fall about the line. Figure 11 shows the best plot fits and the shape parameter  $\beta$  is greater than one, indicating the product is suffering normal wear failure rate. Figure 11 show the best plot fits and the shape parameter  $\beta$  is greater than one, indicating the product is suffering normal wear failure rate. The 3-parameter Weibull plot shows a much better fit than the 2- parameter as shown Figure 11. Furthermore, observing that the 2-parameter Weibull is not a perfect distribution for these data than the 3-parameter. The 3-parameter Weibull plots show the data follow the straight line as shown in the Figure 11.

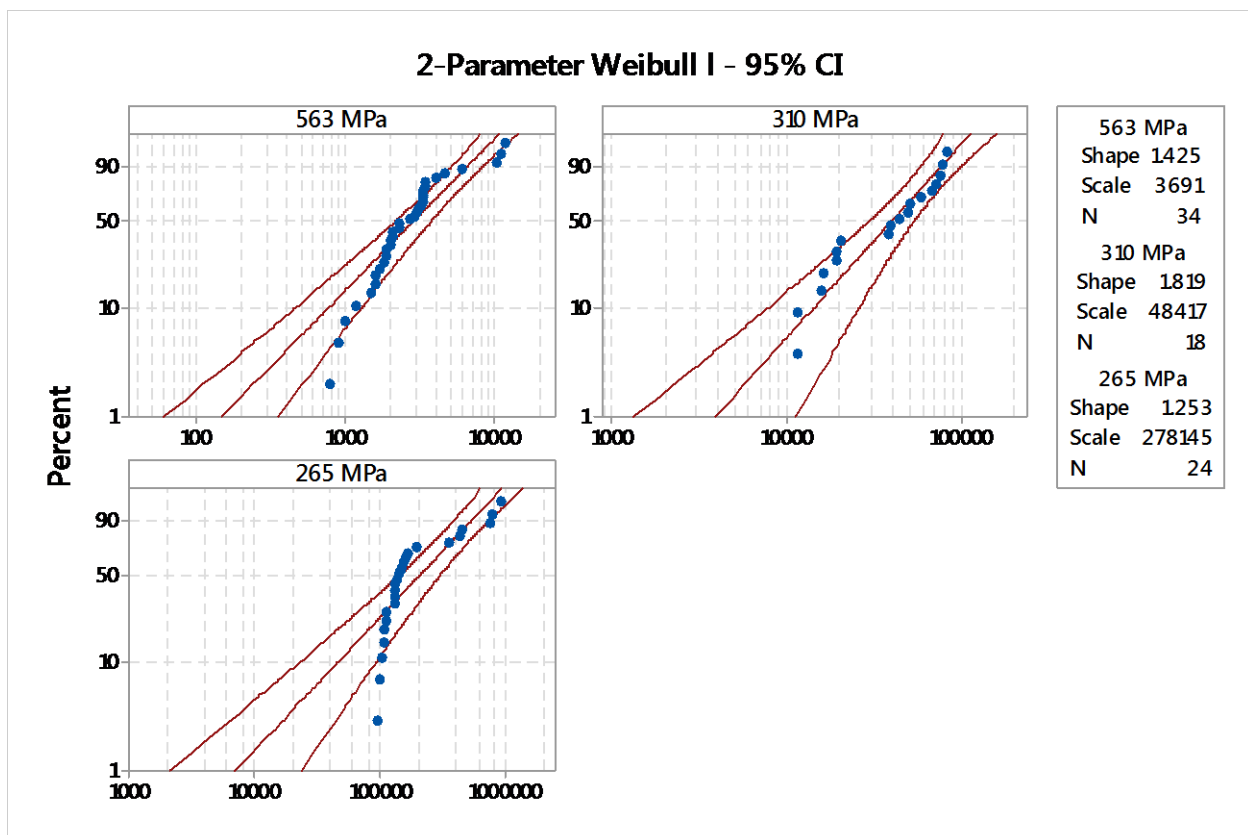


**Fig. 10.** Plot of 2-parameter Weibull distribution.

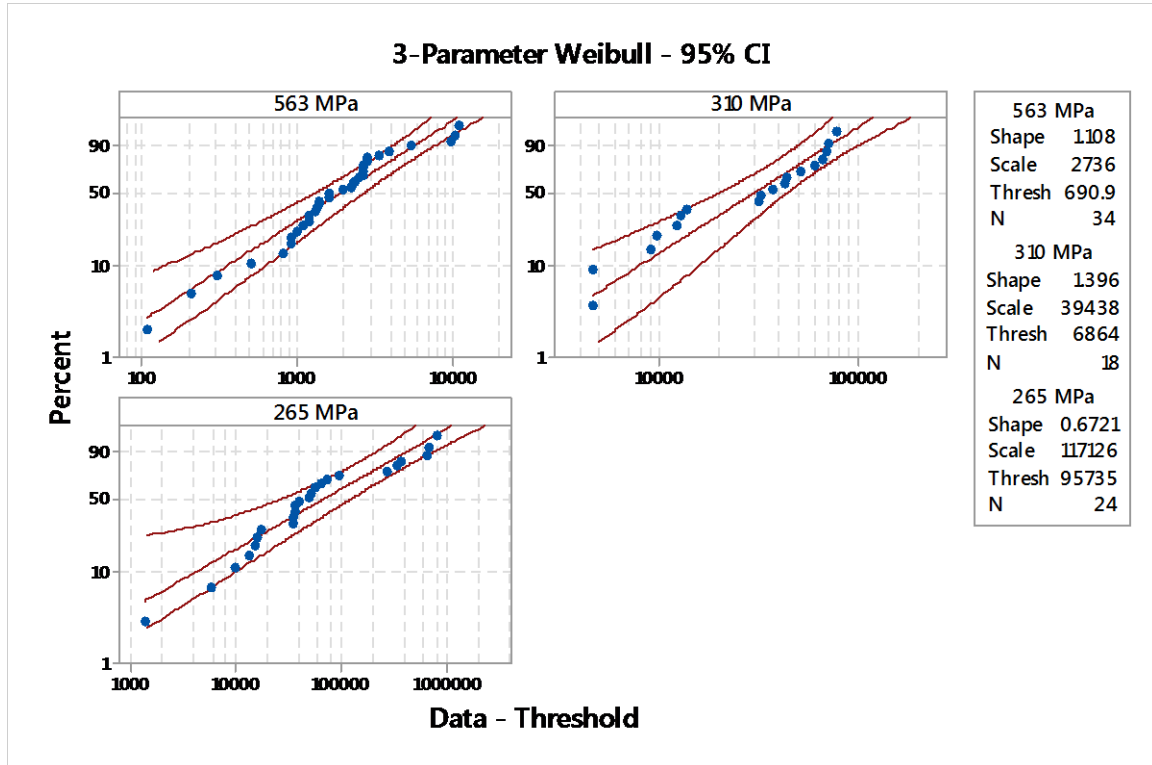


**Fig.11.** Plot of 3-parameter Weibull distribution.

## 6. Conclusion and future work

In this paper, the bending fatigue is proposed with a mini-specimen technique (Krouse-type) to create an S-N curve for HT9 under constant deflections. The measured stress was higher than the simulated one by  $53 \pm 0.002$  MPa. The error is higher in stress value due to dimensional inaccuracies on the deflection and length of the specimen, indicating that perhaps using a longer sample to minimize error in stress level. The Weibull distribution modulus tested the number of cycle under stress level at 563, 310, and 265 MPa. A decreasing shape value shows that the measured data was more scattered and widely distributed. Additional stress level points are recommended. The data appear the fitted line well; therefore the 3- parameter Weibull distribution may be an appropriate choice for the data. Future work will include different nuclear materials and shaped

samples, particularly longer ones. Longer samples are still considered adequate to fit in rest reactors (such as ATR [18]). In addition, we plan machining new specimens with using wire EDM in order to reduce the surface effects and obtain a more reliable fatigue measurements suitable for mini-specimens.

### Acknowledgments

The first author's graduate program is funded by the King Abdul-Aziz City for Science & Technology, Saudi Arabia.

### References

- [1] N. KASAHARA, "Development of thermal load and fatigue evaluation methods based on their mechanism," in *Working Group for advancement of Thermal fatigue evaluation methods in the NISA project*, 2012, no. May.
- [2] C. M. Obermark and R. S. Mishra, "Development of a Reversible Bending Fatigue Test Bed to Evaluate Bulk Properties Using Sub-Size Specimens."
- [3] ASTM, "Standard Test Method for Bending Fatigue Testing for Copper-Alloy Spring Materials," *Annu. B. ASTM Stand.*, vol. 96, pp. 3–7, 2009.
- [4] Y. Chen, "Irradiation Effects of Ht-9 Martensitic Steel," *Nucl. Eng. Technol.*, vol. 45, no. 3, pp. 311–322, Jun. 2013.
- [5] R. B. Abernethy, *Chapter 1. an overview of weibull analysis 1.1*. 2006.
- [6] A. S. Haidyrah, C. H. Castano, and J. W. Newkirk, "An experimental study on bending fatigue test with a krouse - type fatigue specimen," in *2014 ANS Winter Meeting and Nuclear Technology Expo*, 2014, pp. 1–4.
- [7] S. Dongare, F. Liou, and J. W. Newkirk, "Development of a Technique for Testing of Tensile Properties with Miniature size specimens for metal additive manufacturing," Missouri University of Science & Technology, 2012.
- [8] X. Ren, K. Sridharan, and T. R. Allen, "Corrosion of ferritic–martensitic steel HT9 in supercritical water," *J. Nucl. Mater.*, vol. 358, no. 2–3, pp. 227–234, Nov. 2006.

- [9] M. Sivapragash, P. R. Lakshminarayanan, R. Karthikeyan, K. Raghukandan, and M. Hanumantha, "Fatigue life prediction of ZE41A magnesium alloy using Weibull distribution," *Mater. Des.*, vol. 29, no. 8, pp. 1549–1553, Jan. 2008.
- [10] A. S. Haidyrah and C. H. Castano, "Bending Fatigue Mini-Specimens (Krouse Type) for Nuclear Materials," in *Poster presented at Third International Workshop on Structural Materials for Innovative Nuclear Systems (SMINS-3)*, 2013, p. 1.
- [11] Ahmed S. Haidyrah, J. W. Newkirk, and C. H. Castano, "Characterization a Bending Fatigue Mini-Specimen Technique (Krouse Type) of Nuclear Materials," in *2015 TMS Annual Meeting & Exhibition*, 2014, pp. 1–8.
- [12] Robert R. Fujczak, "The Effects of Fatigue Loading Frequency on Fatigue Life of High-Strength Pressure Vessel Steels," WATERVLIET, N.Y. 12189-4050, 1994.
- [13] Fatigue Dynamics Inc., "Instruction Manual Model LFE-150 Variable Speed Life,Fatigue analysis.pdf." Walled Lake ,MI 48390, p. 47.
- [14] G. F. Knoll, *Radiation Detection and Measurement*, vol. 2006. Wiley, 2000.
- [15] C. Lipson and N. J. Sheth, *Statistical Design and Analysis of Engineering Experiments*, First Edit. McGraw-Hill Book Company, 1973.
- [16] R. Sakin and İ. Ay, "Statistical analysis of bending fatigue life data using Weibull distribution in glass-fiber reinforced polyester composites," *Mater. Des.*, vol. 29, no. 6, pp. 1170–1181, Jan. 2008.
- [17] W. M. Group, "Product Excellence using 6 Sigma ( PEUSS ) W e i b u l l a n a l y s i s," .
- [18] J. R. Kennedy, S. Robertson, R. Soelberg, and C. Knight, "ATR NSUF," 2013.

#### IV. Influence of thermal aging on the mini specimen (krouse - type) bending fatigue of nuclear materials

Ahmed S. Haidyrah<sup>1</sup>, Joseph W. Newkirk<sup>2</sup>, Carlos H. Castaño<sup>1\*</sup>

<sup>1</sup>Nuclear Engineering, Missouri University of Science & Technology, 224 Fulton Hall, Rolla, MO, USA 65401

<sup>2</sup>Materials Science & Engineering, Missouri University of Science & Technology, 282 McNutt Hall, Rolla, MO, USA 6540

**Keywords.** bending fatigue test, bending fatigue mini specimen, S-N curve, Thermal Aging, Krouse-type, FEA code ABAQUS, Weibull distribution, Minitab 17, SRIM.

#### ABSTRACT

The mini-specimen bending fatigue (Krouse-type) of nuclear materials was studied with thermal aging at 1000 C° for 8 hours. These mini-specimens were similar (but smaller) to those described in the ASTM B593 standard. They were machined by wire EDM and tested both as-received and under thermal aging conditions. The specimen's cycle bending fatigue behavior was examined under constant deflection at a 60 Hz frequency and a stress ratio (R) of -1. Weibull analysis was used to execute failure probability calculations. The commercial software Minitab 17 were used to calculate the distribution of fatigue life. I have used 2 and 3- parameters Weibull analysis to introduce the probability of failure. The maximum stress distribution on the specimen was recognized by FEA code ABAQUS. The grain boundary for both the as-received and the thermal aging conditions were identified by SEM and optical microscopy. The thermal aging process had little impact on the mini-specimen's fatigue life. The stopping and range of ions in matter (SRIM) program simulation was used to simulate the damage induced by an H ion and an He ion into Incoloy alloy MA956 layer.

---

\* Corresponding author. Tel:+1 (573) 341-676

E-mail address: Email: [castanoc@mst.edu](mailto:castanoc@mst.edu) (Carlos H. Castaño)

## 1. Introduction

A study of the bending fatigue of materials in nuclear systems can be used to predict the behavior and lifetime of a reactor's components under oscillating load conditions. Fatigue issues are becoming more important as nuclear systems age [1]. The material under examination in a bending fatigue experiment is repeatedly bent until failure occurs. The fatigue life before the material breaks is recorded and plotted against the bending stress. The Krouse-type design utilized in this study is similar in geometry to an ASTM standard specimen. The Krouse-type specimen is however, is smaller than the ASTM B593 [2,3] standard was used to test the mini-specimen's fatigue properties. The objective of this study was to create an S-N curve. An Incoloy alloy MA956 is commonly used to design a reactor core in a pressurized water reactor (PWR). The Incoloy alloy MA956 is a ferritic oxide dispersion strengthened (ODS) [4] has a particularly good resistance to high temperature oxidation. Raymond et al studied the fatigue behavior of the Incoloy alloy MA956. They found that the stress of specimens aged at 600 C° was slightly higher than specimens aged at 700 C°. The FEA code ABAQUS was used in this study to verify the stress distribution on the specimen. The Weibull distribution function was used to analyze fatigue scattering problems. This function was used because it has excellent applicability and accuracy. Unfortunately, it needs a large amount of experimental data. The Weibull distribution was examined to determine how well the data fit a straight line. In several cases, study the bad fit may be related to either the quality of the data or the behavior of the failure [5]. This study was conducted in an attempt to clarify the bending fatigue of the Incoloy alloy MA956 mini-specimen. A fatigue life was recorded, and the effect of stress on the specimen was investigated.

## 2. Experimental procedure

### 2.1. Specimens

A Krouse-type mini-specimen (depicted in Figure 1) was used for this study. It was modified according to the dimensions recommended by the ASTM standard B593 [2]. A wire EDM was used to machine it. The specimen's straight lines given in Figure 1 made an angle of 26° with the horizontal axis. A force was applied at the point where two straight

lines intersected along the specimen's straight edges (point A in Figure1) to create bending [6]. A digital caliper was used to measure all of the specimens' dimensions. The specimen's measurements including tolerances are listed in Table 1.

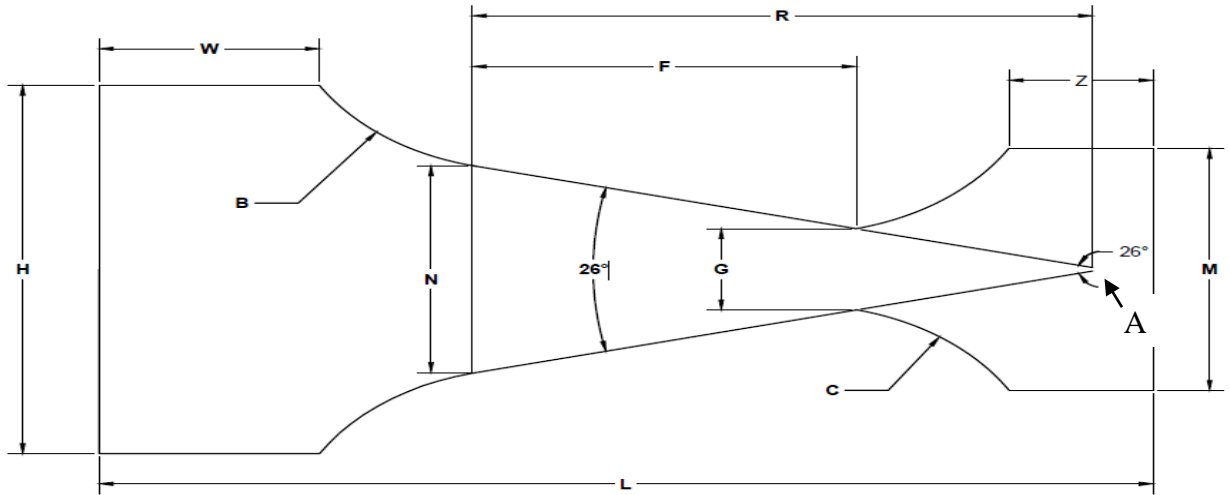


**Fig. 1.** Diagram of the mini fatigue test specimen. (All dimensions are given in millimetres) [3].



**Table 1**

Mini Fatigue Test Specimen dimensions compared with the ASTM B593 Standard.

	<b>Description</b>	<b>ASTM B593 Standard specimen dimension, in [mm]</b>	<b>Mini fatigue test specimen (Krouse-type) dimension, mm</b>
<b>F</b>	Length of test region	-	<b>3.06 ±0. 1</b>
<b>H</b>	Width of grip section 1	1.38 in(35.052mm)	<b>6.4 ±0. 2</b>
<b>M</b>	Width of grip section 2	0.75 in(19.05 mm)	<b>3.28 ±0. 1</b>
<b>t</b>	Thickness	0.008 to 0.031 in (0.203 to 0.787 mm)	<b>1.09 ±0. 01</b>
<b>L</b>	Overall length	2.31 in(58.674 mm)	<b>12.53 ±0.01</b>
<b>G</b>	width of narrowest section	-	<b>1.83 ±0. 2</b>
<b>W</b>	Length of grip section 1	0.75 in(19.05 mm)	<b>2.08±0. 1</b>
<b>Z</b>	Length of grip section 2	0.5 in(12.7 mm)	<b>2.71±0.1</b>
<b>C</b>	Radius of fillet 2, min	3/8 in(9.525 mm)	<b>4.19±0. 1</b>
<b>B</b>	Radius of fillet 1, min	3/8 in(9.525 mm)	<b>4.19±0. 1</b>
<b>R</b>	Distance between the connecting pin (apex of triangle) and the width N of the specimen	-	<b>8.04±0.29</b>
<b>N</b>	Width of the specimen at a distance R from the point of load application	-	<b>3.95±0.29</b>

## 2.2. Materials and experiment

An Incoloy alloy MA 956 supplied from Special Metals Wiggin Ltd was used in this study in the form of a rod with a diameter of 30 mm. The chemical composition and mechanical properties of the Incoloy alloy MA956 are listed in Table 2 and 3.

**Table 2**

Chemical composition (in wt %) [7]

Composition	304 Stainless steel
Cr	21.5
Ni	0.5
Al	5.5
Y <sub>2</sub> O <sub>3</sub>	0.5
C	0.1
Cu	0.15
Mn	0.3
Co	0.3
Mo	0-1
Si	0.0
S	0.03
P	0.02
W	0.48
Ti	0.2-0.6
Fe	Bal.

**Table 3**

Mechanical properties of alloy [8]

Alloy	Modulus of Elasticity MPa	Ultimate Tensile Strength, MPa	Yield Strength MPa	Hardness HV
MA956[8]	$2.69 \times 10^5$	650	550	250-300

The specimens were cut from an Incoloy alloy MA956 rod. An abrasive saw was used to cut thin section approximately 0.0787 in (2 mm) from the rod. This method was used to avoid thermal shock, which can cause cracking. A cooling fluid was also used. A grinder was used to mill the cylinder, thus helping guarantee surface flatness [9]. The Incoloy alloy MA956 rod was then machined with a wire EDM to generate the Krouse-type mini-specimens. Both on a LEF-150 bending fatigue machine and VSS-40H presented

as in Figures 2 and 3 were used to generate the S-N curve of the Incoloy alloy MA956 for specimen as-received and thermal aging condition at a frequency 60 Hz and with a stress ratio R of -1. Thermal aging was conducted in a furnace at temperatures of 1000 C for 8 hours. Both a scanning electron microscope (SEM) and optical microscopy were used to examine [10]. The mini-specimens were tested in specially modified adapters, as pictured shown in Figure 2. This machine provided a constant amplitude cyclic motion with an adjustable pre-set stroke from 0 to 2'' [11]. The pre-set stroke produced a reliable specimen deflection for calculating stress. Each test specimen was loaded in the unit with a fix deflection. The unit was nitially run at a low speed. The wide end was attached to a bed plate while the thin end was deflected cyclically. The crank stroke's length was adjusted until the desired loads were obtained. A digital gauge (with a precision of  $\pm 3.048 \mu\text{m}$ ) was used to measure deflection simultaneously for the specimen and the reciprocating arm. The digital indicator was used to measure the deflection, the indicator's contact point tip was placed on top of the specimen [12]. The number of cycles was recorded, and the stress level was calculated from the beam equation (7). The bending fatigue were stopped after 10 million cycles without failure.

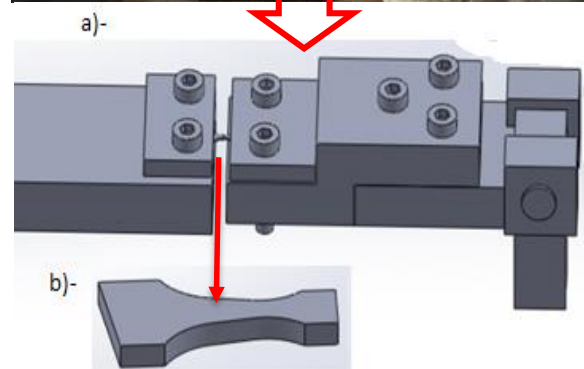
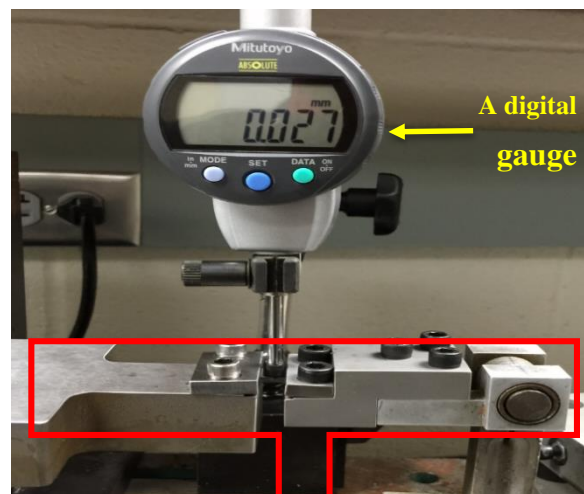
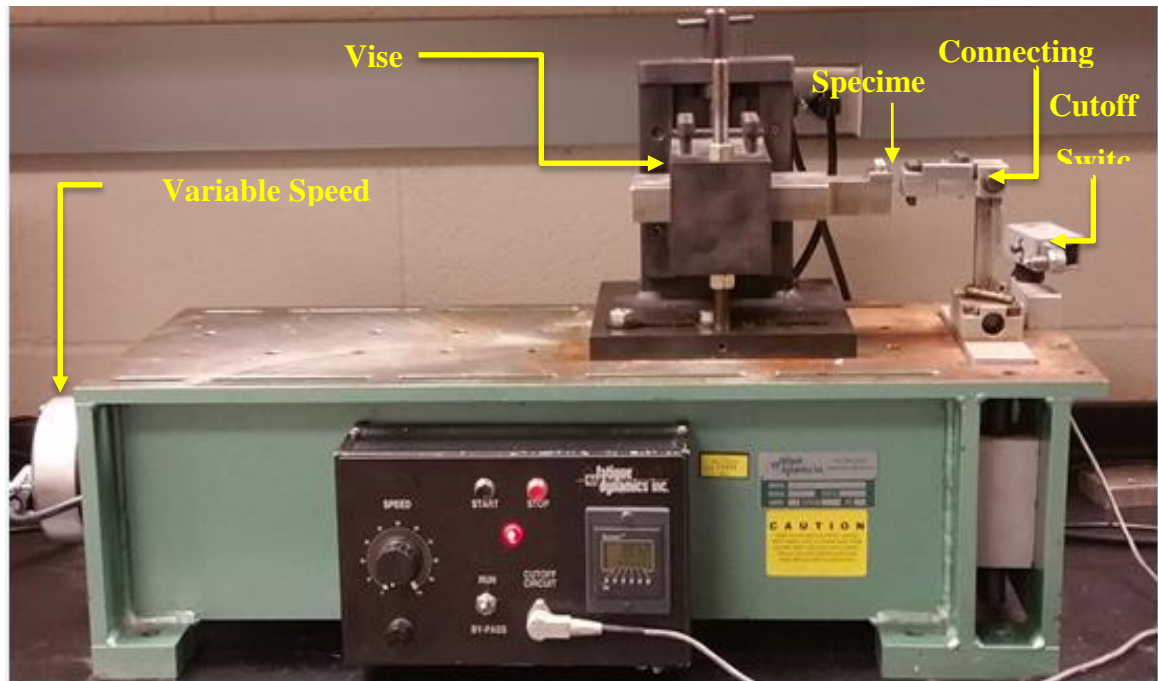


**Fig. 2.** LEF-150 bending fatigue machine. a) Adapters, b) Mini-specimen.

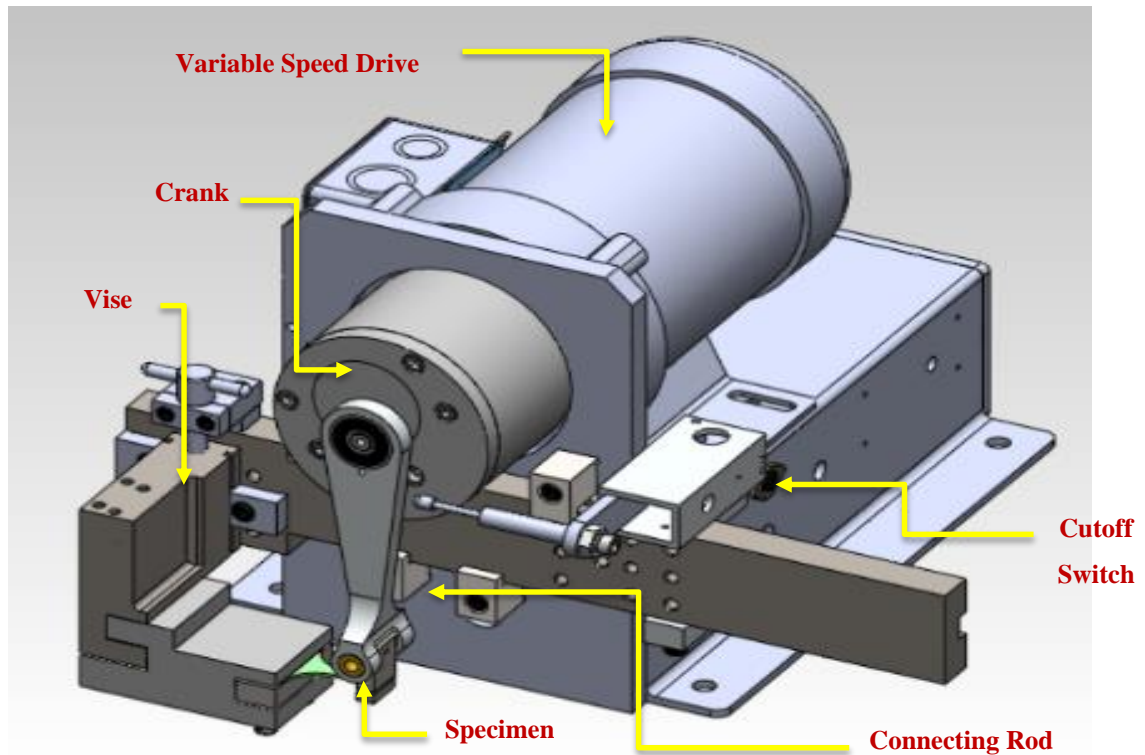


**Fig. 3.** VSS-40H bending fatigue machine

The maximum bending stress can be derived for a rectangular beam from the flexure formula [13].

$$\sigma = \frac{MC}{I} \quad (1)$$

where  $\sigma$  is the desired bending stress in MPa,  $M$  is the bending moment,  $P$  is the force in Newtons.  $L$  is the length in mm,  $C$  is the distance from the neutral axis =  $\left(\frac{t}{2}\right)$ ,  $t$  is the thickness in mm, and  $I$  is moment of inertia =  $\left(\frac{bt^3}{12}\right)$ .

From equation (1),

$$\sigma = \frac{6PL}{bt^2} \quad (2)$$

where L is the distance between the connecting pin (apex of triangle) and the point of load in mm (in Figure 1), and P is the force in Newton. The specimen thickness in mm is represented by t, and the specimen's width at a distance L from the point of load application (in mm) is represented by b.

$$\Delta = \frac{\sigma L^2}{Et} \quad (3)$$

where  $\Delta$  is the deflection in mm, and E is the modulus of elasticity in MPa. Therefore, the bending stress in the linear (triangular) region of the sample can be calculated as.

$$\sigma = \frac{\Delta Et}{L^2} \quad (4)$$

The force can be calculated as equation (5).

$$P = \frac{\sigma t^2 b}{6L} \quad (5)$$

The relationship between the deflection and the force is

$$P = \frac{\Delta Et^3 b}{6L^3} \quad (6)$$

The formula for the deflection of a triangular shape is [14,15]

$$D = \frac{\sigma L^2}{Et} \quad (7)$$

### 2.3. Finite element modeling

The finite element code ABAQUS was used to determine each specimen's illustrated in Figure 4. This technique applies the load at the end of a small grip section (the free end).

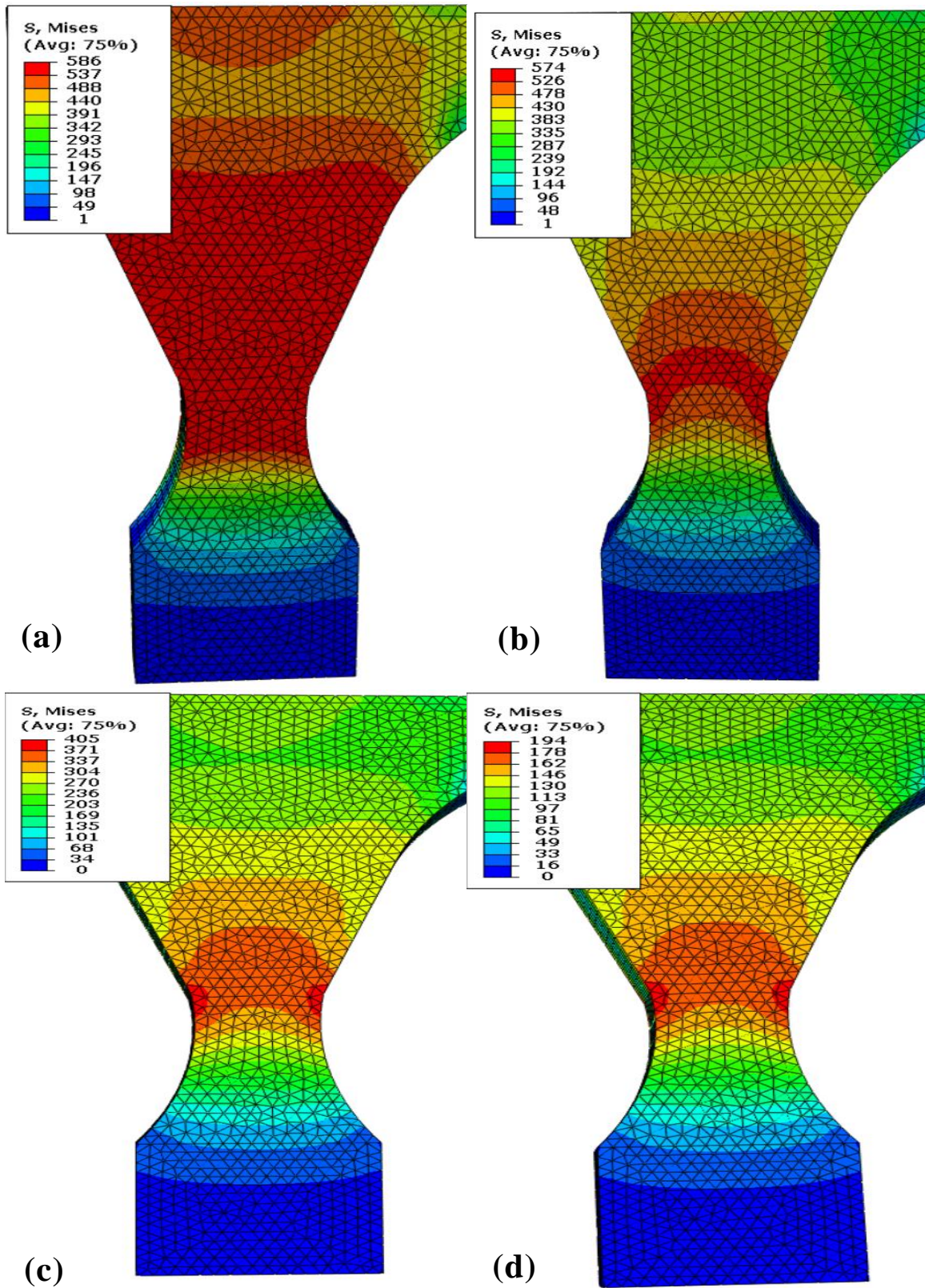


**Fig. 4.** Stress distribution of the model at (a) 18 N, (b) 38 N, (c) 56 N, and (d) 78 N.

## 2.4. STATISTICAL ANALYSIS OF FATIGUE DATA

Fatigue life data will fluctuate from one specimen to another due to variations in dimensions, hardness, surface finish, and so on [16]. The Weibull distribution analysis, a life distribution model with both 2 and 3-parameter, was used to model extreme values (e.g., failure times strengths). The probability density function (PDF) of a 2-parameter distribution can be expressed as [17]

$$f(t) = \frac{\beta}{\eta} \left(\frac{t}{\eta}\right)^{\beta-1} e^{-\left(\frac{t}{\eta}\right)^\beta} \quad \eta \geq 0, \beta \geq 0 \quad (8)$$

where  $\beta$  and  $\eta$  are the shape and scale parameters, respectively. The shape parameter  $\beta$  indicates the point at which 63.2% of the specimen should have failed. A higher shape parameter indicates that the product's overall durability is better. The failure cycle is represented by  $t$  in this study. The cumulative density function (CDF) is obtained in equation 11 [17].

$$F_f(t) = 1 - e^{-\left(\frac{t}{\eta}\right)^\beta} \quad (9)$$

$$F_s(t) = 1 - F_f(t) \quad (10)$$

where  $F_f(x)$  is the probability of failure, and  $F_s(x)$  is the probability of survival. If the natural logarithm of both sides of the equation (10) is taken, the following equation (11) can be written.

$$\ln\left(\ln\left(\frac{1}{1 - F_f(t)}\right)\right) = \beta \ln(t) - \beta \ln(\eta) \quad (11)$$

A Comparison between this equation and the liner form  $y = mx + b$ , produces

$$y = \ln\left(\ln\left(\frac{1}{1 - F_f(t)}\right)\right), m = \beta, \text{ and } b = -\beta \ln(\eta) \quad (12)$$

Each value for the failure probability was used a Bernard's median rank formula [18]:



$$y = \ln \left( \ln \left( \frac{1}{1-F_f(t)} \right) \right), m = \beta, \text{ and } b = -\beta \ln(\eta) \quad (13)$$

$$MR = \frac{i - 0.3}{n + 0.4} \quad (14)$$

where  $i$  is the number of the data points in ascending order, and  $n$  is the total number of data points in the sample. The equation (15) was used to calculate each stress value.

$$y = \ln \left( \ln \left( \frac{1}{1 - MR} \right) \right), \text{ and } x = \ln(t) \quad (15)$$

The Weibull analysis for the estimation of the 3- parameter was [19]

$$F(t) = 1 - e^{-\left[\left(\frac{t-t_0}{\eta}\right)^\beta\right]} \quad (16)$$

$$f(t) = \left(\frac{\beta}{\eta}\right) \left(\frac{t-t_0}{\eta}\right)^{(\beta-1)} \cdot e^{-\left[\left(\frac{t-t_0}{\eta}\right)^\beta\right]} \quad (17)$$

where,  $t_0$  is either the position parameter or the threshold parameter [20]. If the logarithm is taken from both sides of the equation (17), then

$$\ln \left( \ln \left( \frac{1}{1 - F(t)} \right) \right) = \beta \ln(t - t_0) - \beta \ln(\eta) \quad (18)$$

$$y = \ln \left( \ln \left( \frac{1}{1 - F_f(t)} \right) \right), m = \beta, \text{ and } b = -\beta \ln(\eta) \quad (19)$$

$$y = \ln \left( \ln \left( \frac{1}{1 - MR} \right) \right), \text{ and } x = \ln(t - t_0) \quad (20)$$

### 3. Results and discussion

#### 3.1. S-N curve

A comparison between the as-received and the thermal aging mini-specimens. Values at different stress levels are graphed in Fig. 5. The as-received specimens at 408 MPa had a higher as-received fatigue life than did the thermal aging specimens.

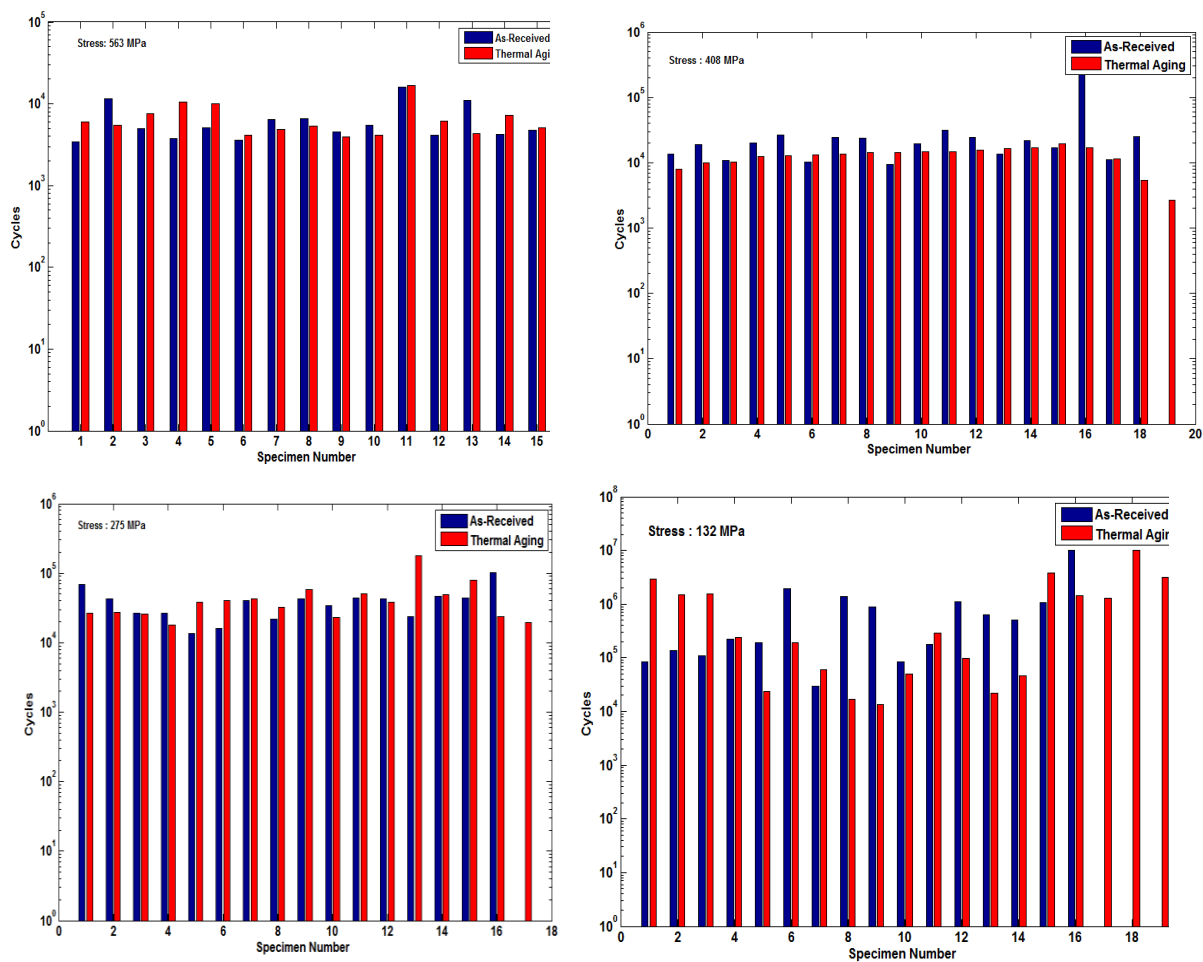


**Fig. 5.** A comparison between the fatigue lives of Incoloy alloy MA956 in both the as-received and the thermal aging conditions at different stress levels.

The S-N curve for as-received and thermal aging specimens fatigue testing are summarized in Fig. 6. These specimens were tested under various stresses. The stress



### 3.2. Microstructural characterization

The initial microstructure of both the as-received and the thermal aging conditions were characterized by SEM (scan electro microscopic) and optical microscopy. The SEM micrographs of the as-received specimen and the thermally aged specimens. Are given in Figs. 7 and 8, respectively. Micro-cracks occurred in the as-received specimen after fatigue testing was complete (see Fig. 7b).

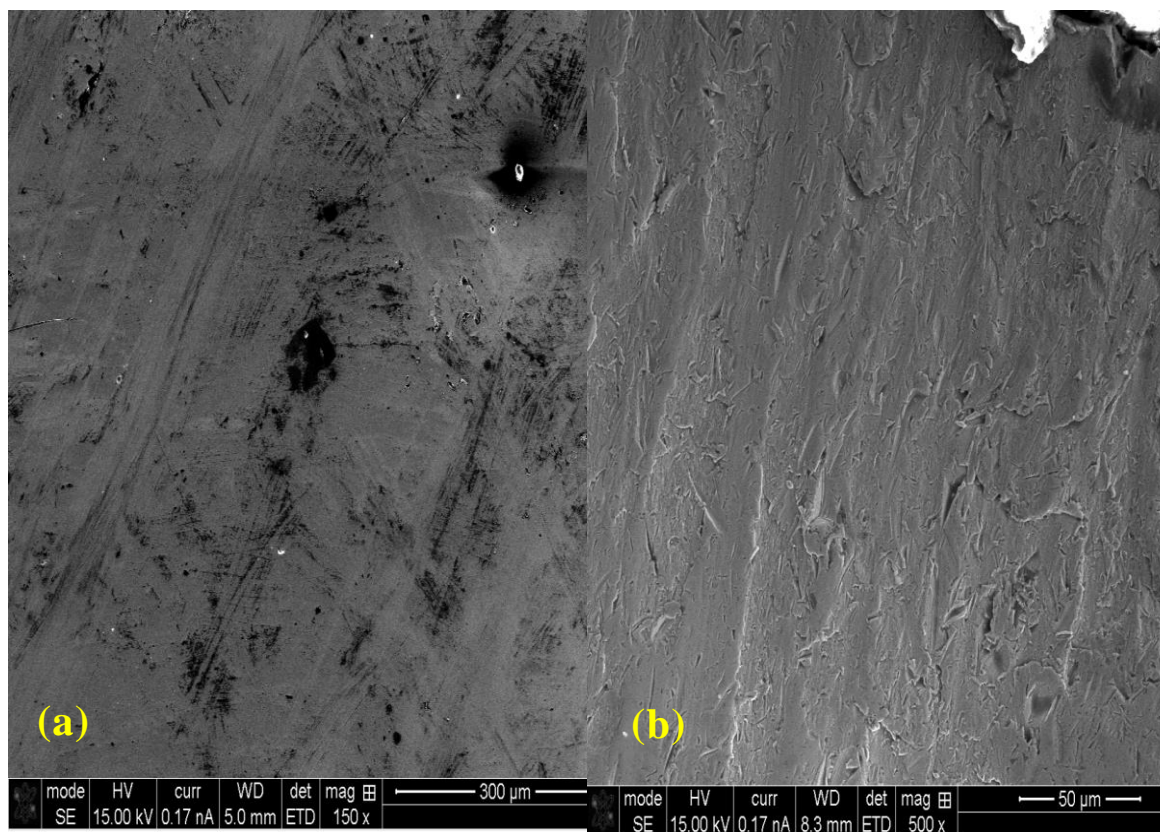


**Fig. 7.** The SEM of the as-received specimen (a) before fatigue and (b) after fatigue.

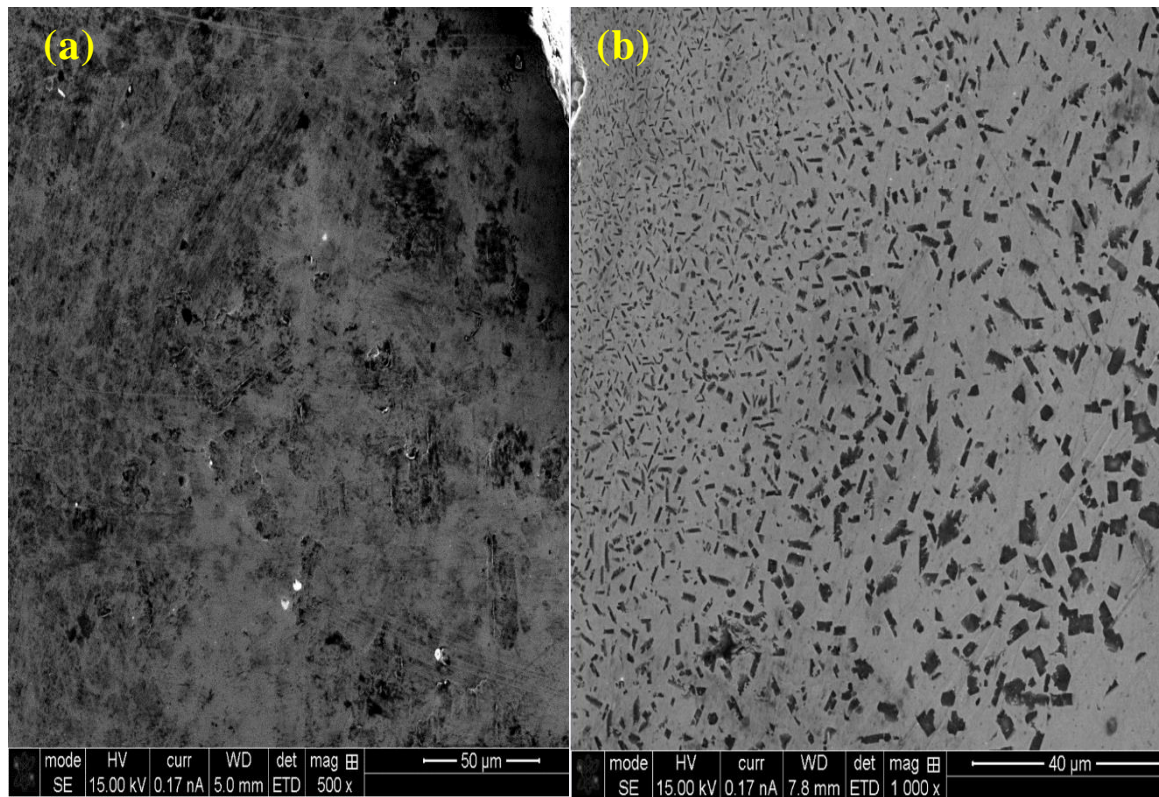


**Fig. 8.** The SEM of thermal aging, (a) before fatigue test and (b) after fatigue test.

The nuclear material's grain boundary should be studied. The grain boundary test for specimen Incoloy alloy MA956 was mounted in an epoxy resin and then polished. Aqua Regia etch was used to etch each specimen. The analysis of the grain boundary for both the as-received and the thermal aging was shown in Fig. 9.

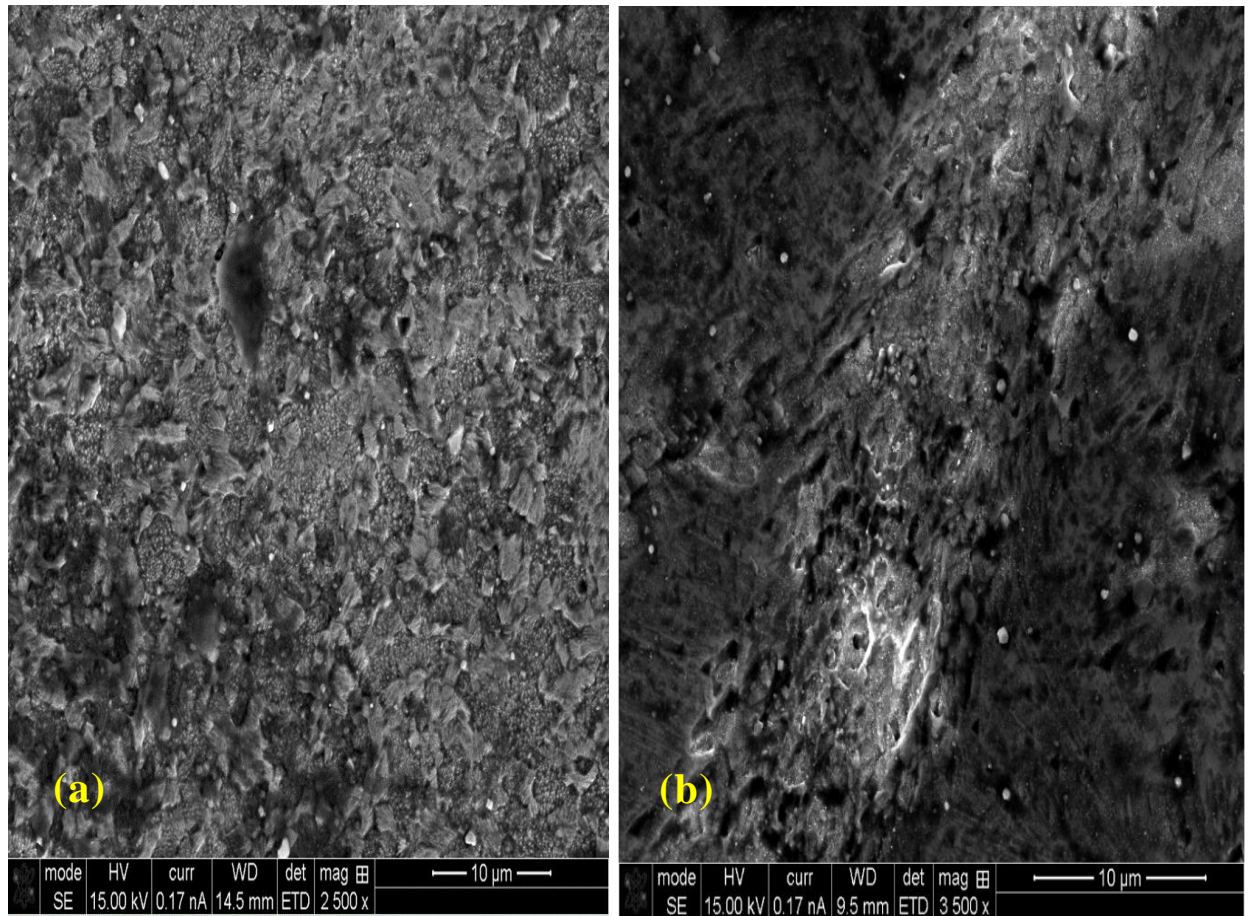
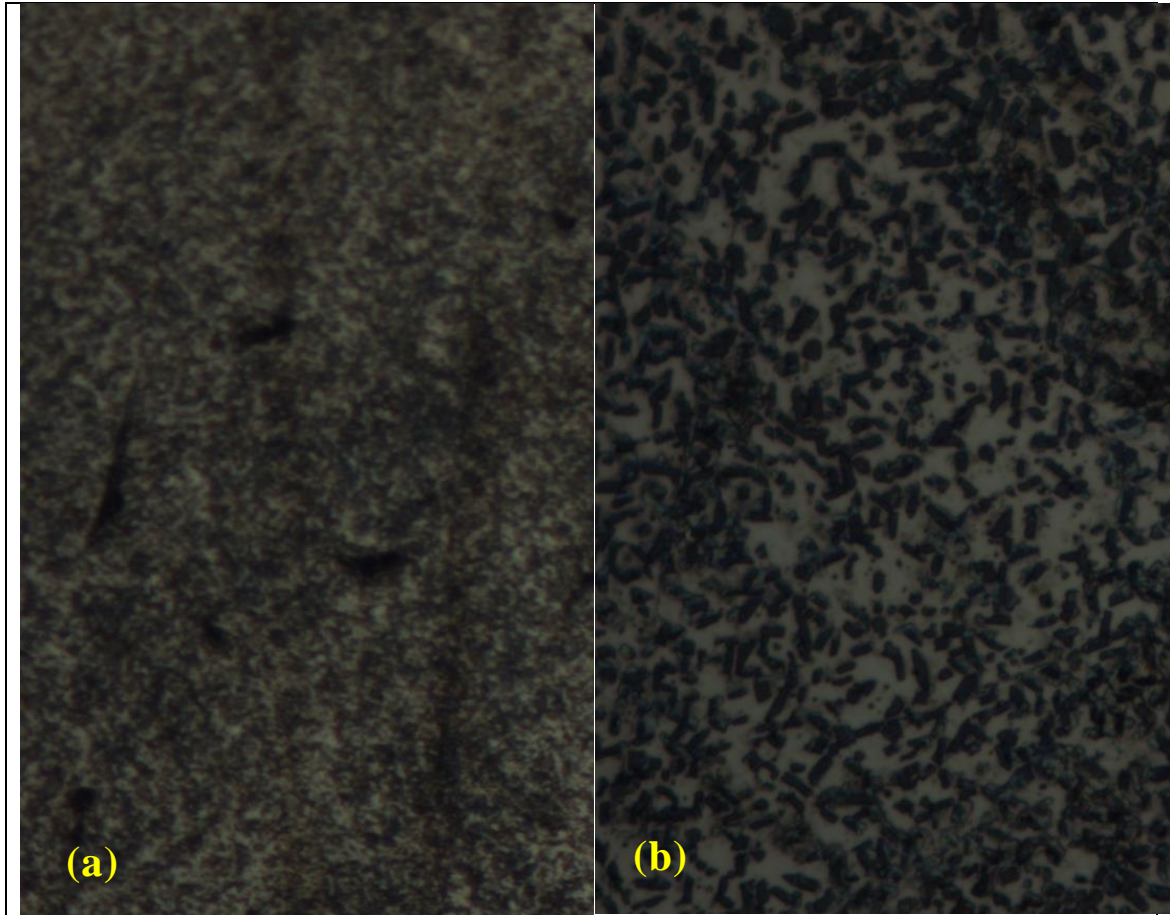


Figure 9. The SEM obtained through an etch test for (a) as-received and (b) thermal aging specimens before the fatigue test was begun.

A Comparison conducted between the as-received and the thermal aging specimens that revealed different grain boundary sizes, as pictured in Fig. 10. The thermal aging specimen's grain boundary was larger than the as-received specimen's as shown in Fig. 10.



**Fig. 10.** Optical Microscopy obtained by etch test for (a) an as-received specimen and (b) a thermal aging specimen before fatigue testing was begun.

The XRD patterns of both the as-received and the thermal aging mini-specimen are given in Fig. 11. Significant differences were noted between in each pattern. The Fe element in the as-received specimen had the strongest diffraction peak.

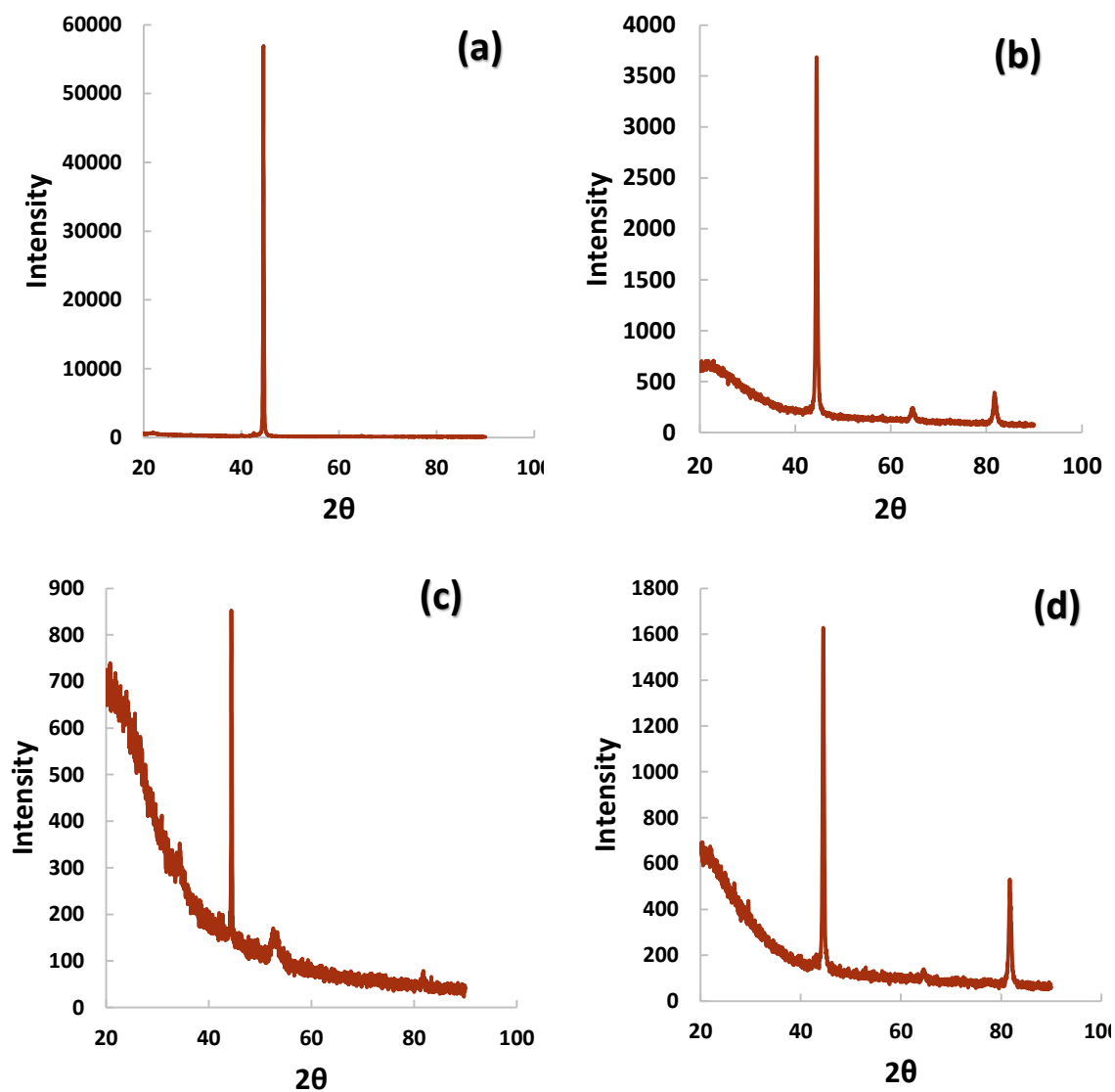


**Fig.11.** XRD patterns of (a) the as-received specimen before fatigue testing was begun (b) the as-received specimen after fatigue testing was complete, (c) the thermal aging specimen before fatigue testing was begun, and (d) the thermal aging specimen after fatigue testing was complete.



### 3.3. Irradiation damage of incoloy alloy MA956

A number of SRIM simulations were conducted on both He and H ions implanted into an Incoloy alloy MA956 specimen. These tests were conducted in an attempt to study the radiation damage inflicted on MA956 mini-specimens. The damage profile is illustrated in Fig. 12. Here, the x-axis denote the ion's penetration depth. The peak damage occurred at approximately  $3.92 \mu\text{m}$ . When irradiated with 2.3 MeV He ion and  $25.38 \mu\text{m}$  when irradiated with 2.3 MeV. The irradiation conditions is subjected to 1 dpa with 47 minutes exposure time during 2.3 MeV He ion and 1 dpa with 47 minutes exposure time using 2.3 MeV ion in Van de Graaf accelerator based on the SRIM results.

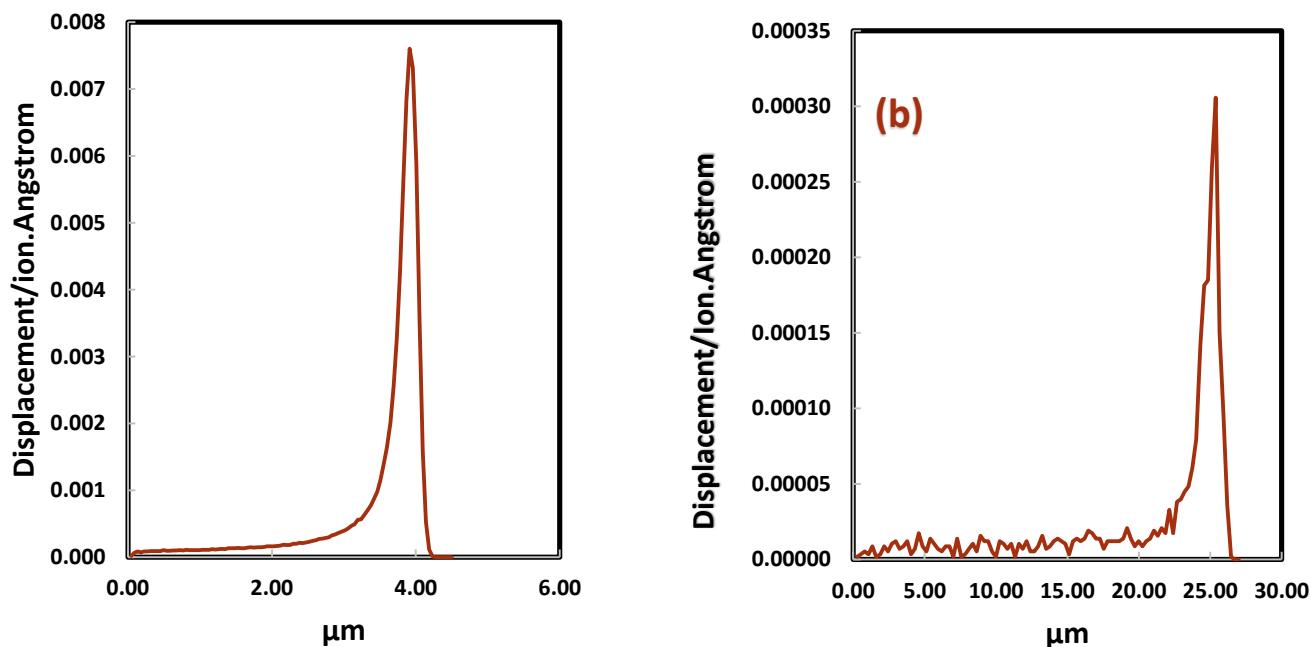


**Fig. 12.** Damage profile of Incoloy alloy MA956 steel when irradiated with 2.3 MeV (a) He ion, (b) H ion.

### 3.4. Hardness

Micro-hardness was measured at different distances with a 9.81 N indentation load. This test was conducted on the broken areas of both the as-received received and the thermal aging specimens. These specimens were mounted onto a bakelite puck and polished on the top. Hardness was then measured across the specimen's thickness. The hardness results measured at the as-received and the thermal aging area in the Incoloy alloy MA956 specimen are illustrated in Fig. 13. The as-received area had a higher hardness than did the thermal aging area at the same load.

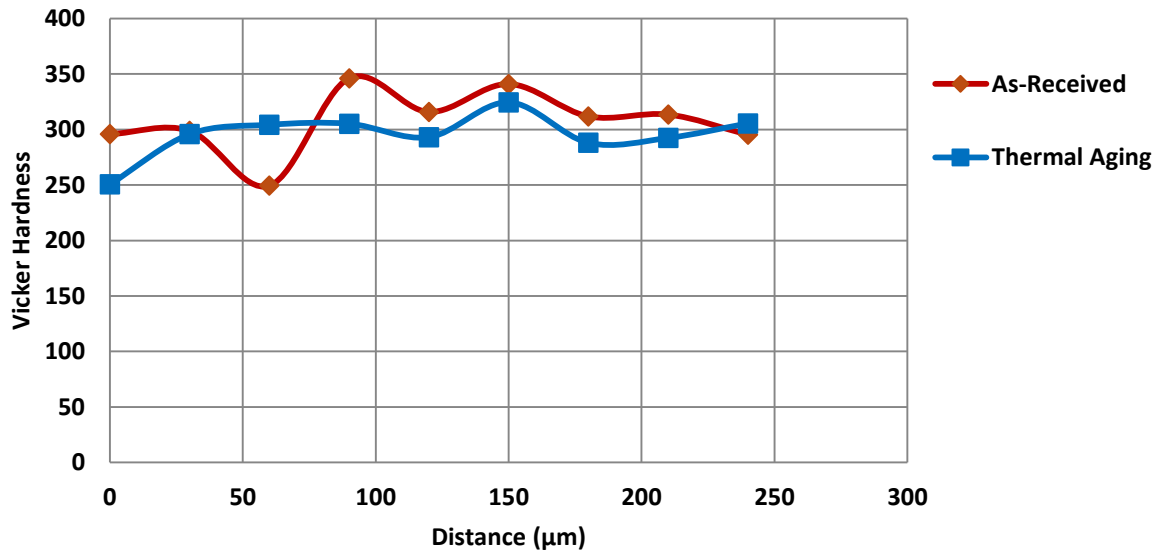


**Fig.13.** Microhardness profiles on specimen.

### 3.5. Analysis of error propagation

Perform an error propagation analysis of equation 3 as follows [21].

$$\sigma_u^2 = \left( \frac{\partial}{\partial \Delta} \left( \frac{\Delta t E}{L^2} \right) \right)^2 \cdot \sigma_D^2 + \left( \frac{\partial}{\partial t} \left( \frac{\Delta t E}{L^2} \right) \right)^2 \cdot \sigma_t^2 + \left( \frac{\partial}{\partial E} \left( \frac{\Delta t E}{L^2} \right) \right)^2 \cdot \sigma_E^2 + \left( \frac{\partial}{\partial L} \left( \frac{\Delta t E}{L^2} \right) \right)^2 \cdot \sigma_L^2 \quad (21)$$

$$\sigma_u = \pm \sqrt{\left(\frac{Et}{L^2} \cdot \sigma_\Delta\right)^2 + \left(\frac{E\Delta}{L^2} \cdot \sigma_t\right)^2 + \left(\frac{t\Delta}{L^2} \cdot \sigma_E\right)^2 + \left(-\frac{2E\Delta t}{L^3} \cdot \sigma_L\right)^2} \quad (22)$$

Table 4 shows an example of one specimen that are measured and repeated five times. The effect of specimen's dimensions on analysis error is listed in Table 4. It has been observed that most of the error is due to length (L) and deflection ( $\Delta$ ) measurements.

**Table 4**  
Error Analysis Calculation

Specimen	L	b	t	$\Delta$	$\left(\frac{Et}{L^2} \cdot \sigma_\Delta\right)^2$	$\left(\frac{E\Delta}{L^2} \cdot \sigma_t\right)^2$	$\left(-\frac{2E\Delta t}{L^3} \cdot \sigma_L\right)^2$	$\sigma_u$	$\sigma$	$\sigma \pm \sigma_u$
Measured1	5.43	3.50	1.22	0.048	1683	42	2778	67	482	482±67
Measured2	5.07	3.46	1.21	0.046	2214	57	4305	81	561	561±81
Measured3	4.85	3.48	1.22	0.049	2549	91	7261	100	696	696±100
Measured4	5.44	3.40	1.22	0.050	1640	38	2418	64	451	451±64
Measured5	4.84	3.47	1.22	0.049	2764	69	5897	93	626	626±93
Average	<b>5.126</b>	<b>3.03</b>	<b>1.098</b>	0.049	2170	59	4532	81	563	563±81
St. Dev	$\sigma_L$	$\sigma_b$	$\sigma_t$	$\sigma_\Delta$	<b>E</b>					
	0.296	0.2	0.0148	0.004	1.72E+05					

### 3.6. Statistics analysis of fatigue data

For the statistical analysis, we have chosen the cycle life data under stress level at 563 MPa, 408 MPa, 275 MPa and 132 MPa.

Table 5 represents the results of Weibull parameters for 2 and 3-paramter of the specimens for each stress level from Figs. 14 and 15. It shows that the different values of  $\beta$  and  $\eta$  at each stress level.

**Table 5**

Weibull parameters summary (SuperSmith)

Stress (MPa)	Weibull analysis							
	2-Parameter				3-Parameter			
	As-Received		Thermal Aging		As-Received		Thermal Aging	
	$\beta$	$\eta$	$\beta$	$\eta$	$\beta$	$\eta$	$\beta$	$\eta$
<b>563</b>	2.873	6844	3.173	7307	0.851	2834	0.811	2752
<b>408</b>	2.122	26299	5.197	15034	0.781	14187	5.781	16435
<b>275</b>	2.345	44242	2.313	47426	1.44	32922	0.932	26320
<b>132</b>	0.744	543222	0.625	558650	0.556	501015	0.446	513454

The value of  $\beta$  is more than one in 2-parameter Weibull analysis at 563,408 and 275 MPa stress levels and less than one at 132 MPa stress level. Fig.14 shows the longnormal distribution fit plots of the test data with 95 % confidence level. The centreline is the trend line and the outer lines are the 95% confidence level , this distribution helps us to evaluate the distribution fit by viewing how the data fall about the line. The transformations used for this distribution is  $\ln(\text{data} - \text{threshold})$  in x-axis and  $\Phi^{-1}(\text{MR})$  in y-axis, where  $\Phi^{-1}(\text{MR})$  is value returned for (MR) by the inverse CDF for the standard normal distribution and (MR) is Median Rank (Benard). The longnormal distribution at 132 MPa shows the data follow the straight line and the best plot fits for both the as-received and thermal aging conditions.

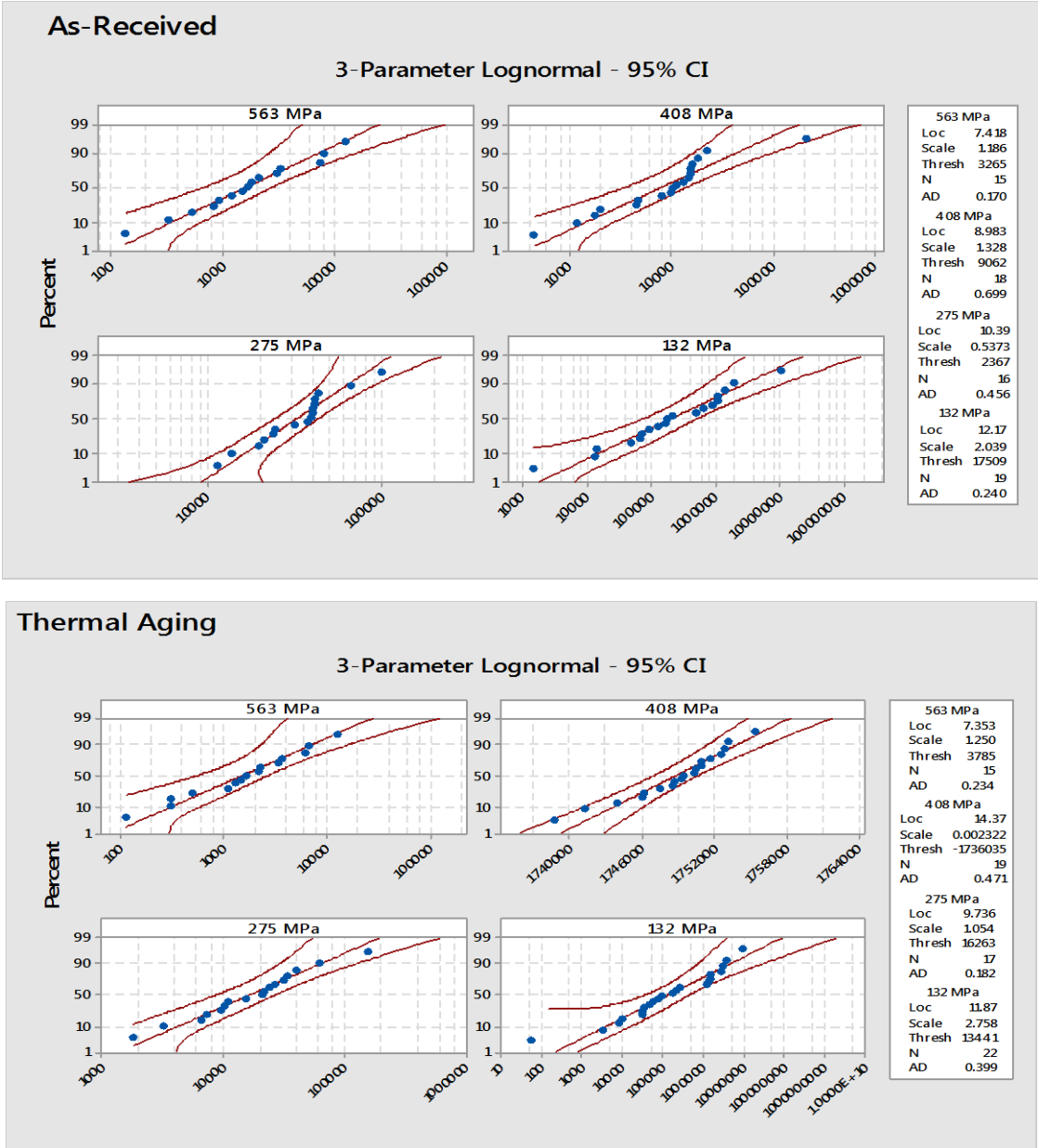


**Fig.14.** Lognormal distribution fit under stress level at 563 MPa, 408 MPa, 275 MPa and 132 MPa stress levels.

In the Minitab plots, observing that the 2-parameter Weibull is not a perfect distribution for these data than the 3-parameter as shown in the Figures 15 and 16. The 3-parameter Weibull plots show the data follow the straight line. Figs. 17 and 18 show the

probability plots that represent the same data fit to the 2-parameter Weibull and a 3-parameter Weibull distribution.

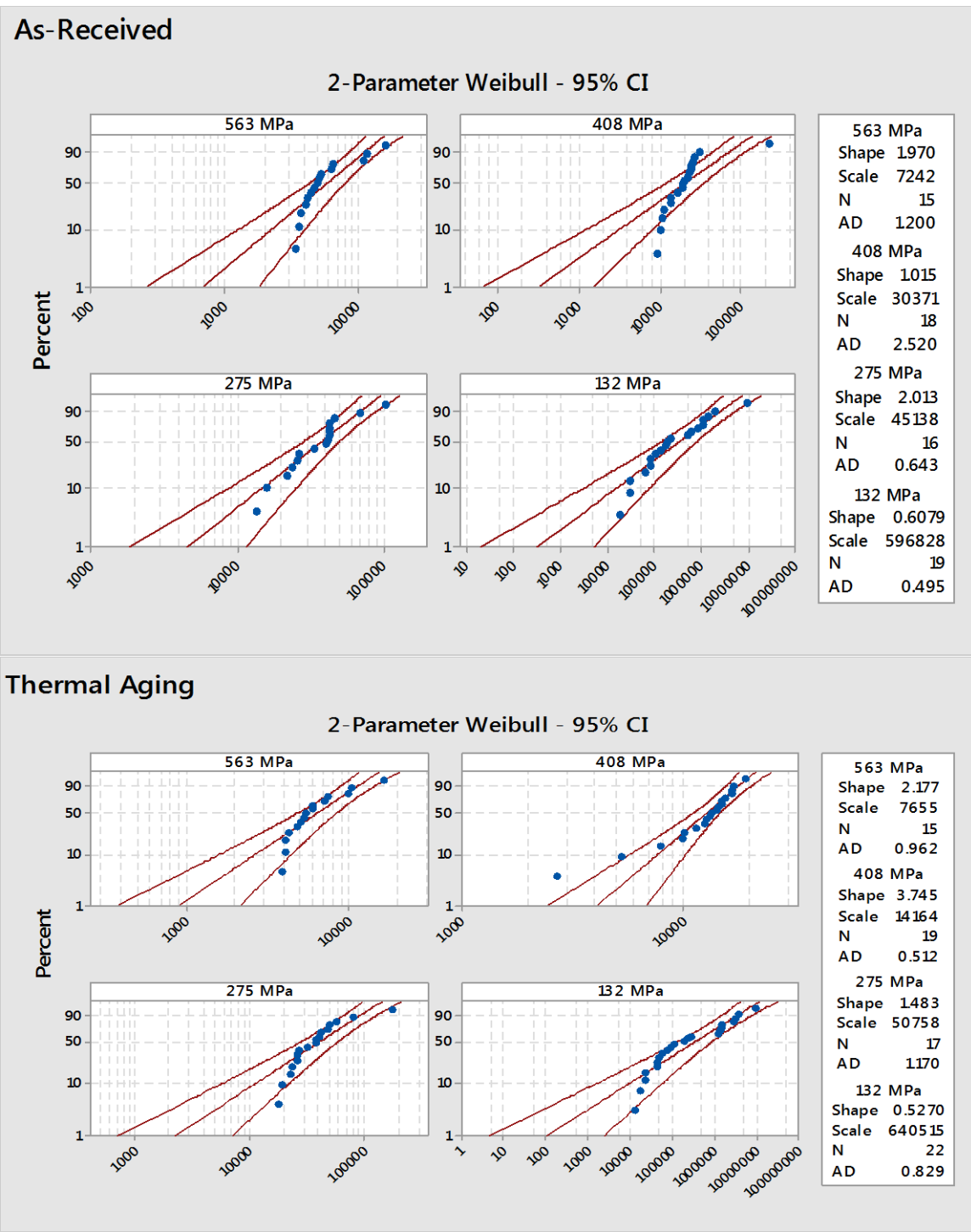


Fig.15. Probability Plot of 563 MPa, 408 MPa, 275 MPa and 132 MPa stress level.

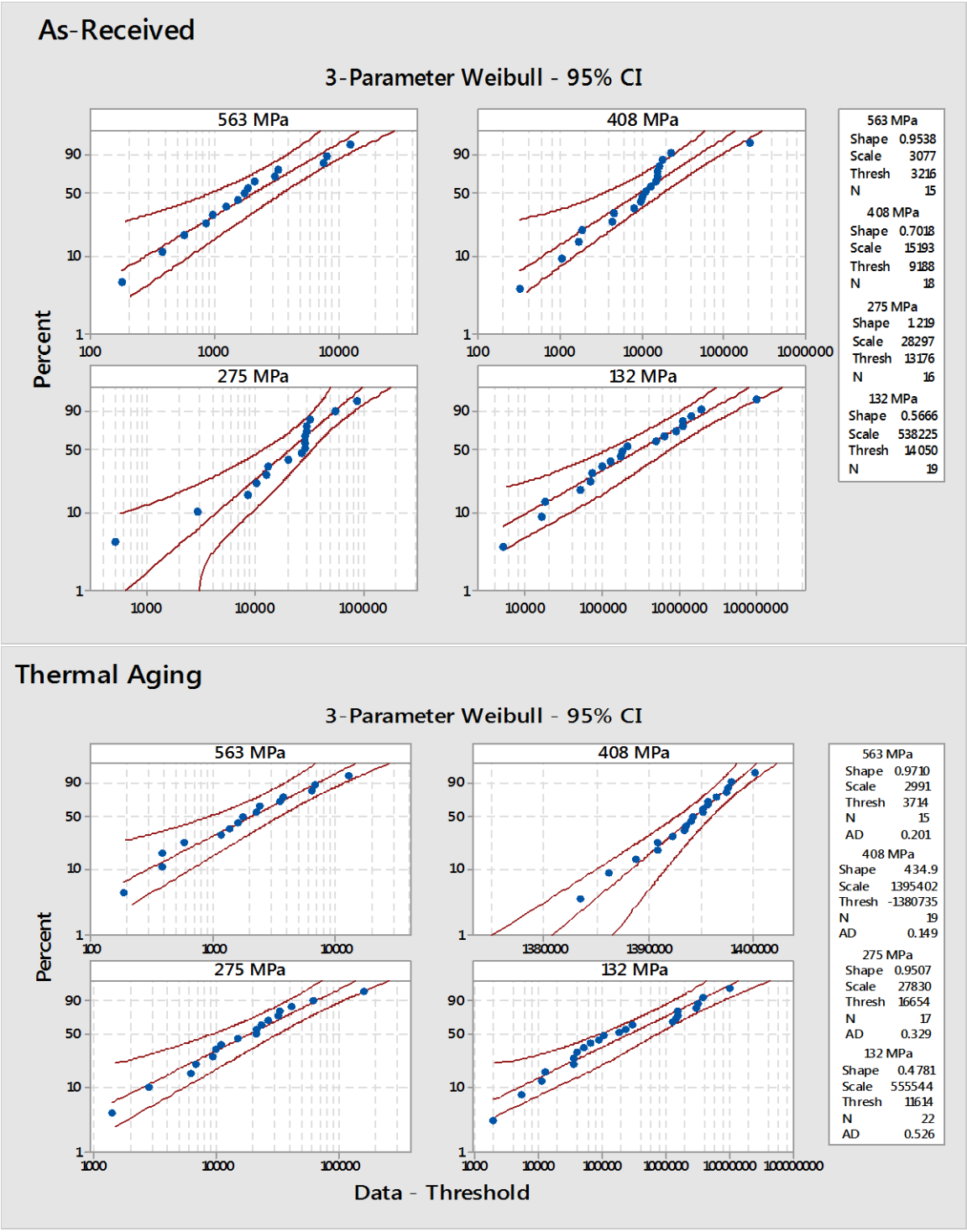


Fig. 16. Probability Plot of 563 MPa, 408 MPa, 275 MPa and 132 MPa stress level



The 2-parameter Weibull does not use the threshold parameter and displays as a curve on the probability plot. The 3-parameter Weibull corrects for threshold parameter so that the data track a straighter line.

#### **4. Conclusion and future work**

The Incoloy alloy MA956 was investigated under both at the as-received and the thermal aging conditions. A wire EDM was used to machine each specimen so that reliable fatigue measurements could be obtained. A mini-specimen technique (Krouse-type) was used to create an S-N curve under constant deflection so that the bending fatigue could be studied. The simulated stress was closer than the measured stress at both high and low stress levels. The error was higher in the length and the deflection measurements, indicating a longer sample may have produced better results.

The Weibull distribution was used to test the number of cycles obtained under four different stress levels. A decreasing shape value revealed that the measured data was more scattered and widely distributed. The data appear to fit the line well. Therefore the 3-parameter Weibull distribution is an appropriate choice for the data because it had a better fit and improved the correlation coefficient values. The longnormal distribution demonstrations that the data follow the straight line and the best plot fits for both the as-received and thermal aging conditions. An SRIM simulation was used to calculate the profile damage for Incoloy alloy MA956. It found to be around 3.92  $\mu\text{m}$  when irradiated with 2.3 MeV He ion and 25.38  $\mu\text{m}$  when irradiated with 2.3 MeV.

The fatigue life for both conditions, however, was nearly the same. Thus, the thermal aging process had little influence on fatigue life. Long-term thermal aging experiment is needed for further research. Future studies will include different nuclear materials and shaped samples, particularly longer ones. Longer samples are still considered adequate to fit in rest reactors (e.g., ATR [22]). The mini specimen (Krouse-Type) technique used to examine the Incoloy alloy MA956 specimen provided the same fatigue life for both the as-received and thermal aging compared to published data. Thus, this technique can be used to create fatigue data.

## References

- [1] N. KASAHARA, “Development of thermal load and fatigue evaluation methods based on their mechanism,” in *Working Group for advancement of Thermal fatigue evaluation methods in the NISA project*, 2012, no. May.
- [2] C. M. Obermark and R. S. Mishra, “Development of a Reversible Bending Fatigue Test Bed to Evaluate Bulk Properties Using Sub-Size Specimens.”
- [3] ASTM, “Standard Test Method for Bending Fatigue Testing for Copper-Alloy Spring Materials,” *Annu. B. ASTM Stand.*, vol. 96, pp. 3–7, 2009.
- [4] R. C. Benn, R. Benn, and P. Relationships, “Microstructure and Property Relationships in Oxide Dispersion Strengthened Alloys,” pp. 238–268, 2015.
- [5] R. B. Abernethy, *Chapter 1. an overview of weibull analysis 1.1*. 2006.
- [6] A. S. Haidyrah, C. H. Castano, and J. W. Newkirk, “An experimental study on bending fatigue test with a krouse - type fatigue specimen,” in *2014 ANS Winter Meeting and Nuclear Technology Expo*, 2014, pp. 1–4.
- [7] AZoM.com Staff Writers, “INCOLOY Alloy MA956,” 2013. [Online]. Available: <http://www.azom.com/article.aspx?ArticleID=9513>.
- [8] Joseph R. Davis, *ASM Specialty Handbook: Heat Resistant Materials*. ASM International (May 1, 1997), 1997.
- [9] S. Dongare, F. Liou, and J. W. Newkirk, “Development of a Technique for Testing of Tensile Properties with Miniature size specimens for metal additive manufacturing,” Missouri University of Science & Technology, 2012.
- [10] M. Sivapragash, P. R. Lakshminarayanan, R. Karthikeyan, K. Raghukandan, and M. Hanumantha, “Fatigue life prediction of ZE41A magnesium alloy using Weibull distribution,” *Mater. Des.*, vol. 29, no. 8, pp. 1549–1553, Jan. 2008.
- [11] A. S. Haidyrah and C. H. Castano, “Bending Fatigue Mini-Specimens (Krouse Type) for Nuclear Materials,” in *Poster presented at Third International Workshop on Structural Materials for Innovative Nuclear Systems (SMINS-3)*, 2013, p. 1.
- [12] Ahmed S. Haidyrah, J. W. Newkirk, and C. H. Castano, “Characterization a Bending Fatigue Mini-Specimen Technique (Krouse Type) of Nuclear Materials,” in *2015 TMS Annual Meeting & Exhibition*, 2014, pp. 1–8.
- [13] Robert R. Fuczak, “The Effects of Fatigue Loading Frequency on Fatigue Life of High-Strength Pressure Vessel Steels,” WATERVLIET, N.Y. 12189-4050, 1994.

- [14] K. Berchem and M. G. Hocking, “A simple plane bending fatigue and corrosion fatigue testing machine,” *Meas. Sci. Technol.*, vol. 17, pp. N60–N66, 2006.
- [15] Fatigue Dynamics Inc., “Instruction Manual Model LFE-150 Variable Speed Life,Fatigue analysis.pdf.” Walled Lake ,MI 48390, p. 47.
- [16] C. Lipson and N. J. Sheth, *Statistical Design and Analysis of Engineering Experiments*, First Edit. McGraw-Hill Book Company, 1973.
- [17] R. Sakin and İ. Ay, “Statistical analysis of bending fatigue life data using Weibull distribution in glass-fiber reinforced polyester composites,” *Mater. Des.*, vol. 29, no. 6, pp. 1170–1181, Jan. 2008.
- [18] W. M. Group, “Product Excellence using 6 Sigma ( PEUSS ) W e i b u l l a n a l y s i s,” .
- [19] M. Teimouri and A. K. Gupta, “On the Three-Parameter Weibull Distribution Shape Parameter Estimation,” vol. 11, pp. 403–414, 2013.
- [20] R. F. Stapelberg, *Handbook of Reliability, Availability, Maintainability and Safety in Engineering Design*. 2009.
- [21] G. F. Knoll, *Radiation Detection and Measurement*, vol. 2006. Wiley, 2000.
- [22] J. R. Kennedy, S. Robertson, R. Soelberg, and C. Knight, “ATR NSUF,” 2013.

## V. A comparison of bending fatigue specimens (Krouse - type) for nuclear materials.

Ahmed S. Haidyrah<sup>1</sup>, Joseph W. Newkirk<sup>2</sup>, Carlos H. Castaño<sup>1†</sup>

<sup>1</sup>Nuclear Engineering, Missouri University of Science & Technology, 301 W. 14th St.,  
Rolla, MO, USA 65409

<sup>2</sup>Materials Science & Engineering, Missouri University of Science & Technology, 1440  
N. Bishop Ave, Rolla, MO, USA 65409

**Keywords:** bending fatigue test, bending fatigue mini specimen, S-N curve, Krouse–type specimen.

### ABSTRACT

Results are presented from a comparison of bending fatigue (Krouse-type) mini specimens to study the fatigue properties of nuclear materials. The initial specimen in this study is a Krouse-type mini specimen called specimen type-1. The objective of this paper is comparing this initial model with three other specimen types to verify the bending fatigue technique for 304 stainless steel suitable for reactor irradiation studies. These specimens are different in size and similar in design to that described in the ASTM B593 standard. A finite element model code ABAQUS is used to compute the stress and deflection for each models. The simulation results illustrate that the value of stress and deflection is influenced by the size and the geometry of each models. This study was conducted to evaluate the high cycle bending fatigue behavior of 304 stainless steel and compare its bending properties with simulations conducted with the ABAQUS. The S-N fatigue results were affected by size difference and bending fatigue reported values for model-1 (Krouse-type) mini specimen was lower than the North American Stainless Steel NASS curve for 304 stainless steel.

---

† Corresponding author. Tel:+1 (573) 341-6766

E-mail address: Email: [castanoc@mst.edu](mailto:castanoc@mst.edu) (Carlos H. Castaño)

## Introduction

Fatigue is a failure process where a material is subjected to cyclic stresses. It is important in the development of nuclear materials for both current and future power plants. Fatigue properties can be used in the prediction of the behavior and lifetime performance of reactors components under oscillating load conditions. Unfortunately, full size samples are too bulky for irradiation in high flux experimental reactors (such as the Advanced Test Reactor, ATR or the High Flux Isotope Reactor, HFIR). Bending fatigue tests of mini-specimens might be the best compromise as it provides a uniform stress distributed in the test specimen and can fit experimental reactors [1]. A material subjected to bending fatigue is repeatedly bend until it breaks. The number of cycles before it breaks is recorded and plotted against the bending stress. The specimen type-1 Krouse-type specimen used as the basis for this study has proportions similar to an ASTM B893 standard [1] although smaller in size [2]. This research was conducted to understand the effect of bigger size and higher volume testing volumes, which reduce surface effects and produce a more reliable fatigue measurement. The main objective is to compare specimen type-1 (mini-specimen Krouse-type) technique with three other form factors. We have used 304 stainless steel in the past to verify the (Krouse-type) fatigue technique with mini-specimens[3]. LEF-150 and VSS40H machines (from Systems Integrators L.L.C) were used to produce an S-N curve. The machine was preset to produce a constant amplitude cyclic motion at an adjustable preset stroke (the machine allows any stroke between zero and two inches). The present stroke permits to calculate the stress to the sample during bending [4]. The 3 specimen types were compared by producing typical S-N curves for 304 stainless steel. We compared against a typical S-N curve for 304 stainless steel with full-size specimens done by North America stainless steel corporation (NASS) [4]. Krouse -specimen types-1, 2, 4 were tested as received and after thermal aging, while specimen type-3 was tested as received. Finite element analysis (FEA) code an ABAQUS was conducted to find out the area under stress and deflection for each model. Each specimen type was subjected to a load of 15 newtons so as to compare the difference between these models. There was no treatment on the surface and the specimens were tested as received [5].

## Experimental procedure

### Specimens

Specimens were modified from the dimensions recommended by the ASTM standard B593 [2]. Krouse-type specimens were machined with waterjet. The bending is calculated by drawing two straight lines from a point of load where it is a point of application of force on the specimen along the edges intersect [3]. All specimens' dimensions were measured using a digital caliper with a precision of  $\pm 25 \mu\text{m}$ . The geometry of Krouse-type specimen types are illustrated in Figs.1, 2, 3 and 4.

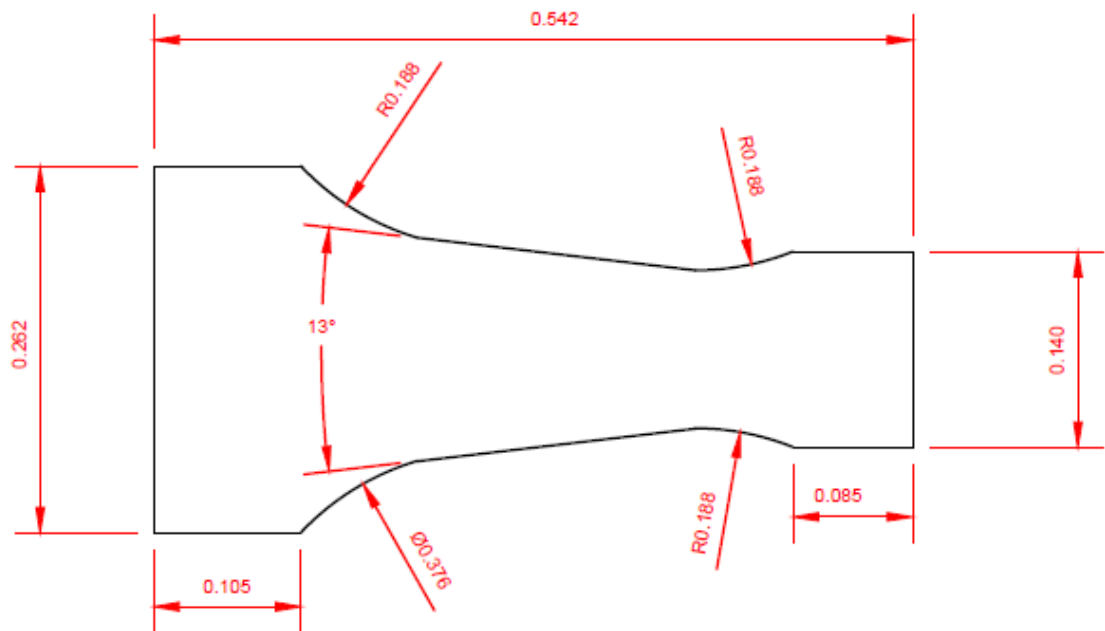


FIG.1- Sketch of specimen type-1 (all dimensions are in inches).

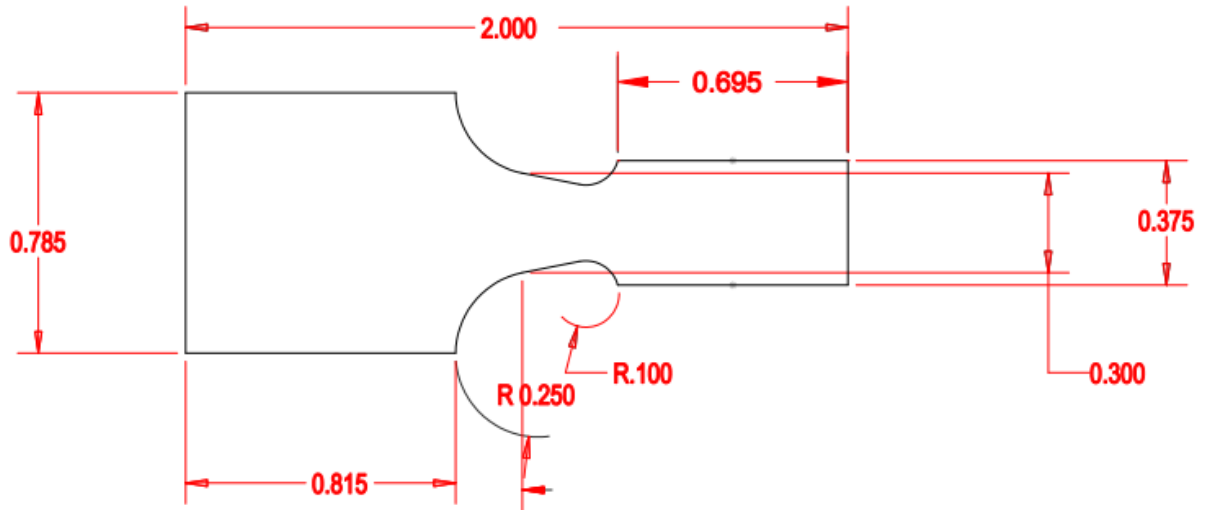


FIG. 2- Sketch of specimen type-2 (all dimensions are in inches).

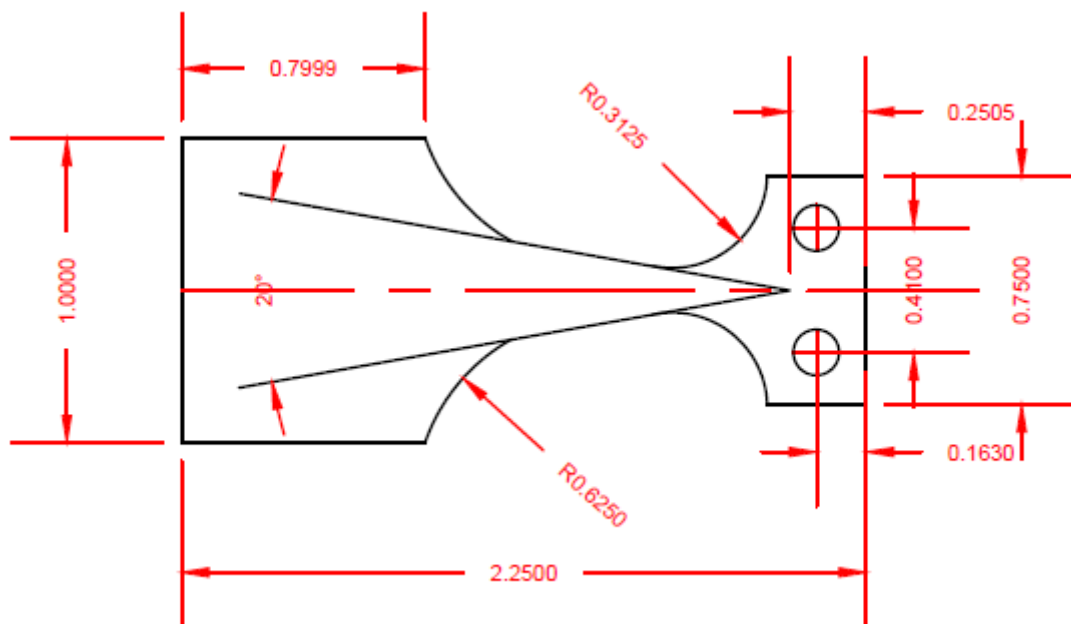


FIG. 3- Sketch of specimen type-2 (all dimensions are in inches).

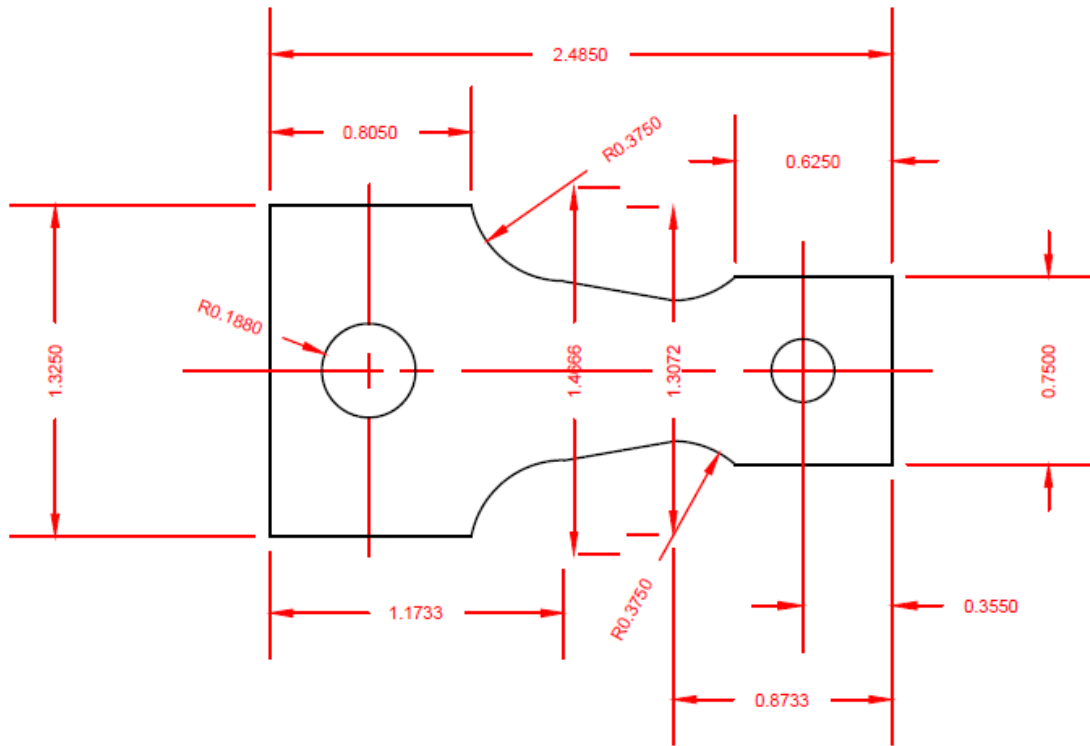


FIG.4- Sketch of specimen type-2 (all dimensions are in inches).

The bending stress can be calculated with the following equation:

$$\sigma = \frac{DEt}{L^2} \quad (1)$$

where  $\sigma$  is the desired bending stress in MPa,  $L$  is the distance between the connecting pin (apex of triangle) and the point of load in mm. The specimen thickness in mm is represented by  $t$  and  $D$  is the deflection in mm, and  $E$  is the modulus of elasticity. The force value can be calculated as

$$P = \frac{\sigma t^2 b}{6L} \quad (2)$$

where  $P$  is the force in Newton and the width of the specimen at a distance  $L$  from the point of load application in mm is represented by  $b$ .



The formula for the deflection of a triangular shape is [6]:

$$\Delta = \frac{SL^2}{Et} \quad (3)$$

where  $\Delta$  is the deflection in mm, and E is the modulus of elasticity in MPa. The triangular shape is advantageous because the stress is constant along the length of the test section.

### Material and specimen preparation

The chemical composition and mechanical properties of 304 stainless steel[7] are listed in Tables 1 and 2.

TABLE 1- *Chemical composition (in wt %) of 304 stainless steel.*

Composition	304 Stainless steel
Chromium	18-20
Nickel	8-12
Carbon	0-0.08
Manganese	0-2
Copper	0-1
Molybdenum	0-1
Silicon	0-1
Phosphorus	0-0.03
Sulfur	0-0.045
Cobalt	0-0.2
Nitrogen	0-0.1
Iron	Remaining percentage

TABLE 2- *Mechanical properties of 304 stainless steel.*

<b>Properties</b>	
<b>Modulus of Elasticity, MPa</b>	1.93x 10 <sup>5</sup>
<b>Ultimate Tensile Strength, MPa</b>	517-620
<b>Yield Strength, MPa</b>	206-275
<b>Hardness, HRB</b>	80-99
<b>Density , g/cm<sup>3</sup></b>	8.027

The specimens were cut from 304 stainless steel sheet with a thickness of 0.075in (1.905). The 304 stainless steel sheet was then machined with water jet to generate the Krouse-type specimens as shown in Fig. 5. All these specimen types would fit irradiation positions in the ATR.

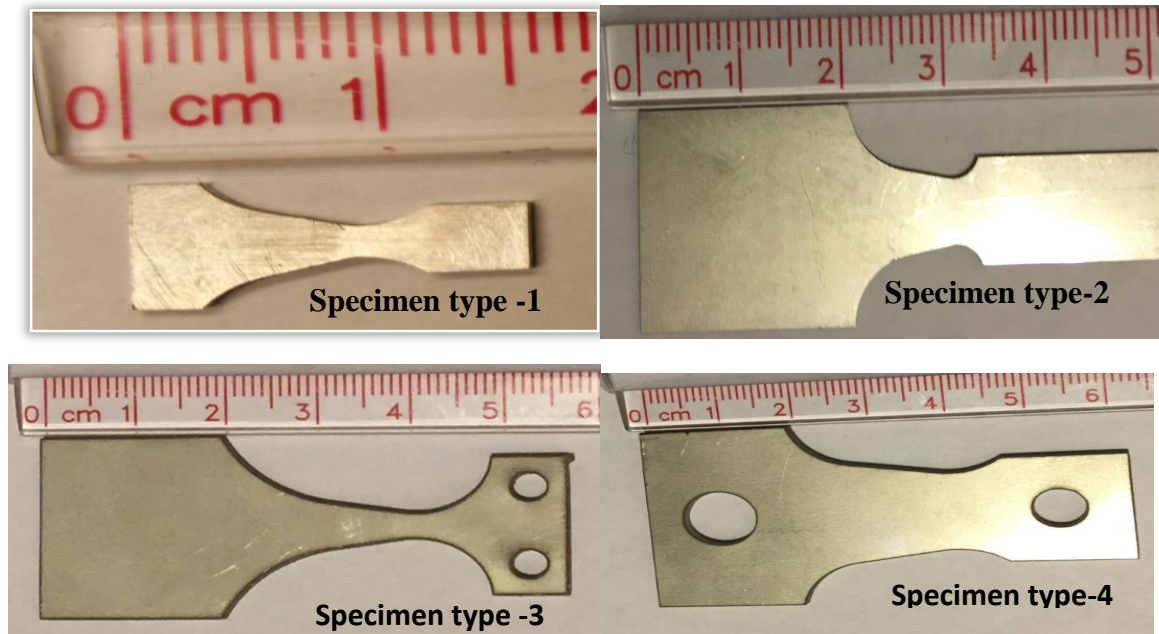


FIG. 5- *Physical geometry of specimen types.*

### **Thermal aging treatment**

Short-term thermal aging treatment was conducted in this study for specimen type-1, 2 and 4. The thermal treatment consisted of heating the specimens to 1000 °C and holding this temperature for 8 hours. The objective of this thermal treatment is to simulate long term operation of the nuclear materials in a nuclear reactor, since the design lifetime of the nuclear reactor is 60 years.

### **Bending fatigue test**

A LEF-150 and a VSS-40H bending fatigue machines were used to generate the S-N curve of the 304 stainless steel as shown in Fig. 6 [6]. The fatigue tests were carried out at 60 Hz with a ratio of minimum stress to maximum stress in one cycle of loading ( $R = -1$ ) and all tests were made at room temperature. Each specimen type was loaded in the unit and a deflection was set. The wide end was clamped to the bed plate (vise) while the narrow end was cyclically deflected. The sample is run until the fatigue crack had propagated through the specimen. The length of the crank stroke is adjusted until the desired loads are obtained

and a new specimen is tested. A digital gauge (with a precision of  $\pm 25 \mu\text{m}$ ) was used to measure deflection. The relationship between the specimen's deflection and the stroke was verified to be linear (as expected).

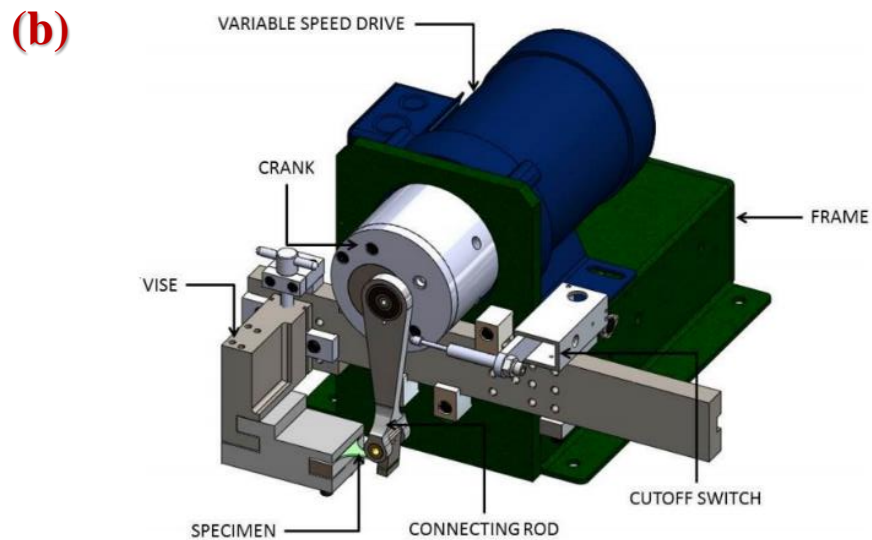
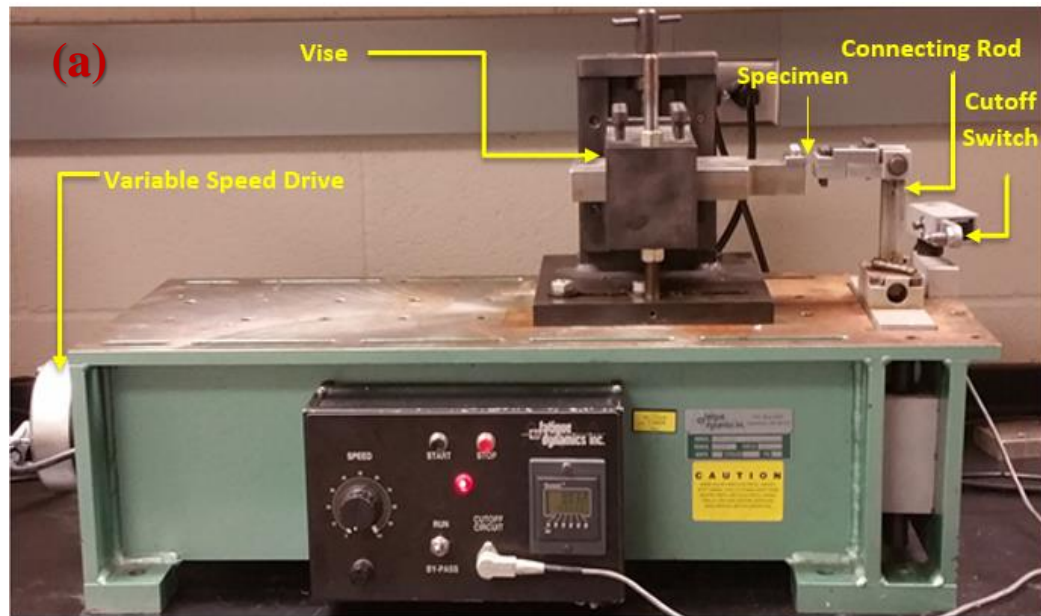


FIG.6- Experiment device of bending fatigue, (a) LEF-150 bending fatigue machine, (b) VSS-40H bending fatigue machine.

## Finite element model results

Analysis of maximum stress of the specimen types are shown in Fig. 7.

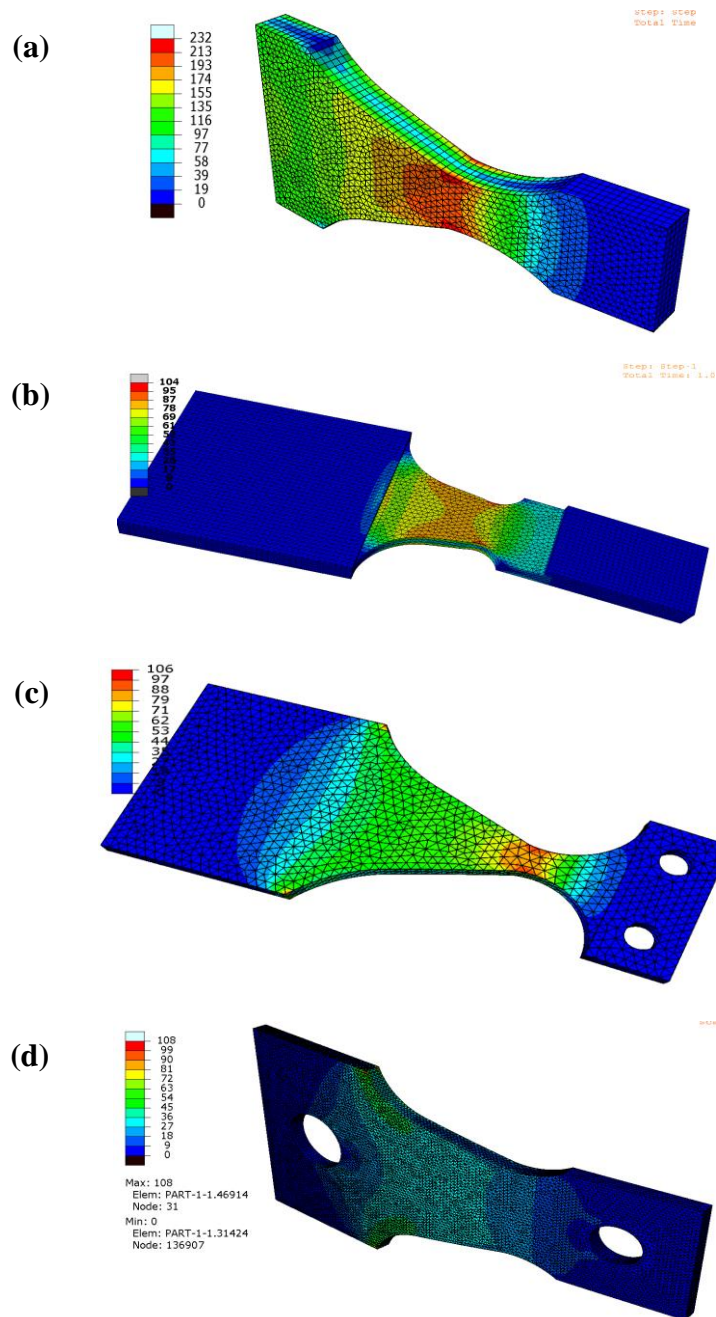


FIG. 7- Stress analysis for the specimen types (a) specimen type-1, (b) specimen type-2, (c) specimen type-3, and (d) specimen type-4.

The finite element model in ABAQUS 6.12 [8], was used to compute the stress in the specimens for 304 stainless steel. The Krouse-type specimen types were simulated with a 15 newton load and the analysis confirms the effect of specimen size on the value of stress, i.e. as the size of specimen reduces, the value of stress each specimen type increases.

### **Results and discussion**

The bending fatigue data for the specimens were recorded and plotted. The model's geometry and material properties were used to calculate the stress for each specimen [2]. Equation 1 was used to calculate the bending stress. The bending fatigue behavior of 304 stainless steel is presented in Figs 8, 9, 10 and 11. Fig. 8 presents the S-N curve experimental and the S-N typical (NASS) curve for specimen type -1 (the target specimen) for the as-received and thermal aging conditions. The bending fatigue stated that the values for 304 stainless steel were lower than the typical S-N curve for both conditions with 87 MPa endurance limit.

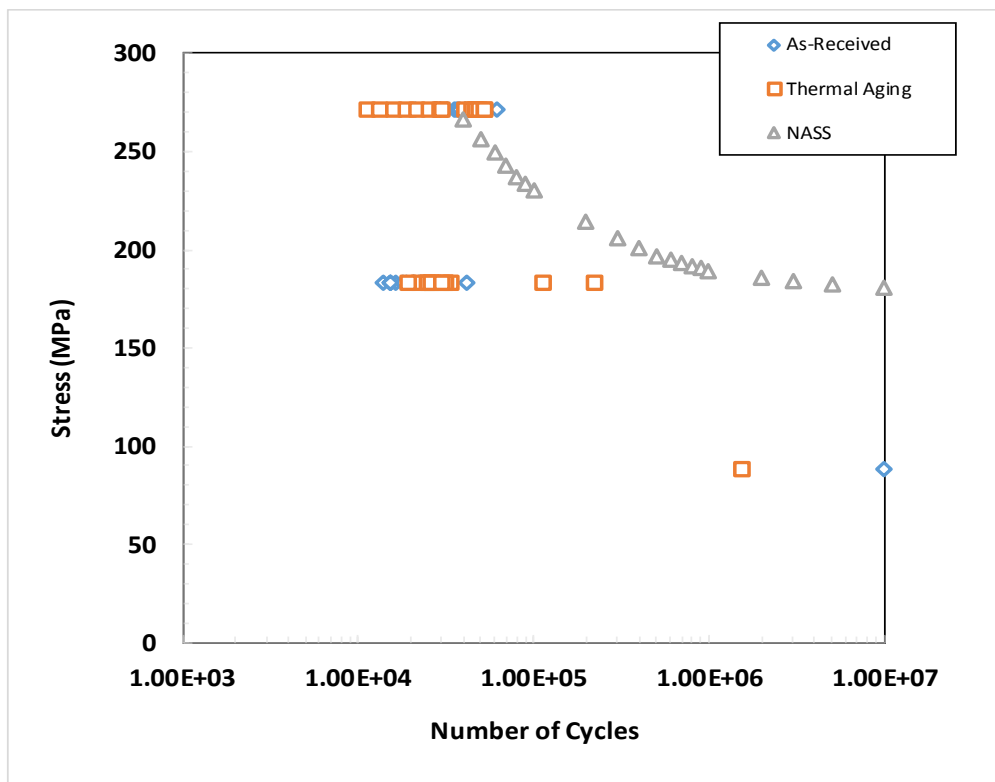


FIG. 8- Results for specimen type-1 for 304 stainless steel compared with typical 304 stainless steel.

Fig.9 shows already a better agreement between experimental and typical (NASS) for S-N curve for the as-received and thermal aging conditions for specimen type 2. In addition, there are no significant differences in fatigue life between the as-received and thermally aged at 1000 °C for 8 hours for specimen type -2.

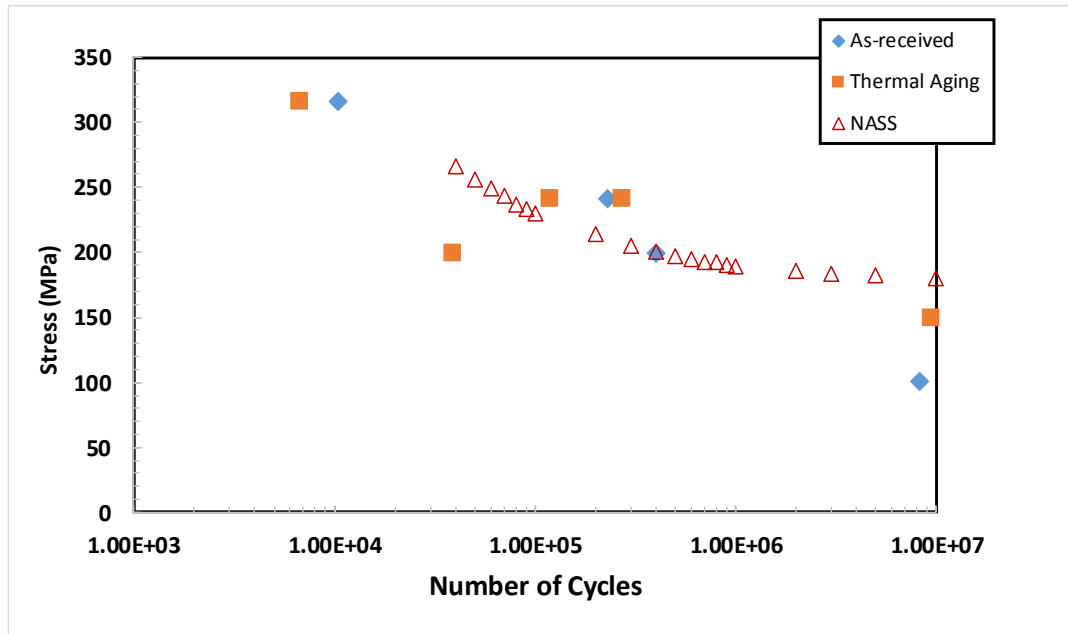
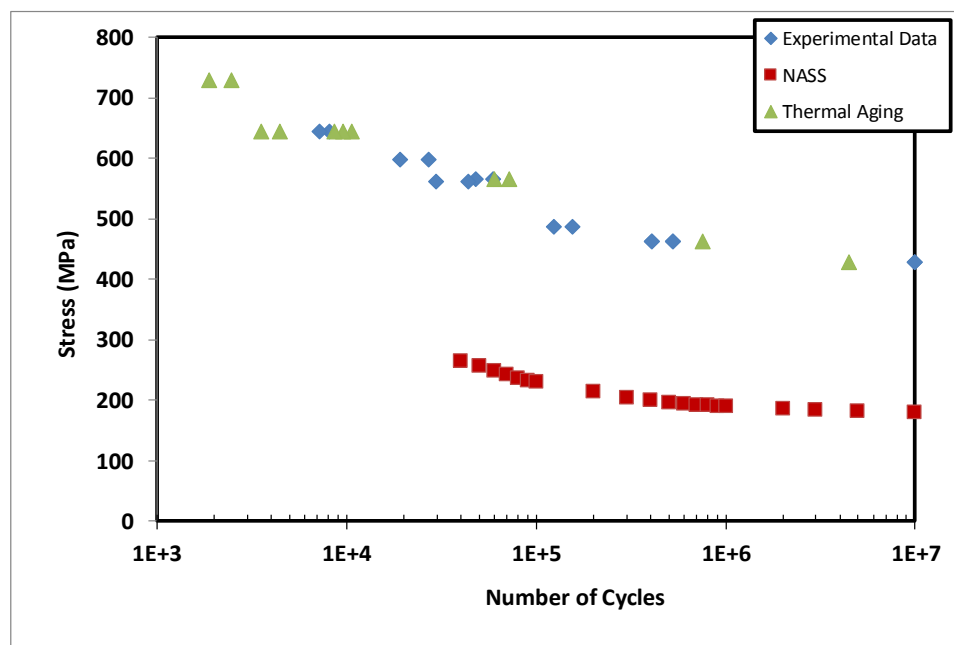


FIG. 9- Results for specimen type-2 for 304 stainless steel compared with typical 304 stainless steel.

The S-N curve for specimen type-3 was too spread than the NASS curve and average percentage error of stress between two curves was high by 119 %.





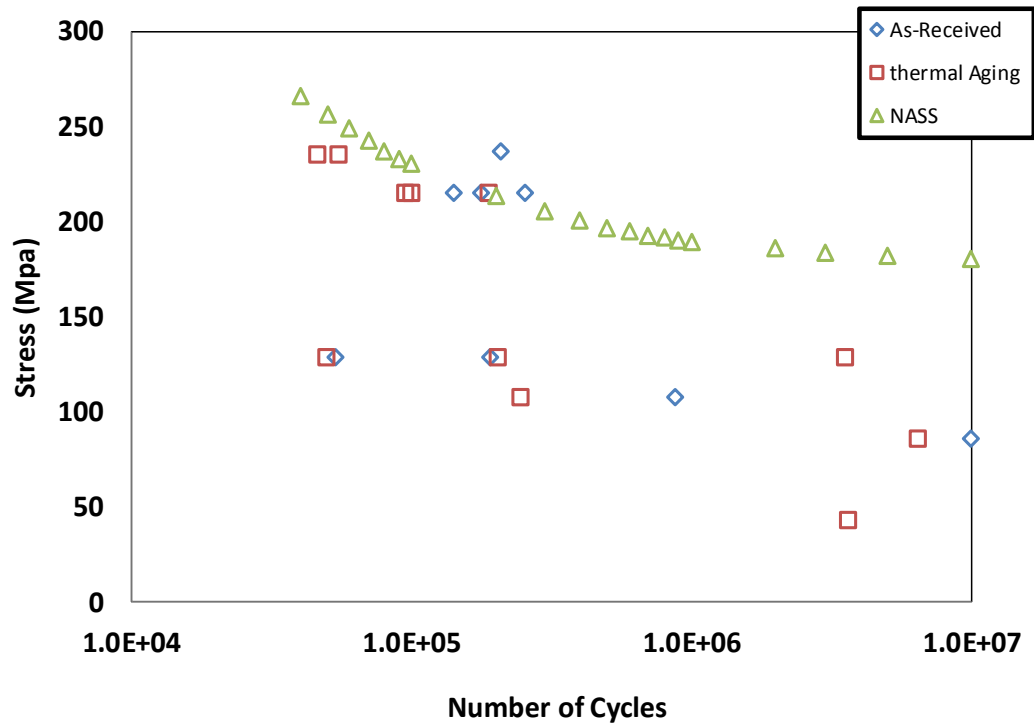


FIG. 11. Results for model 2 for 304 stainless steel compared with typical stainless steel 304L

The result comparison revealed that the stress value for each specimen types were influenced by the geometry and size of specimen. Table 3 illustrates the comparing between FEA simulated and experimental results. The stress was calculated by using equation 1 and 3. It is observed that the higher percentage error for stress correspond to specimen type -1 by 43.10 %.

TABLE 3 - *Simulated and experimental comprising results*

Specimen type No.	ABAQUS simulation MPa	Experiment MPa	% error
1	232	132	43.10
2	104	61	41.34
3	47	56	19.15
4	108	72	33.33

Table 4 shows the error analysis for each specimen type. The measurements were made for one specimen and repeated five times in order to reach a good estimate of the true stress value. The effect of specimen's dimensions on analysis error is listed in Table 4 and it has been observed that the most of the error was in specimen type-1.

Table 4. Error Analysis Calculation [9]

Specimen type #	L	b	t	P	$\left(\frac{6P}{bt^2} \cdot \sigma_L\right)^2$	$\left(-\frac{6PL}{t^2b^2} \cdot \sigma_b\right)^2$	$\sigma_u$	$\sigma$	$\sigma \pm \sigma_u$
1	5.13	3.03	1.903	15	5.98	7.80	4	44	42 ± 4 MPa
2	19.45	8.17	1.903	15	0.62	1.20	1	59	59 ± 1 MPa
3	16.52	7.45	1.903	15	1.06	0.33	1	55	55 ± 1 MPa
4	57.85	19.76	1.903	15	0.005	0.20	0.45	73	73 ± 0.45 MPa

It can be seen from this analysis, the amount of the errors are depend on the measurement accuracy of length (L) and width (b) of the specimen.

## Conclusion

Fatigue life is influenced by the variation of the stress value for each Krouse-type. This variation comes from the differences in size for each specimen type. The obtained results from the experimental and simulation were carried out in four specimen types. These types have different in geometries and validate with typical S-N curve made by NASS. The comparison between FEA simulated and experimental was observed that the higher percentage error for stress was in specimen typed-2 by 43.10 % . The results of experimental data for Krouse-type specimen of the specimen type-1, 3 and 4 have been found to be different with the NASS data and in good agreement in specimen type -2. The specimen type -1 is the target specimen for our technique and show the measured fatigue life was lower than the NASS under constant deflection. While the fatigue results were not much influenced by short-term thermal aging. The fatigue results were too spread to obtain good S-N curves in specimen type-3. These results indicate the need for additional material testing and substantial further research is required. Future work will include studying the primary fracture surface of each specimen type to determine the level and morphology of failure.

## References

- [1] ASTM, "Standard Test Method for Bending Fatigue Testing for Copper-Alloy Spring Materials," *Annu. B. ASTM Stand.*, vol. 96, pp. 3–7, 2009.
- [2] C. M. Obermark and R. S. Mishra, "Development of a Reversible Bending Fatigue Test Bed to Evaluate Bulk Properties Using Sub-Size Specimens."
- [3] A. S. Haidyrah, C. H. Castano, and J. W. Newkirk, "An experimental study on bending fatigue test with a krouse - type fatigue specimen," in *2014 ANS Winter Meeting and Nuclear Technology Expo*, 2014, pp. 1–4.
- [4] North American Stainless, "Flat Products Stainless Steel Grade Sheet," Ghent, KY 41045-9615.
- [5] Y. Katoh, "Effect of Specimen Size on Fatigue Properties of Reduced Activation ferritic/ Martensitic Steel," pp. 535–545, 2001.
- [6] Fatigue Dynamics Inc., "Instruction Manual Model LFE-150 Variable Speed Life,Fatigue analysis.pdf." Walled Lake ,MI 48390, p. 47.

- [7] McMaste-Carr, "More About Stainless Steel Alloys," 2010.
- [8] DS Simulia, "Abaqus CAE User's Manual (6.12)," p. 1174, 2012.
- [9] Glenn F. Knoll, *Radiation Detection and Measurement*. 2010.

## 5. CONCLUSION & FUTURE WORK

This research investigated the testing and bending fatigue of mini specimen (krouse-type) for any materials using the proposed setup of the new and small machine and modified exist machine to produce bending fatigue in a mini specimen size. All experiments were undertaken and carried out using stress ratio ( $R = -1$ ) with frequency 60 Hz to ascertain the krouse-type fatigue specimen for materials under constant deflection

The first research was to ascertain if krouse-fatigue specimen under constant deflection had any nuclear material. The initial design was modified using a bending fatigue machine. The results of using this showed a lower stress levels that what were accepted or typical S-N curve for stainless steel stainless steel 304 L and it also supported the need for additional nuclear material testing and research.

The second research was prepared to confirm if bending fatigue mini-specimen technique (krouse-type) could generate the S-N curve for HT9 under constant deflection. The measured data for fatigue life lower was lower than what is accepted for 304 stainless steel for polished mini specimens. From the observations the results were as a result of polishing the surface which was supposed to spread to obtain a good S-N curve. As such the need for further testing for new specimen with higher volumes to try and reduce surface effects that will result to more reliable fatigue measurements that is suitable for mini specimens. To achieve this we intent to use the main fracture surface will be examined by scanning electron microscopy (SEM) to the required level and use morphology for more future works. The results will determine if there is need for any further research.

The third work was creating the S-N curve for HT9 under constant deflections. The fatigue endurance limit was measured to be 94 MPa. The measured stress was higher than the simulated one by  $53 \pm 0.002$  MPa. The error levels were found to be high because of the dimensional inaccuracies on the deflection and length of the specimen due to stress. This was indicative that a longer sample length would have minimized stress levels. The Weibull distribution modules tested the number of cycle under stress level at 563, 310, and 265 MPa. A scattered and widely distributed data lead to decreasing shape value. The data appears fitted line in well so the need to choose the 3-parameters Weibull

distribution. It is recommended that additional stress level points be applied. The Weibull distribution model could be appropriate if the data is in with the line of stress.

The fourth work was with the Incoloy alloy MA956 and the bending fatigue was conducted and created S-N curve. The specimens were machined using wire EDM to obtain conclusive fatigue measurements. The bending fatigue were analysed using (Krause-type) to create an S-N curve under constant deflection the replicated stress was closer than measured at high and low stress level. The error was higher suggesting the use of longer samples. Using the Weibull distribution tested the number of cycles that were obtained from four different stress levels. It showed that the measured data was more scattered and widely distributed. The data appear fitted in line well making the 3-parameter Weibull distribution the best choice for data. This also showed that it was better fit to show a much better fit and improve the coefficient value. The profile damage for Incoloy alloy MA956 was calculated using SRIM simulation and calculated that around 3.92  $\mu\text{m}$  when irradiated with 2.3 MeV He ion and 25.38 $\mu\text{m}$  when irradiated with 2.3 MeV. When we compare the as-received with the thermal aging specimens we conclude that the as received display higher hardness and smaller grain boundary and show micro cracks after fatigue test while the fatigue life of both conditions are nearly the same, and summarizes that there is not much influence of the thermal aging process on the fatigue life. The mini specimen (Krause-Type) technique for Incoloy alloy MA956 provide the same fatigue life for the published data and this technique can also be used to generate more fatigue data. The fatigue endurance limit was measured to be 132 MPa.

The fifth work was executed upon four different specimen types and these specimens happened to have considerable differences in their geometries. As such these needed to be validated with a typical S-N curve prepared by NASS. The resulting comparison between simulated FEA and experimental produced the following observations:

1. Percentage error for stress was higher in specimen type-2 by as much as 43.10%.
2. There exists considerable difference in NASS data and Experimental data, for Krause-type specimens namely specimen type-1, type-3 and type-4.
3. However, NASS data and experimental data seem to be in good agreement in case of specimen type-2.

4. Under constant deflection specimen type-1 (target specimen) shows that the measured fatigue life is at a much lower value, than the one observed from NASS data.

For future research.

1. Further research is necessary with different nuclear materials and shaped specimens, particularly longer ones. The longer specimens are still considered adequate to fit in rest reactors (such as ATR).
2. Machining new specimens with using wire EDM in order to reduce the surface effects and obtain a more reliable fatigue measurements suitable for mini-specimens.
3. The behavior of specimen's deflection will be monitoring using a new technique, such as digital deflect meter to verify the bending progress.
4. Because the lifetime for some nuclear reactors is 60 years, long-term thermal aging experiment is needed.
5. Determine the fatigue properties of irradiated.



## APPENDIX

To determine the maximum bending stress and beam deflections generated on surface.

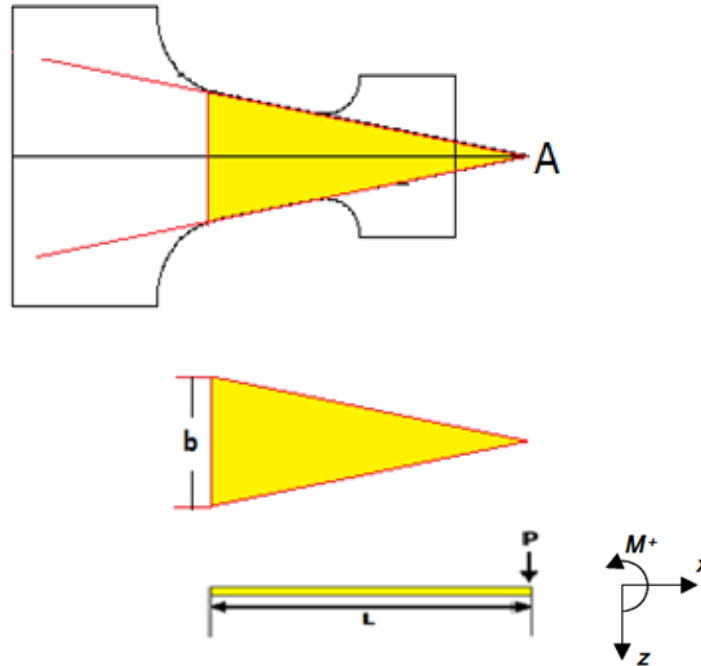


Figure A. 1. Cantilever beam bending tests

Derived for rectangle beam from flexure formula.

$$\sigma = \frac{MC}{I} \quad (\text{A.1})$$

where,

$\sigma$  = stress

$M$  = local bending moment = Force x distance =  $PL$

$L$  = overall length

$b$  = width at the base of the wedge-shaped beam

$C$  = Distance from neutral axis =  $\frac{t}{2}$

$t$  = thickness of the specimen

The moment of inertia of a rectangular cross section is given according to equation (A.2):

$$I = \frac{bt^3}{12} \quad (\text{A.2})$$

In the case of a wedge-shaped beam, local  $b_{(x)}$  and therefore  $I$  values depend on the position along the  $x$ -axis:

$$b_{(x)} = \frac{b}{L} \cdot (L - x) \quad (\text{A.3})$$

By substituting equation (A.2) in equation (A.3), we get:

$$I_{(x)} = \frac{b \cdot (L - x) \cdot t^3}{12L} \quad (\text{A.4})$$

The bending moment  $M$  also depends on the position along the  $x$ -axis and it can be determined from Figure A.1:

$$M_{(x)} = -P(L - x) \quad (\text{A.5})$$

Where  $P$  is the force applied by the connecting rod at position  $x = L$ . Substituting equations (A.3), (A.4) and (A.5) into equation (A.1), we get:

$$\sigma = \frac{MC}{I} = \frac{-P(L - x) \cdot \left(\frac{t}{2}\right)}{\frac{b \cdot (L - x) \cdot t^3}{12L}} = -\frac{12 PLt}{2bt^3} = -\frac{6PL}{bt^2}$$

$$\sigma = -\frac{6PL}{bt^2} \quad (\text{A.6})$$

The maximum deflection which is the deflection at the cantilever tip of a wedge shaped beam and maximum stress is described by the differential equation of the deflection curve:

$$\frac{d^2z}{dx^2} = -\frac{M}{E \cdot I} \quad (\text{A.7})$$

where,  $E$  is modulus of elasticity. Substituting equations (A.5) and (A.4) in equation (A.7), we get:

$$\frac{d^2z}{dx^2} = -\frac{P(L-x) \cdot 12 \cdot L}{E \cdot b \cdot (L-x) \cdot t^3} \quad (\text{A.8})$$

$$\frac{d^2z}{dx^2} = -\frac{P \cdot 12 \cdot L}{E \cdot b \cdot t^3} \quad (\text{A.9})$$

$$\frac{dz}{dx} = \frac{12 \cdot P \cdot L}{E \cdot b \cdot t^3} \cdot x + C_1 \quad (\text{A.10})$$

$$z(x) = \frac{6 \cdot P \cdot L}{E \cdot b \cdot t^3} \cdot x^2 + C_1x + C_2 \quad (\text{A.11})$$

We need two boundary conditions to determine the integration constants:

$$\text{B. C 1: at } x = 0, \quad \frac{dz}{dx} = 0 \quad (\text{A.12})$$

$$\text{B. C 2: at } x = 0, \quad z = 0 \quad (\text{A.13})$$

From equation (A.10), we get  $C_1 = 0$  and from equation (A.11), we get  $C_2 = 0$

$$z(x) = \frac{6 \cdot P \cdot L}{E \cdot b \cdot t^3} \cdot x^2 \quad (\text{A.14})$$

Deflecting  $\Delta$  at point  $x = L$ , the tip of the wedge, then the equation (A.14) becomes:

$$\Delta = \frac{6 \cdot P \cdot L^3}{E \cdot b \cdot t^3} \quad (\text{A.14})$$

$$P = \frac{\Delta \cdot E \cdot b \cdot t^3}{6 \cdot b \cdot L^2} \quad (\text{A.15})$$

Substituting equation (A.15) into equation (A.6), we get:

$$\Delta = \frac{\sigma \cdot L^2}{E \cdot t} \quad (\text{A.16})$$

Equation (A.16) is the formula for the deflection of the specimen in mm.

**REFERENCE**

- [1] T. S. M. Corporation, “INCOLOY alloy MA956.”
- [2] J. R. Kennedy, S. Robertson, R. Soelberg, and C. Knight, “ATR NSUF,” 2013.
- [3] R. V Furstenu and S. B. Grover, “The Advanced Test Reactor Irradiation Facilities and Capabilities,” in *PHYTRAI: First International Conference on Physics and Technology of Reactors and Applications*, 2007, p. 8.
- [4] G. R. R. and B. A. Chin, “Development of miniature bending fatigue specimens,” *J. Nucl. Mater.*, vol. 181, pp. 2–4, 1991.
- [5] C. M. Obermark and R. S. Mishra, “Development of a Reversible Bending Fatigue Test Bed to Evaluate Bulk Properties Using Sub-Size Specimens.”
- [6] H. W. Cao, P. Yang, and B. Z. Bao, “Design of Bending Fatigue Machine for Flexible Electronics,” *Adv. Mater. Res.*, vol. 383–390, pp. 483–489, 2011.
- [7] M. Li and J. Stubbins, “Fatigue Response and Life Prediction of Selected Reactor Materials,” *J. ASTM Int.*, vol. 1, no. 5, p. 11334, 2004.
- [8] R. C. Benn, R. Benn, and P. Relationships, “Microstructure and Property Relationships in Oxide Dispersion Strengthened Alloys,” pp. 238–268, 2015.
- [9] ASTM, “Standard Test Method for Bending Fatigue Testing for Copper-Alloy Spring Materials,” *Annu. B. ASTM Stand.*, vol. 96, pp. 3–7, 2009.

## VITA

Ahmed Suliman R. Haidyrah was born in Riyadh, Saudi Arabia. He received a B.S. degree in 2000 from King Fahd University of Petroleum and Minerals (KFUPM) in Chemical Engineering, Dhahran, Saudi Arabia and an M.S. degree in 2008 from King Saud University (KSU) in chemical engineering, Riyadh, Saudi Arabia. He enrolled in Nuclear Engineering Program at the Missouri University of Science & Technology in fall 2010 under the supervision of Professor Carlos H. Castaño in the area of nuclear materials. In May, 2015, he received the Doctor of Philosophy degree in Nuclear Engineering at the Missouri University of Science and Technology (Rolla, Missouri, USA).